FUNCTIONAL INTERACTION BETWEEN PTEN AND NEDD4

IN IGF SIGNALING

A Dissertation

Presented to the Faculty of Weill Cornell Graduate School

of Medical Sciences

in Partial Fulfillment of the Requirements for the Degree of

Doctor of Philosophy

By

Yuji Shi

January 2015

FUNCTIONAL INTERACTION BETWEEN PTEN AND NEDD4 IN IGF SIGNALING

Yuji Shi, Ph.D.

Cornell University 2015

PTEN is a master regulator of multiple cellular processes and a potent tumor suppressor. Its biological function is mainly attributed to its lipid phosphatase activity that negatively regulates the PI3K-AKT signaling pathway. A fundamental and highly debated question remains whether PTEN can also function as a protein phosphatase in cells. This study demonstrates that PTEN is a protein tyrosine phosphatase that selectively dephosphorylates insulin receptor substrate-1 (IRS1), a mediator for transduction of insulin and IGF1 signaling. IGF signaling is defective in cells lacking NEDD4, a PTEN ubiquitin ligase, whereas AKT activation triggered by EGF or serum is unimpaired in these cells. Surprisingly, the defect of IGF signaling caused by NEDD4 deletion, including the of phosphorylation of IRS1, upstream of PI3K, can be rescued by PTEN ablation, suggesting PTEN may be a protein phosphatase for IRS1. The nature of PTEN as an IRS1 phosphatase is demonstrated by direct biochemical analysis and confirmed by cellular reconstitution. Further, we find that NEDD4 supports insulin-mediated glucose metabolism, and is required for the proliferation of IGF1 receptor (IGF1R)-dependent but not EGFR-dependent tumor cells. Taken

together, PTEN is a protein phosphatase for IRS1, and its antagonism by the ubiquitin ligase NEDD4 promotes IGF/insulin signaling.

Finally, we also identified a novel form of PTEN, which is a translational variant, termed UPP, and characterized it using biochemical and cellular studies. UPP is a fast turnover subpopulation of PTEN, and demonstrates a distinctive subcellular localization from PTEN. Co-localization imaging studies indicated that UPP is involved in endocytosis membrane trafficking and adherens junctions. UPP still functions as a lipid phosphatase for PIP3, antagonizing PI3K signaling. Furthermore, UPP was found to be a better binding partner for the PTEN protein substrate, IRS1, in cells.

BIOGRAPHICAL SKETCH

Yuji Shi was born in 1983, at Jianyang of Sichuan province, a small city in southwest of China. She went to school there until graduation from high school in 2002. The same year, she was enrolled in Tsinghua University in Beijing. In 2006, she finished her undergraduate thesis studies on *Structures of Su(var)3-9* in Dr. Zihe Rao's laboratory and received her B.S. degree with a major in biological sciences. In 2006, she was enrolled in the graduate program of BCMB at Weill Graduate School of Medical Sciences of Cornell University in New York City. In 2007, she joined the laboratory of Dr. Xuejun Jiang at Memorial Sloan-Kettering Cancer Center to study the regulation of tumor suppressor PTEN. During the years, she published one first-author, one second-author paper and one first-author review.

ACKNOWLEDGMENTS

I am greatly grateful for the opportunity of working in Dr. Xuejun Jiang's laboratory. His wisdom and passion for biological science has guided me through the whole process. I really appreciate his patience and encouragement.

I wish to express my gratitude to my thesis committee members, Dr. Songhai Shi, Neal Rosen and Eric Holland for their help and scientific advice for my thesis. I also want to thank Dr. Sarat Chandarlapaty for the discussion and great help for my paper, Dr. Cole Haynes and Dr. Michael Overholtzer for their supply of equipment.

It is so fortunate for me to have so many wonderful lab members ready to help and discuss science. Particularly Dr. Xinjiang Wang and Dr. Noor Gammoh offered their guidance and assistance for many years. Also Dr. Junru Wang provided excellent technical support. Joy Lee volunteered to contribute to the project for 6 months.

I want to thank my dear friends for their constant support. Especially, Ph.D. candidate Daniel Marks offered great suggestion and emotional support for the past four and half years and eventually proof-read my thesis. Last but not least, I owe my life and Ph.D. degree to my beloved mom who endures years of separation and loneliness for my degree.

TABLE OF CONTENTS

Biographical Sketch ---------- iii

Acknowledgements ---------- iv

Table of Contents ---------- v

List of Abbreviations ---------- vi

List of Figures ---------- viii

Chapter One: General Introduction ---------- 1

Chapter Two: Function of NEDD4 in IGF Signaling ---------- 15

Introduction ---------- 15

Results ---------- 16

Discussion ---------- 33

Chapter Three: PTEN is Protein Tyrosine Phosphatase for IRS1 ---------- 36

Introduction ---------- 36

Results ---------- 37

Discussion ---------- 55

Chapter Four: Characterize a New Form of PTEN Tumor Suppressor ---------- 58

Introduction ---------- 58

Results ---------- 59

Discussion ---------- 88

Chapter Five: Materials and Methods ---------- 90

Materials ---------- 90

Methods ---------- 94

References ---------- 101

LIST OF ABBREVIATIONS

NEDD4: Neural precursor cell expressed developmentally down-regulated protein 4

PTEN: Phosphatase and tensin homolog on chromosome ten

IRS1: Insulin receptor substrate 1

IRS2: Insulin receptor substrate 2

IGF1: Insulin-like growth factor 1

IGF2: Insulin-like growth factor 2

EGF: Epidermal growth factor

EGFR: Epidermal growth factor receptor

IGF1R: Insulin-like growth factor 1 receptor

MAPK: Ras-mitogen-activated protein kinase

RTK: receptor tyrosine kinase

PI3K: phosphoinositide 3-kinase

AKT: also known as protein kinase B (PKB)

PIP_3: phosphatidyl inositol-3,4,5-trisphosphate

PIP_2: phosphatidylinositol-4,5-biphosphate

PH: pleckstrin homology

PTB: phosphotyrosine-binding

mTORC2: mammalian target of rapamycin complex 2

UPP: upper protein band of PTEN

ER: endoplasmic reticulum

MEFs: mouse embryonic fibroblasts

LIST OF FIGURES

Figure 1.1 ---------- 3

Figure 1.2 ---------- 6

Figure 1.3 ---------- 14

Figure 2.1 ---------- 18

Figure 2.2 ---------- 19

Figure 2.3 ---------- 20

Figure 2.4 ---------- 23

Figure 2.5 ---------- 24

Figure 2.6 ---------- 25

Figure 2.7 ---------- 29

Figure 2.8 ---------- 31

Figure 2.9 ---------- 32

Figure 3.1 ---------- 40

Figure 3.2 ---------- 41

Figure 3.3 ---------- 42

Figure 3.4 ---------- 46

Figure 3.5 ---------- 47

Figure 3.6 ---------- 48

Figure 3.7 ---------- 49

Figure 3.8 ---------- 52

Figure 3.9 ---------- 53

Figure 3.10 ---------- 54

Figure 4.1 ---------- 61

Figure 4.2 ---------- 62

Figure 4.3 ---------- 63

Figure 4.4 ---------- 65

Figure 4.5 ---------- 70

Figure 4.6 ---------- 71

Figure 4.7 ---------- 72

Figure 4.8 ---------- 74

Figure 4.9 ---------- 75

Figure 4.10 ---------- 76

Figure 4.11 ---------- 79

Figure 4.12 ---------- 81

Figure 4.13 ---------- 83

Figure 4.14 ---------- 86

Figure 4.15 ---------- 87

CHAPTER ONE

GENERAL INTRODUCTION

Insulin and IGF signaling pathway

Insulin, insulin-like growth factor-1 (IGF1) and insulin-like growth factor-2 (IGF2) belong to a group of secreted growth factors with essential roles in growth, development, and metabolism (Yakar and Adamo, 2012). Insulin and IGF1 are structurally homologous growth factors, which function through binding to specific receptors (Insulin receptor and IGF1 receptor (IGF1R) respectively) on the surface of target cells. The closely related receptors share the same tetrameric structure composed of two extracellular α subunits including the ligand-binding domain and two transmembrane β subunits containing the tyrosine kinase domain. Binding of ligands to α subunits leads to activation and auto-phosphorylation of tyrosine residues in the β subunits (Pautsch et al., 2001). Signaling is subsequently mediated by the phosphorylation of specific substrates by the activated receptors.

The principal substrates for insulin and IGF1 receptors are insulin receptor substrate proteins (IRS proteins), which mediate activation of two main downstream signaling pathways (White, 1998). After tyrosine phosphorylation at multiple sites, IRS1 binds to either the regulatory p85 subunit of phosphatidylinositol 3-kianse (PI3K), or the adaptor molecule Grb2, which associates with son-of-sevenless (SOS)

to activate the Ras--mitogen-activated protein kinase (MAPK) pathway (Figure 1.1). The PI3K-AKT pathway is responsible for most of the metabolic actions of insulin, while the MAPK pathway regulates gene expression and cooperates with the PI3K pathway to control cell growth and differentiation.

PI3K belongs to a conserved family of lipid kinases involving in intracellular signaling propagation (Cantley, 2002). PI3K phosphorylates phosphatidylinositol-4,5-biphosphate (PIP_2) in the plasma membrane to generate phosphatidylinositol-3,4,5-triphosphatate (PIP_3). PIP_3 is a critical second messenger which binds to various signaling proteins containing the pleckstrin homology (PH) domains, including the serine/threonine kinase AKT and PDK1 (Manning and Cantley, 2007). AKT is activated by phosphorylation at T308 in the activation loop by PDK1 and phosphorylation on the hydrophobic motif S473 by mTOR complex 2 (mTORC2). Activated AKT promotes cell survival, growth, proliferation, and inhibit apoptosis, through phosphorylating various downstream targets.

The functions of the insulin and IGF components in development were demonstrated by mice with genes disrupted by homologous recombination (Taniguchi et al., 2006). IGF1R knockout led to the immediate postnatal death from respiratory failure, with a dramatic reduction in body weight (more than 50% reduction) (Liu et al., 1993). While heterozygous mice are normal, but show a ~15% decrease in body mass. In contrast, insulin receptor-disrupted mice are born normal, but develop early postnatal diabetes and die of ketoacidosis (Kitamura et al., 2003). IRS1-deficient mice

are born alive, but have defective insulin response in the muscle and general retardation in body growth due to IGF1 resistance (Liu et al., 1993).

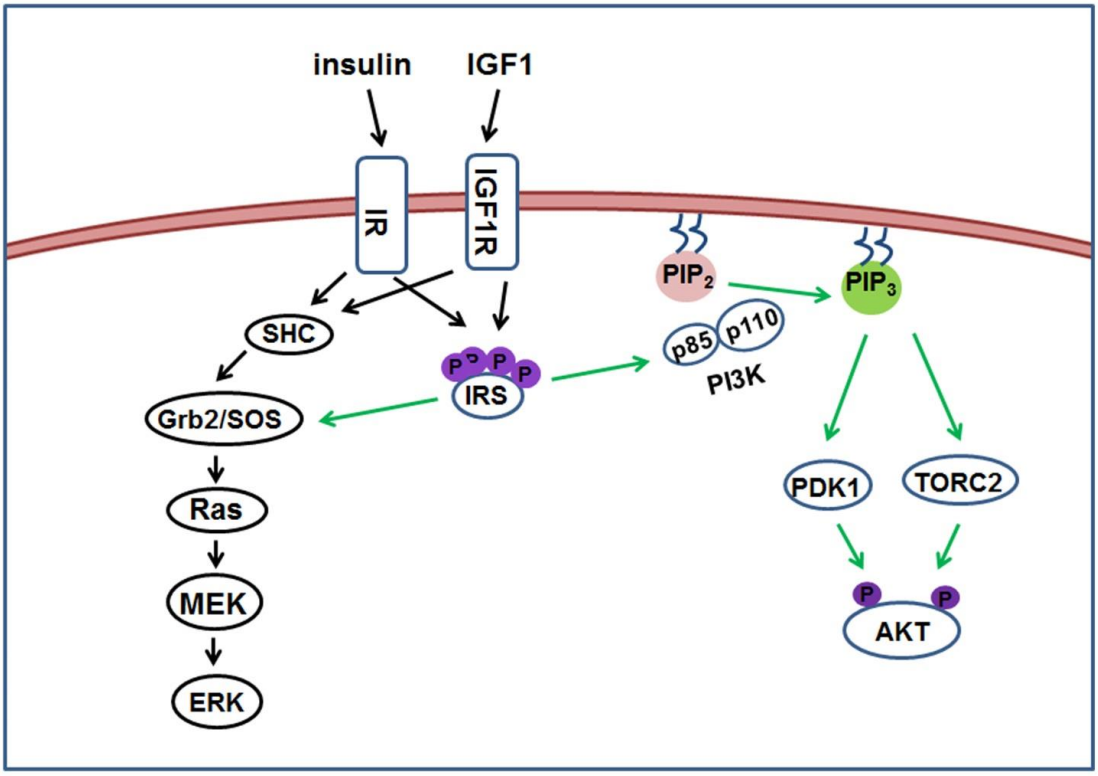

Figure 1.1

IGF and Insulin Signaling Pathways. The binding of growth factors insulin and IGF1 to their receptors on cell surface lead to the recruitment of adaptor proteins, including SHC and IRS proteins. Tyrosine phosphorylation of IRS promotes binding of PI3K and Grb2/SOS, resulting in the activation of the downstream AKT and MAPK pathway.

The IRS proteins possess pleckstrin-homolog (PH) domains and phosphotyrosine-binding (PTB) domains at the N-terminus that are responsible for the high affinity for IR/IGF1R (Boura-Halfon and Zick, 2009). There are up to 20 potential tyrosine-phosphorylation sites between the center and C-terminus of the IRS proteins. After tyrosine phosphorylation by IR/IGF1R, IRS proteins can bind to proteins that contain Src-homolog-2 (SH2) domains. Phosphorylation of tyrosines 465, 612, 632, 662, 941 and 989 of IRS1 YXXM motifs are predicted to bind the SH2 domain of the p85 regulatory subunit of PI3K, resulting in activation of the p110 catalytic subunit (Sesti et al., 2001) . Studies have shown that Tyr612 and Tyr632 in human IRS1 (corresponding to positions 608 and 628 in rat or mouse IRS1) are important for full activation of insulin-stimulated PI3K activity and translocation of GLUT4 in adipose cells (Esposito et al., 2001).

Tumor suppressor PTEN

Since its discovery in 1997 (Li and Sun, 1997; Li et al., 1997; Steck et al., 1997), PTEN (phosphatase and tensin homolog) has been established as one of the most frequently mutated tumor suppressor genes in human cancer, including endometrial carcinoma, glioblastoma multiforme, skin and prostate cancers (Salmena et al., 2008). Biochemically, PTEN is a phosphatase for the lipid second messenger PIP_3, catalyzing its conversion to PIP_2 (Maehama and Dixon, 1998). Therefore, PTEN functions as a major regulator of the cellular concentration of PIP_3 to antagonize the signaling cascades downstream of receptor tyrosine kinases (RTKs) and PI3K ((Figure 1.2). Interestingly, PTEN might also possess protein phosphatase activity with several

potential protein substrates reported (Gu et al., 1999; Mahimainathan and Choudhury, 2004; Raftopoulou et al., 2004; Tamura et al., 1998).

Importantly, PTEN is involved in regulating many cellular processes. Many of these functions can be attributed to its lipid phosphatase activity. For example, PTEN regulates cell proliferation and apoptosis. These effects are mediated by suppressing AKT activation and subsequent alteration of the function of AKT substrates, such as forkhead box protein O (FOXO), the E3 ubiquitin ligase Mdm2, and Bcl2 antagonist of cell death (BAD) (Tamura et al., 1999).

PTEN has a crucial role in regulating the self-renewal and differentiation of human embryonic stem cells and hematopoietic stem cells as well as the timing of follicle activation through the regulation of oocyte growth (Reddy et al., 2008). PTEN also regulates the chemotaxis of neutrophils, and all these functions require its lipid phosphatase activity (Heit et al., 2008). Moreover, PTEN can regulate various cellular events independently of its lipid phosphatase activity. For example, it can inhibit cell cycle progression by modulating the activity of the anaphase promoting complex/cyclosome (APC/C) in the nucleus in a manner that is independent of PTEN's enzymatic activity (Song et al., 2011). Furthermore, it can inhibit cell invasion and migration, likely through its protein phosphatase activity (Tamura et al., 1998). PTEN can control the size of DNA-damaged cells by regulating the actin-remodeling process through a mechanism that is likely independent of its lipid phosphatase activity (Kim et al., 2011). Deficiency of any of these functions can contribute to tumorigenesis.

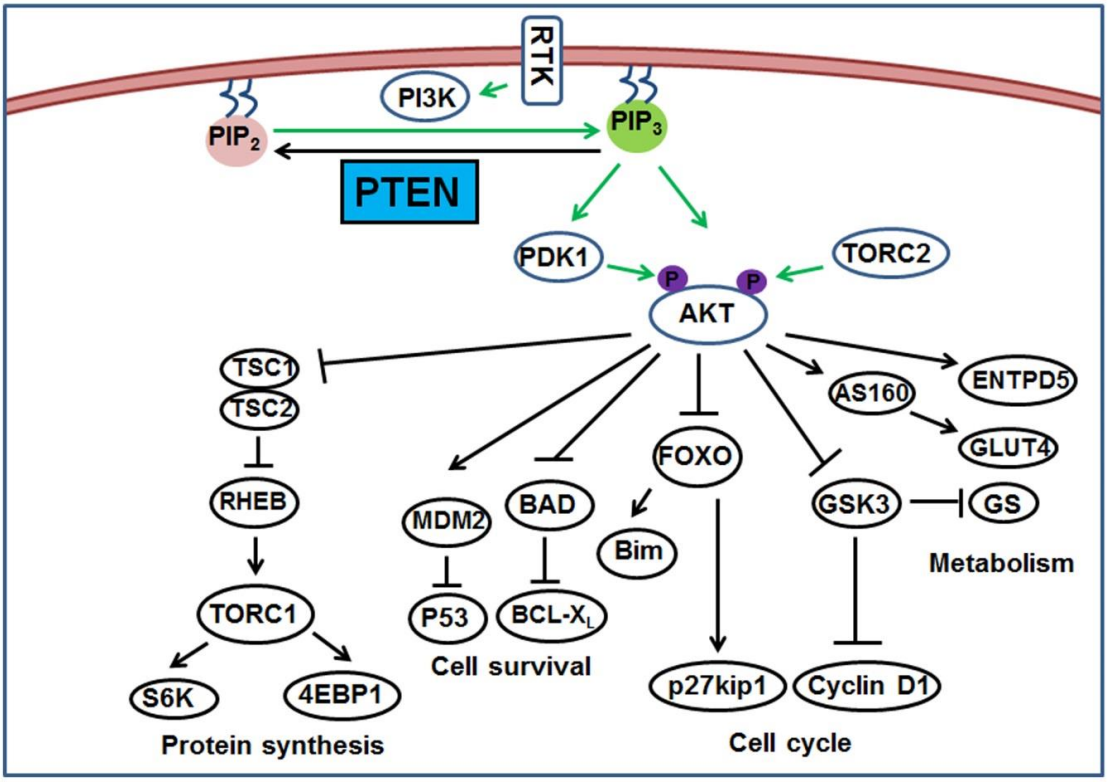

Figure 1.2

PTEN is the major negative regulator of PI3K-AKT pathway. Physiologically, PTEN is a lipid phosphatase for PIP3 at the plasma membrane, antagonizing the activity of PI3K. PTEN negatively regulates PIP3 levels, which are essential for AKT activation and multiple biological processes.

PTEN contains multiple domains, including an N-terminal phosphatase domain, a central C2 domain and a C-terminal tail (Song et al., 2012). The phosphatase and C2 domains form a minimal enzymatic unit that is sufficient for metabolizing PIP_3. The C-terminal tail is a long flexible fragment that is mainly involved in PTEN regulation.

The functional diversity of PTEN demands a collection of delicate regulatory mechanisms, including transcriptional and posttranslational regulation in a tissue- and context-dependent manner. The *PTEN* promoter is regulated by many transcription factors, which operate at specific times and in different cell types (Shi et al., 2012). PTEN mRNA is susceptible to post-transcriptional regulation by a variety of microRNAs (miRNAs), including miR-21, which is the most frequently up-regulated onco-miRNA in solid tumors (Meng et al., 2007). Additional complexity results from the regulation of PTEN expression by non-coding RNAs, such as the *PTEN* pseudogene *PTENP1* mRNA (Poliseno et al., 2010). *PTENP1* genetically resembles PTEN in its protein coding region. Unlike *PTEN* mRNA, however, *PTENP1* mRNA cannot be translated into a protein as a result of a mutation in its initiator codon. The *PTENP1* mRNA is generally subject to the same miRNA-mediated regulation and thus can function as decoys to sequester miR-21. Interestingly, in sporadic colon cancer, *PTENP1* undergoes a copy number loss that is concurrent with *PTEN* down-regulation. Similarly, ZEB2, another endogenous RNA, was reported to serve as an miRNA decoy for the *PTEN* mRNA, and its loss contributes to melanomagenesis (Karreth et al., 2011). However, it is important to bear in mind that only 25% of cancer patients

show a correlation between PTEN protein loss and its mRNA level (Chen et al., 2011), which emphasizes the importance of PTEN regulation at the posttranscriptional and posttranslational levels.

PTEN is subject to various posttranslational modifications, including phosphorylation, acetylation, oxidation, S-nitrosylation and ubiquitination (Figure 1.3). These modifications regulate the enzymatic activity of PTEN, its interaction with other proteins and its subcellular localization.

Phosphorylation: The first phosphorylation sites mapped on PTEN were a cluster of serine and threonine residues in its C-terminal tail (Vazquez et al., 2000). Mutation of these residues to alanine leads to elevated membrane affinity, higher enzymatic activity and more rapid degradation of PTEN. When these residues are phosphorylated, the C-terminal tail can interact with the N-terminal C2 and phosphatase domains, which suggests that phosphorylation of the C-terminal tail functions as an auto-inhibitory mechanism, controlling both PTEN membrane recruitment and lipid phosphatase activity (Odriozola et al., 2007; Rahdar et al., 2009). Several kinases have been reported to phosphorylate PTEN. Casein kinase 2 (CK2) mainly phosphorylates Ser370 and Ser385 (Torres and Pulido, 2001), whereas glycogen synthase kinase 3 beta (GSK3-β) targets Ser362 and Thr366 (Al-Khouri et al., 2005). In contrast with the function of C-terminal tail phosphorylation, it seems that Thr366 phosphorylation can promote PTEN degradation (Maccario et al., 2007). Additionally, glioma tumor suppressor candidate region 2 (GLTSCR2, also known as PICT-1) has been shown to interact with PTEN, enhance its phosphorylation at Ser380

and stabilize it (Okahara et al., 2006; Yim et al., 2007). Moreover, RhoA-associated kinase (ROCK) has been shown to phosphorylate PTEN at Ser229, Thr232, Thr319 and Thr321, which are all located in the C2 domain, and promote its membrane targeting in chemoattractant-stimulated leukocytes (Li et al., 2005). A Src family tyrosine kinase, RAK has been reported to interact with PTEN and phosphorylate it on Tyr336, thereby protecting it from neural precursor cell expressed, developmentally downregulated-4-1 (NEDD4-1)-mediated proteasomal degradation (Yim et al., 2009).

Acetylation: Similar to phosphorylation, acetylation can also regulate PTEN activity. The histone acetyltransferase p300/CBP-associated factor (PCAF) has been reported to interact with PTEN and promote PTEN acetylation on Lys125 and Lys128 in response to growth factors (Okumura et al., 2006). As these residues are within the catalytic pocket, PTEN acetylation by PCAF negatively regulates its enzymatic activity. PTEN is also acetylated on Lys402, within the C-terminal PDZ domain-binding motif Thr–Lyz–Val sequence (Ikenoue et al., 2008). This potentially affects the interaction between PTEN and PDZ domain-containing proteins. Nuclear cap-binding protein (CBP) and the sirtuin SIRT1 have been identified as the major PTEN acetyltransferase and deacetylase, respectively.

Oxidation: Another mechanism that can potentially regulate the catalytic activity of PTEN is direct oxidation by reactive oxygen species (ROS). ROS can oxidize Cys124 in the active site, thereby forming an intramolecular disulfide bond with Cys71 (Lee et al., 2002). Oxidative inactivation of PTEN has been reported in studies using hydrogen peroxide or endogenous ROS production in macrophages

(Kwon et al., 2004; Leslie et al., 2003). PTEN activity can also be indirectly inhibited by oxidation through modulation of PTEN binding partners. Oxidation of the antioxidant DJ-1 (also known as PARK7) leads to its binding to PTEN and the subsequent inhibition of the PTEN lipid phosphatase activity (Kim et al., 2009).

S-nitrosylation: A few studies have demonstrated the importance of another redox mechanism, S-nitrosylation, in the regulation of PTEN. The level of S-nitrosylation on PTEN substantially increases in the early stages of Alzheimer's disease, and this correlates with reduced PTEN protein levels and elevated AKT phosphorylation (Kwak et al., 2010a). Nitrogen Oxide (NO) signaling induces PTEN S-nitrosylation, thereby inactivating the lipid phosphatase, down-regulating its protein level through NEDD4-1-mediated degradation, and leading to downstream AKT activation. Another report has shown that PTEN is selectively S-nitrosylated on Cys83 by low concentrations of NO (Numajiri et al., 2011). Moreover, S-nitrosylated PTEN has been detected in the core and penumbra regions of ischemic mouse brains, likely as a protective mechanism to promote AKT activation.

Ubiquitin ligase NEDD4

The modification of ubiquitination is made by sequential transfer of activated ubiquitin to substrate protein, involving ubiquitin-activating enzyme (E1), ubiquitin-conjugating enzyme (E2) and ubiquitin ligase (E3) (Mani and Gelmann, 2005). E3s catalyze the transfer of ubiquitin to Lys residues in the substrate and covalent conjugation between the carboxyl group of the carboxy-terminal Gly residue of

ubiquitin and the ε–amino group of an internal Lys in the substrate, therefore dictating the specificity of ubiquitination. A substrate protein can be mono-ubiquitinated at one site, multi-ubiquitinated at various residues or poly-ubiquitinated through formation of chains of ubiquitin (Ikeda and Dikic, 2008). Usually the fate of the substrate depends on the length and architecture of ubiquitin chain. Among the seven Lys residues (K6, K11, K29, K33, K48 and K63), Lys 48 and Lys 63 are the most commonly utilized. Generally, K48-linked polyubiquitination targets substrates for degradation by the 26S proteasome, while monoubiquitination and K63-linked polyubiquitination regulate multiple cellular processes, including signal transduction and protein subcellular localization (Rotin and Kumar, 2009).

NEDD4-1 belongs to one of the two main classes of E3 ligases, HECT (Homologous to E6-AP C-Terminus) E3 enzymes (Yang and Kumar, 2010). Mammalian NEDD4 contains an N-terminal calcium/lipid and/or protein binding C2 domain, three (in mouse or rat) or four (in human) WW domains (protein-protein interaction domains), and a C-terminal HECT domain (Anan et al., 1998; Kumar et al., 1997; Staub et al., 1996). The *Nedd4* gene was initially identified by a subtraction cloning as a transcript which highly expressed in the mouse embryonic brain and decreased as development progressed (Kumar et al., 1992). NEDD4 protein is detected in various embryonic tissues and widely expressed in mammalian adult tissues. NEDD4 protein, around 120 kDa, localizes to the cellular cytoplasm, mainly in the perinuclear region and cytoplasm periphery (Anan et al., 1998; Kumar et al., 1997). NEDD4 interacts with specific E2 enzymes containing Ubc4, UbcH5B, UbcH5C,

UbcH6 and UbcH7 (Anan et al., 1998). Systematic analysis of the types of ubiquitin chains showed that NEDD4, with UbcH5, formed exclusively Lys63 ubiquitin chains (Kim et al., 2007).

Using a biochemical purification approach, NEDD4 was identified as an E3 ligase that ubiquitinates PTEN (Wang et al., 2007b). NEDD4 physically interacts with PTEN and its overexpression leads to both mono- and poly-ubiquitination of PTEN. Interestingly, mono-ubiquitination of PTEN appears to be crucial for its nuclear import (Trotman et al., 2007). Consistent with the function of the C-terminal tail of PTEN in regulating its stability, deletion of this region makes PTEN a stronger binding partner and better substrate for NEDD4 (Wang et al., 2008). However, in most experimental systems, PTEN appears to be a rather stable protein. Under normal growth condition, inhibition of NEDD4 expression does not affect cellular PTEN levels or AKT activation in several examined cell types, suggesting that regulation of PTEN by NEDD4 might be only relevant under specific biological contexts. For example, NEDD4 is required for neuronal axonal branching in retinal ganglion cells (RGCs) and mainly functions through down-regulating PTEN (Drinjakovic et al., 2010). Blocking NEDD4 function severely inhibits terminal branching in RGCs, whereas PTEN knockdown rescues the branching deficiency. Also, NEDD4-mediated PTEN ubiquitination is essential for regulating PI3K–AKT signaling for neuronal survival in response to Zn^{2+} (Kwak et al., 2010b). Furthermore, in cultured neuronal models, NO signaling not only induces PTEN S-nitrosylation but also results in

enhanced PTEN protein degradation through NEDD4-mediated ubiquitination (Kwak et al., 2010a).

Several cellular proteins have been reported to modulate the association between NEDD4 and PTEN, which might provide mechanistic insights into the context-dependent regulation of PTEN by NEDD4. In breast cancer cells, the tyrosine kinase RAK positively regulates PTEN stability by phosphorylating PTEN on Tyr336. This prevents PTEN from binding to NEDD4 and its subsequent degradation (Yim et al., 2009). The PY (Pro–Pro–x–Tyr)-motif containing membrane proteins NEDD4-family interacting proteins (NDFIP) 1 and 2, which are potent activators of NEDD4 family members, were shown to promote NEDD4-mediated ubiquitination and degradation of PTEN (Howitt et al., 2012; Mund and Pelham, 2010).

Studies investigating the oncogenic activity of NEDD4 in various cell culture and mouse models indicate NEDD4 is critical for targeting PTEN for degradation in a variety of cancers. Over-expression of NEDD4 promotes oncogenic K-Ras-mediated transformation in $p53^{-/-}$ primary MEFs in soft-agar-colony formation experiments (Wang et al., 2007b). Analysis of invasive human bladder cancer samples showed that PTEN levels were inversely correlated with the levels of NEDD4. Xenograft mouse models using two human prostate cancer cell lines, DU-145 (PTEN positive) and PC3 (PTEN negative) show that NEDD4 RNAi inhibits tumor growth in a PTEN-dependent manner. Immunohistochemical analysis on tissue microarrays of non-small cell lung carcinoma (NSCLC) revealed NEDD4 over-expression in 80% of tumors, which correlated with the loss of PTEN protein (Amodio et al., 2010). Furthermore,

inhibition of NEDD4 expression significantly reduces in vitro proliferation of NSLC cells and tumor growth in xenografts. Finally, FoxM1, a transcription factor over-expressed in human glioma tissue, with its expression level correlated with glioma grade, up-regulates the expression of NEDD4, promoting PTEN ubiquitination and degradation in glioma cells (Dai et al., 2010).

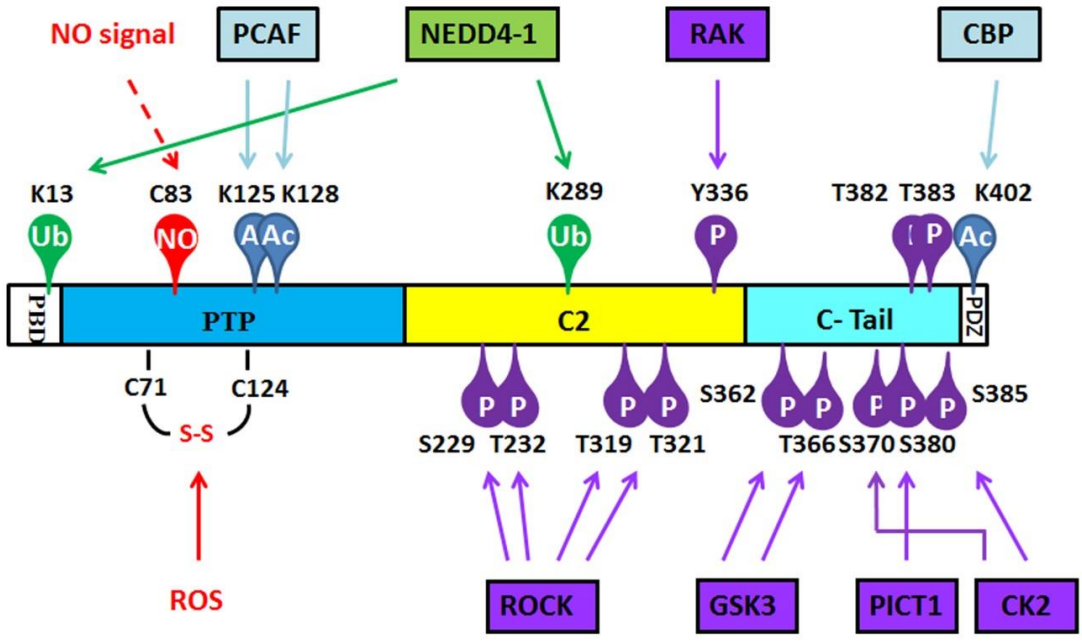

Figure 1.3

Post-translational modifications of PTEN. Summary of enzymes and key residues of post-translational modification of PTEN.

CHAPTER TWO

FUNCTION OF NEDD4 IN IGF SIGNALING*

INTRODUCTION

The physiological function of NEDD4 was demonstrated by knockout mice studies (Cao et al., 2008; Fouladkou et al., 2008). NEDD4-null mice are small, due to delayed embryonic development, severe growth retardation and neonatal lethality, a phenotype reminiscent of that observed in mice with deletion of AKT1, IGF1 or IGF1R (Cao et al., 2008). Moreover, NEDD4$^{-/-}$ mouse embryonic fibroblasts (MEFs) showed decreased IGF1, insulin signaling and reduced mitogenic activity, suggesting that NEDD4 is a positive regulator of cell proliferation and animal growth. The growth defect of the NEDD4$^{-/-}$ embryos was attributed to a decrease of cell surface IGF1R and subsequent IGF1 signaling. Furthermore, there was an increase in the protein level of GRB10, an adaptor protein and negative regulator of IGF1 signaling (Smith et al., 2007; Wang et al., 2007a), in the NEDD4$^{-/-}$ MEFs.

Previous studies showed that PTEN was regulated by ubiquitination and a substrate of the NEDD4 ubiquitin ligase (Wang et al., 2007b). However, under normal growth conditions, inhibition of NEDD4 expression does not affect either cellular PTEN levels or AKT activation in several examined cell types (Fouladkou et

*: citation 4

al., 2008), suggesting that regulation of PTEN by NEDD4 might be only relevant under specific biological contexts (Shi et al., 2012).

In this study, we sought to investigate whether insulin and IGF signaling required NEDD4-mediated PTEN suppression. By conducting both cellular and in vitro biochemical analysis, we discovered that suppression of PTEN by NEDD4 played a physiologic role in maintaining AKT activation induced specifically by IGFs but not by other tested agonists. Consistent with this function, NEDD4 regulated IGF1R-dependent cancer cell growth and insulin-mediated glucose metabolism.

RESULTS

NEDD4 is required for IGF/insulin signaling but not EGF signaling

We found that in NEDD4$^{-/-}$ MEFs, activation of AKT phosphorylation in response to IGF1 or insulin was greatly diminished compared to paired NEDD4$^{+/+}$ MEFs, whereas induction of AKT phosphorylation by serum or EGF was intact in NEDD4$^{-/-}$ MEFs (Figure 2.1A). Similar to IGF1, IGF2 cannot stimulate AKT phosphorylation in NEDD4$^{-/-}$ MEFs, though IGF2-induced AKT activation is normal in NEDD4$^{+/+}$ MEFs (Figure 2.1B). Consistently, NEDD4 deletion did not abrogate EGF signaling when different doses of EGF were used to trigger the pathway (Figure 2.1C). Even though EGF-induced AKT phosphorylation was comparable in both

MEFs, EGFR phosphorylation was slightly higher in NEDD4$^{-/-}$ MEFs. To further confirm the effect of NEDD4 in IGF signaling, we engineered wild type (WT) MEFs to express two different shRNA sequences against NEDD4 in a doxycycline (Dox)-inducible manner. Time course analysis of the cell lines showed that Dox caused marked reduction of NEDD4 expression within 2 days but little change of PTEN or Grb10 protein levels (Figure 2.2A). Similar to data from NEDD4 knockout MEFs, Dox-induced depletion of NEDD4 protein suppressed the ability of IGF1 to induce the phosphorylation of both AKT and tyrosine phosphorylation on upstream IRS1 (Figure 2.2B).

The kinetics of signaling by IGF1, insulin and EGF were then examined in more detail. In WT MEFs, IGF1 rapidly induced the phosphorylation of IGF1R and IRS1, which persisted without decline for at least 60 minutes (Figure 2.3A). This was associated with a potent and equally persistent induction of AKT phosphorylation. After Dox-induced NEDD4 knockdown, although IGF1R phosphorylation was unaffected, induction of IRS1 phosphorylation at Y608 5 minutes after IGF1 stimulation was significantly repressed and remained so up to 60 minutes later. This was accompanied by markedly reduced induction of AKT phosphorylation. Insulin signaling was similarly defective after NEDD4 knockdown, though phosphorylation of Insulin receptor was intact (Figure 2.3B). In contrast, NEDD4 knockdown had no effect on the magnitude or kinetics of the induction by EGF of phosphorylation of EGFR or AKT (Figure 2.3C). Thus, NEDD4 was specifically required for induction of the PI3K/AKT pathway by IGF1 and insulin but not by EGF or serum.

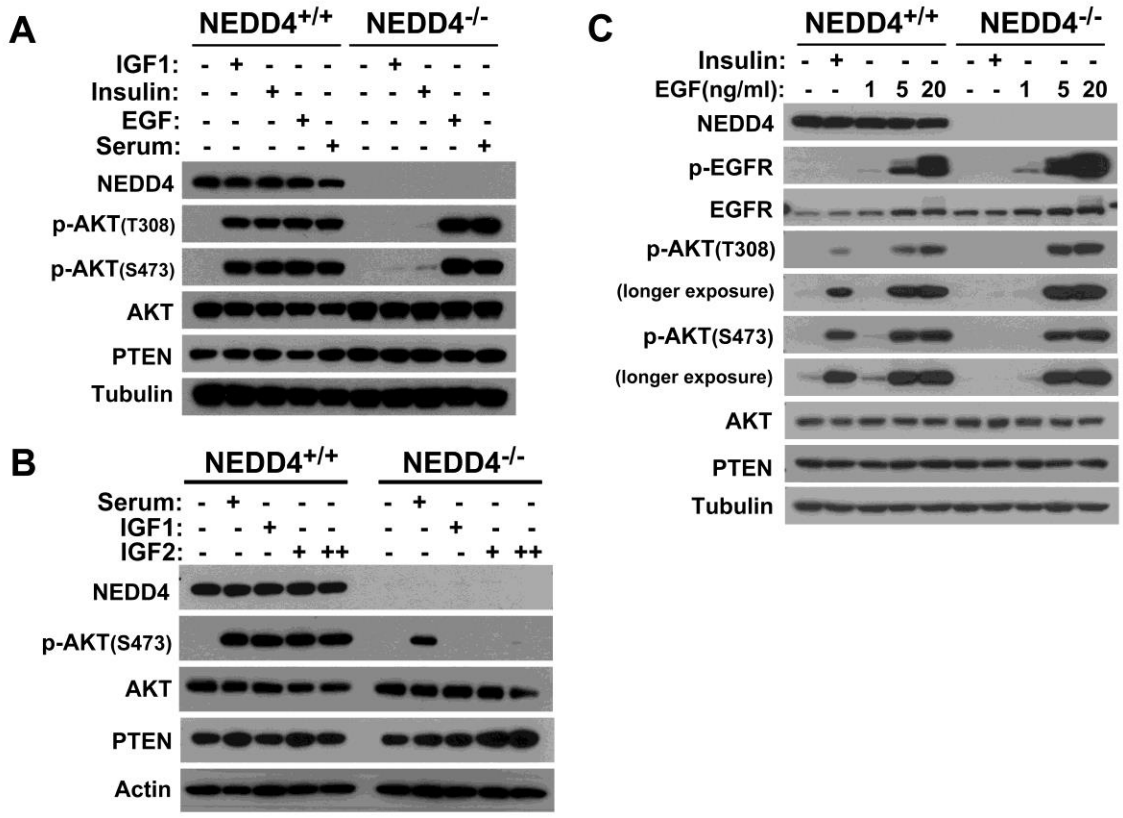

Figure 2.1

NEDD4 specifically regulates IGF/insulin signaling but not EGF or serum signaling. (A) IGF1 and insulin signaling but not EGF or serum signaling is defective in NEDD4$^{-/-}$ MEFs. NEDD4$^{+/+}$ and NEDD4$^{-/-}$ MEFs were serum-starved for 3 hrs, and then stimulated with either 50 ng/ml IGF1, 100 ng/ml Insulin, 10% serum or 100 ng/ml EGF for 5 min. (B) IGF2 signaling is defective in NEDD4$^{-/-}$ MEFs. NEDD4$^{+/+}$ and NEDD4$^{-/-}$ MEFs were serum starved for 3 hrs, then stimulated with either 10% serum, 50 ng/ml IGF1 or 50 ng/ml, 100 ng/ml IGF2 for 5 min. (C) Dose response of EGF showing NEDD4 is not required for EGF signaling. NEDD4$^{+/+}$ and NEDD4$^{-/-}$ MEFs were serum-starved for 3 hrs, and then stimulated with either insulin (100 ng/ml) or EGF (1, 5 or 20 ng/ml as indicated) for 5 min.

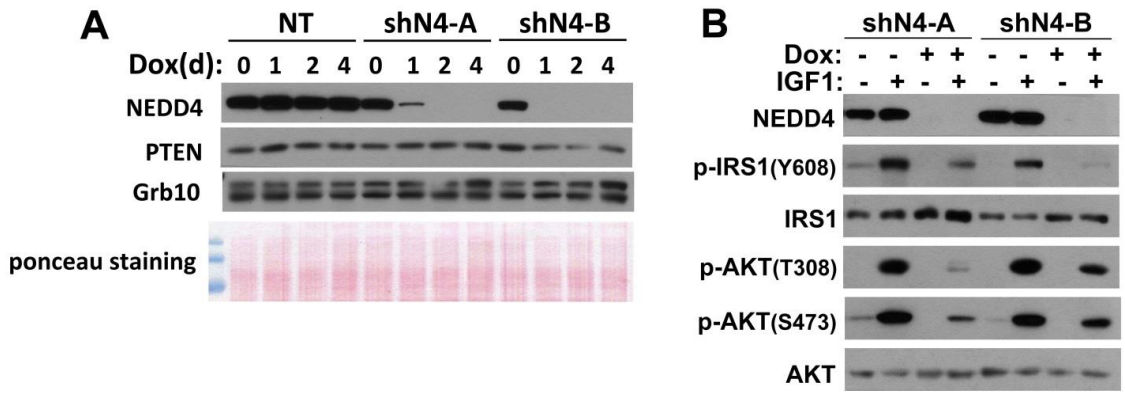

Figure 2.2

Inducible NEDD4 RNAi blocks IGF1 signaling. (A) Analysis of WT MEFs with Dox-inducible NEDD4 shRNA. WT MEFs harboring non-targeting (NT) and Dox-inducible NEDD4 shRNA constructs (shN4-A or shN4-B) were treated with or without 1 μg/ml Dox for indicated time. (B) Inducible NEDD4 RNAi blocks IGF1 signaling. WT MEFs harboring Dox-inducible NEDD4 shRNA constructs (shN4-A or shN4-B) were treated with or without 1 μg/ml Dox for 3 days, serum-starved for 3 hrs, and then stimulated with 50 ng/ml IGF1 for 5 min.

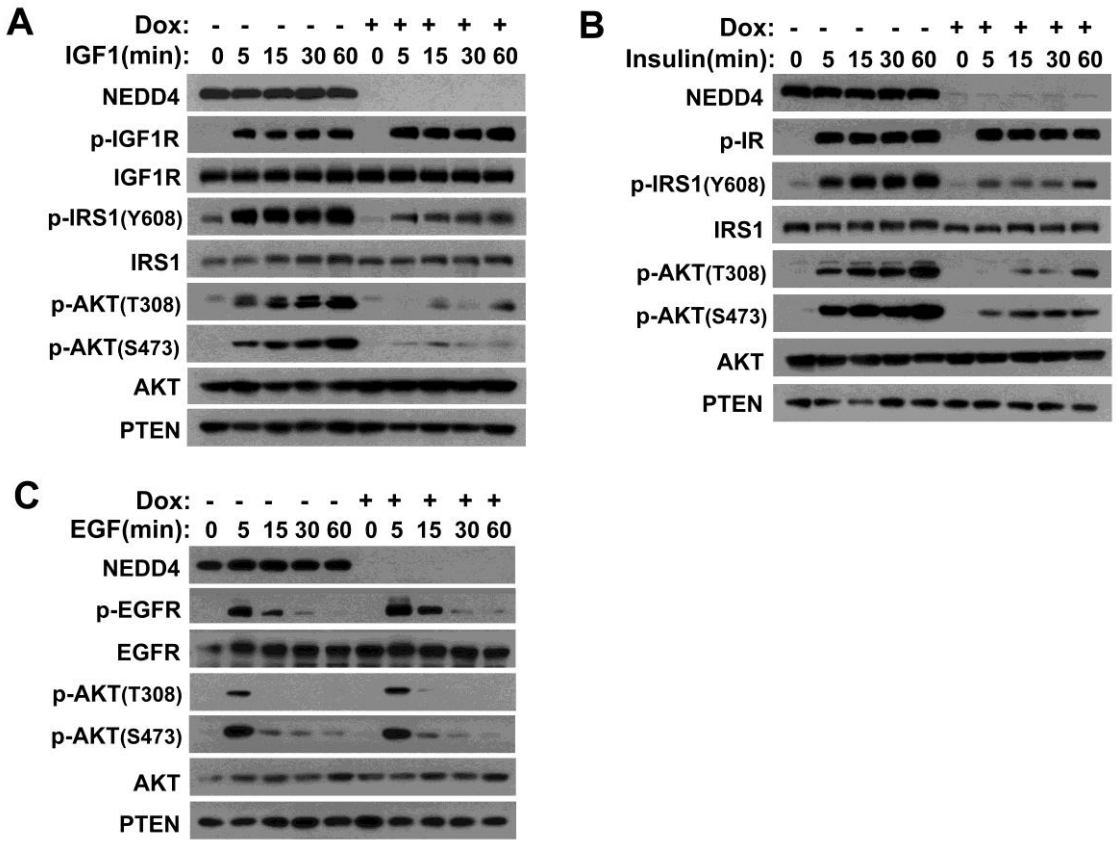

Figure 2.3

Kinetic analysis of the effect of NEDD4 elimination on IGF/insulin/EGF signaling. (A) Time course showing NEDD4 RNAi ablates IGF1 signaling. MEFs harboring a Dox-inducible NEDD4 shRNA construct were treated with or without 1 μg/ml Dox for 3 days, serum-starved for 3 hrs, and then stimulated with 50 ng/ml IGF1 for the indicated time. (B) Time course showing NEDD4 RNAi ablates insulin signaling. 100 ng/ml Insulin was used for indicated time after 3 hrs of serum starvation. (C) Time course showing NEDD4 RNAi does not block EGF signaling. 100 ng/ml EGF was used for indicated time after 3 hrs of serum starvation.

The role of NEDD4 in IGF signaling is PTEN-dependent

In NEDD4-deficient cells, ligand activation of IGF1R and insulin receptor was normal, as monitored by the induction of their tyrosine phosphorylation. For IGF1R, both its early phosphorylation at Y1135/1136 (Pautsch et al., 2001) and that at the juxtamembrane Y980 site were not inhibited by NEDD4 deletion (Figure 2.4A). However, induction of both IRS1 and AKT phosphorylation was defective when NEDD4 was absent.

Because NEDD4 is an E3 ubiquitin ligase for PTEN, we examined whether the requirement of NEDD4 for IGF/insulin signaling was due to its suppression of PTEN function. Indeed, when PTEN was knocked down in NEDD4$^{-/-}$ MEFs by two different Dox-inducible shRNA constructs, IGF1-induced IRS1 phosphorylation and AKT phosphorylation were restored, with no effect on IGF1R phosphorylation (Figure 2.4B). To rule out the possibility of off-target effects of RNAi, we introduced back shRNA-resistant PTEN for rescue experiments. Indeed, expression of shRNA-resistant PTEN in the NEDD4$^{-/-}$ MEFs, consistently prevented rescue of IGF1-induced AKT activation by PTEN shRNA (Figure 2.4C). These data suggested that NEDD4 enabled IGF signaling by suppressing PTEN function.

To determine how NEDD4 regulates PTEN upon IGF1 treatment, first, we tested if IGF1 addition could increase the interaction between NEDD4 and PTEN by co-immunoprecipitation (Co-IP) experiments. Interestingly, endogenous PTEN interacted with endogenous NEDD4 constitutively (Figure 2.5A). To explore the

possible mechanisms by which PTEN regulated IRS1 phosphorylation in a NEDD4-sensitive manner, we tested whether PTEN interacted with IRS1. As shown in Figure 2.5B, S-tagged PTEN interacted with exogenous IRS1 in 293T cells and this interaction was blocked by over-expression of wild-type but not enzymatically inactive NEDD4, suggesting NEDD4 inhibited the interaction between PTEN and IRS1 through its E3 ligase activity.

However, we did not observe changes in gross PTEN protein expression when NEDD4 expression was knocked down in MEFs or when cells were stimulated with IGF1. So what was the precise mechanism by which NEDD4 regulated PTEN in response to IGF/insulin stimulation? Previous systematic analysis of the types of ubiquitin chains showed that NEDD4 in collaboration with E2, UbcH5, formed homogenous chains exclusively Lys63 chains (Kim et al., 2007). So we tested if PTEN polyubiquitination by NEDD4 was through K48 or K63 chain, in vitro PTEN ubiquitination assay. Employing various ubiquitin mutants, we confirm that NEDD4 mainly formed K63-specific polyubiquitination chain on PTEN in vitro (Figure 2.6), suggesting suppression of PTEN by NEDD4 was probably through mechanisms other than proteasomal degradation, which is exclusively mediated through K48 polyubiquitination chains.

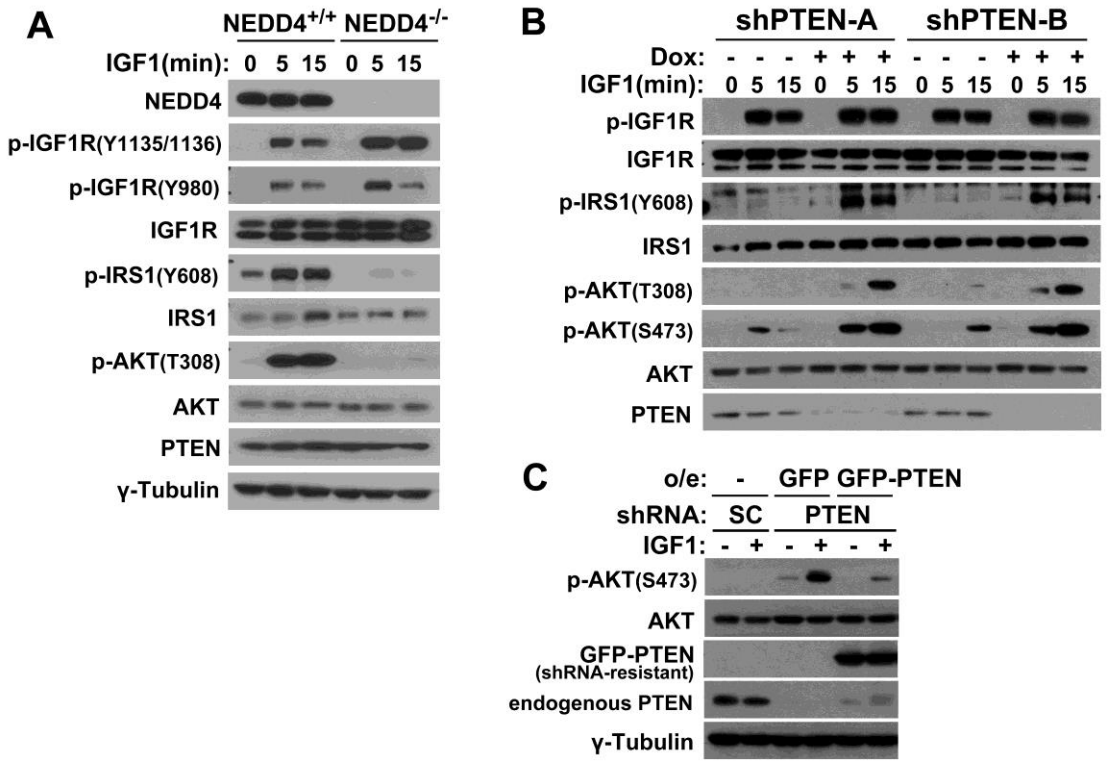

Figure 2.4

NEDD4 functions through PTEN in IGF1 signaling pathway. (A) IGF1-induced AKT and IRS1 phosphorylation, but not IGF1R phosphorylation, is defective in NEDD4$^{-/-}$ MEFs. NEDD4$^{+/+}$ and NEDD4$^{-/-}$ MEFs were serum-starved for 3 hrs, and then stimulated with 50 ng/ml IGF1 for indicated time. Activation of IGF1R, IRS1, and AKT was monitored by using indicated antibodies. (B) Inducible PTEN RNAi restores IGF1 signaling in NEDD4$^{-/-}$ MEFs. NEDD4$^{-/-}$ MEFs harboring inducible PTEN shRNA constructs (shPTEN-A or shPTEN-B) were treated with or without 1 μg/ml Dox for 3 days, serum-starved for 3 hrs, and then stimulated with 50 ng/ml IGF1 for indicated time. (C) shRNA-resistant PTEN counters the effect of PTEN-shRNA in NEDD4$^{-/-}$ MEFs. NEDD4$^{-/-}$ MEFs harboring inducible PTEN shRNA were reconstituted with either GFP or shRNA-resistant GFP-PTEN, and then subjected to serum-starvation followed by 50 ng/ml IGF1 stimulation for 5 min. o/e: overexpression. SC: scramble.

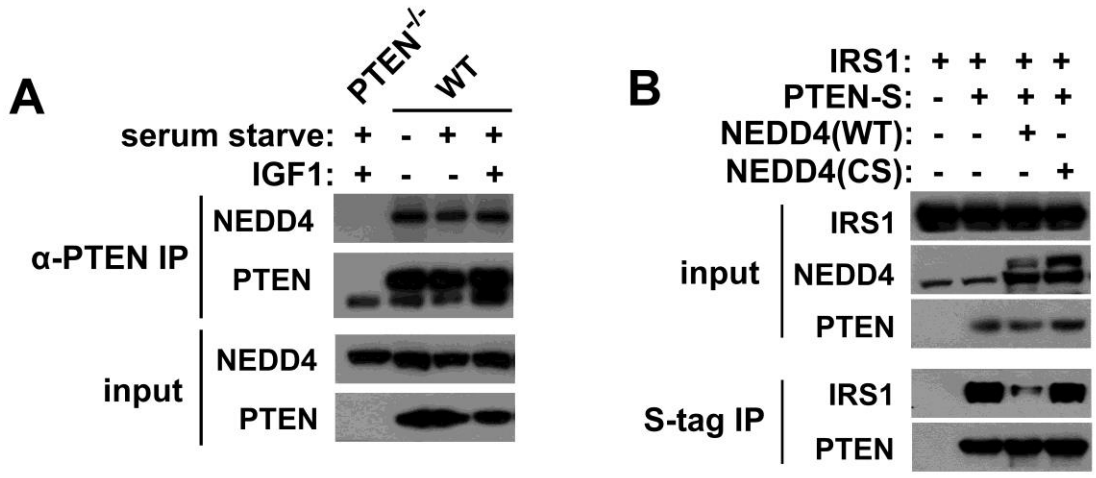

Figure 2.5

NEDD4 inhibits interaction between PTEN and IRS1. (A) PTEN interacts with NEDD4 constitutively in MEFs. WT MEFs were treated as indicated, and then endogenous PTEN was immunoprecipitated by PTEN antibody. (B) NEDD4 inhibits the interaction between PTEN and IRS1 in a NEDD4 E3 ligase activity-dependent manner. 293T cells were co-transfected with vector or S-tagged PTEN (PTEN-S) and indicated NEDD4 plasmids. The cell lysates were immunoprecipitated with S-agarose and followed by immunoblotting for PTEN and IRS1.

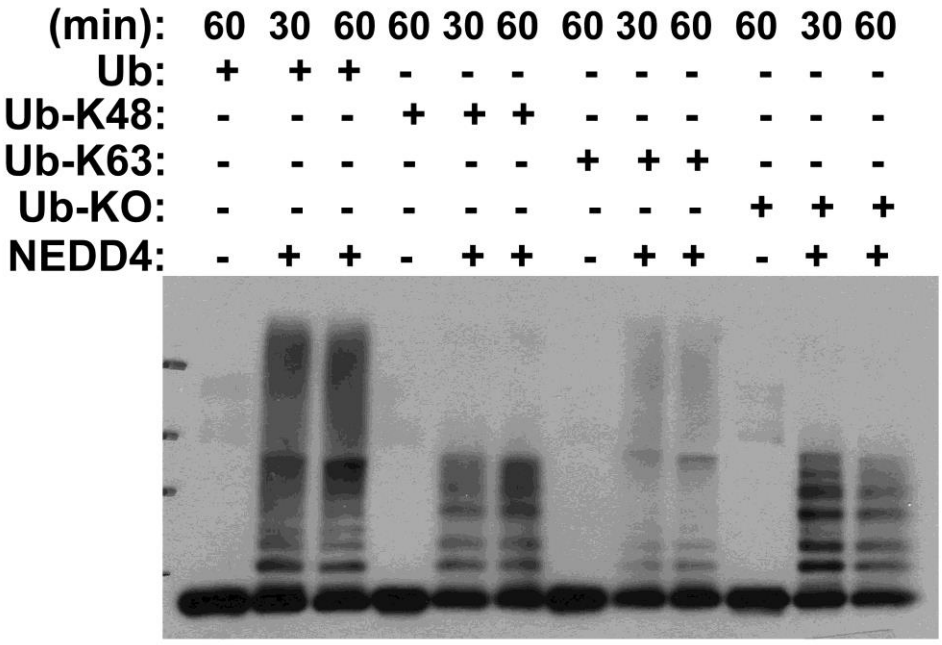

Figure 2.6

NEDD4 forms K63-specific polyubiquitination chain on PTEN. Purified recombinant PTEN protein was mixed with WT or ubiquitin mutants in PTEN ubiquitination assay. Assays were allowed to process for indicated time.

The effect of NEDD4 on the biological function of IGF/insulin signaling

To investigate the impact of NEDD4 on the biological functions of IGF/insulin signaling, we first asked whether the requirement of NEDD4 in IGF1/insulin signaling had any effect on cell growth. Interestingly, we noticed that NEDD4 RNAi in WT MEFs led to decrease in basal IRS1 tyrosine phosphorylation, even though PTEN levels did not change (Figure 2.7A). Some cancer cells require IGF1R activity for the maintenance of proliferation, including the Ewing's sarcoma cell line TC71 and the breast cancer cell line MCF7 (both PTEN-positive). Using pharmacologic inhibitors for IGF1R (OSI-906) and EGFR (erlotinib), we confirmed that IGF1R activity but not EGFR activity was required for maintaining AKT activation in TC71 (Figure 2.7B). By contrast, non-small cell lung cancer cell line PC9 (PTEN-positive), which contained an activating mutant of EGFR, was dependent on EGFR signaling but not IGF1R signaling (Figure 2.7B). Similarly, we validated that IGF1R, but not EGFR, activity was required for maintaining AKT activation in MCF7 (Figure 2.7C). However, breast cancer cell line MDA-MB468 (PTEN-negative) was dependent on neither (Figure 2.7C). Consistently, RNAi knockdown of NEDD4 also blocked AKT activation and upstream IRS1 tyrosine phosphorylation in TC71 (Figure 2.7D). And NEDD4 was dispensable for AKT activation in PC9 cells (Figure 2.7E). NEDD4 RNAi caused a decrease in AKT phosphorylation in MCF7 while MDA-MB-468 did not require NEDD4 expression for AKT activation (Figure 2.7F).

NEDD4 was also selectively required for the proliferation of TC71 cells. In the IGF1R-dependent TC71 cells, NEDD4 knockdown potently reduced cell proliferation (Figure 2.8A), whereas in PC9 cells, NEDD4 knockdown had no discernible effect (Figure 2.8B).

Because insulin signaling was a major physiological regulator of glucose metabolism (Kitamura et al., 2003), NEDD4 could also be involved in glucose metabolism. For this reason, we examined the effect of NEDD4 knockdown on insulin-regulated glucose metabolism in MEFs. As expected, elimination of NEDD4 by Dox-induced RNAi significantly reduced glucose uptake (Figure 2.9A) and associated lactate production (Figure 2.9B), whereas glutamine uptake (Figure 2.9C) and associated glutamate production (Figure 2.9D) were not affected.

Figure 2.7

NEDD4 is required for AKT activation of IGF1R-dependent tumor cells. (A) NEDD4 RNAi effect on basal p-IRS1 in MEFs. (B) AKT activation in TC71 requires IGFR but not EGFR, while AKT activation in PC9 cells requires EGFR but not IGFR. TC71 cells were treated with either 5 μM IGF1Ri or 5 μM EGFRi for 1 hr. PC9 cells were treated with either 5 μM IGF1Ri or 5 μM EGFRi for 24 hrs. (C) The effect of IGF1R inhibitor, EGFR inhibitor on AKT activity in MCF7 and MDA-MB-468 cells. MCF7 and MDA-MB-468 cells were treated with either 5 μM IGF1Ri or 5 μM EGFRi for 3 hrs. (D) Dox-inducible NEDD4 RNAi blocks AKT activation in TC71 cells. (E) Dox-inducible NEDD4 RNAi does not block AKT activation in PC9 cells. NT: non-targeting shRNA. (F) The effect of NEDD4 RNAi on AKT activity in MCF7 and MDA-MB-468 cells.

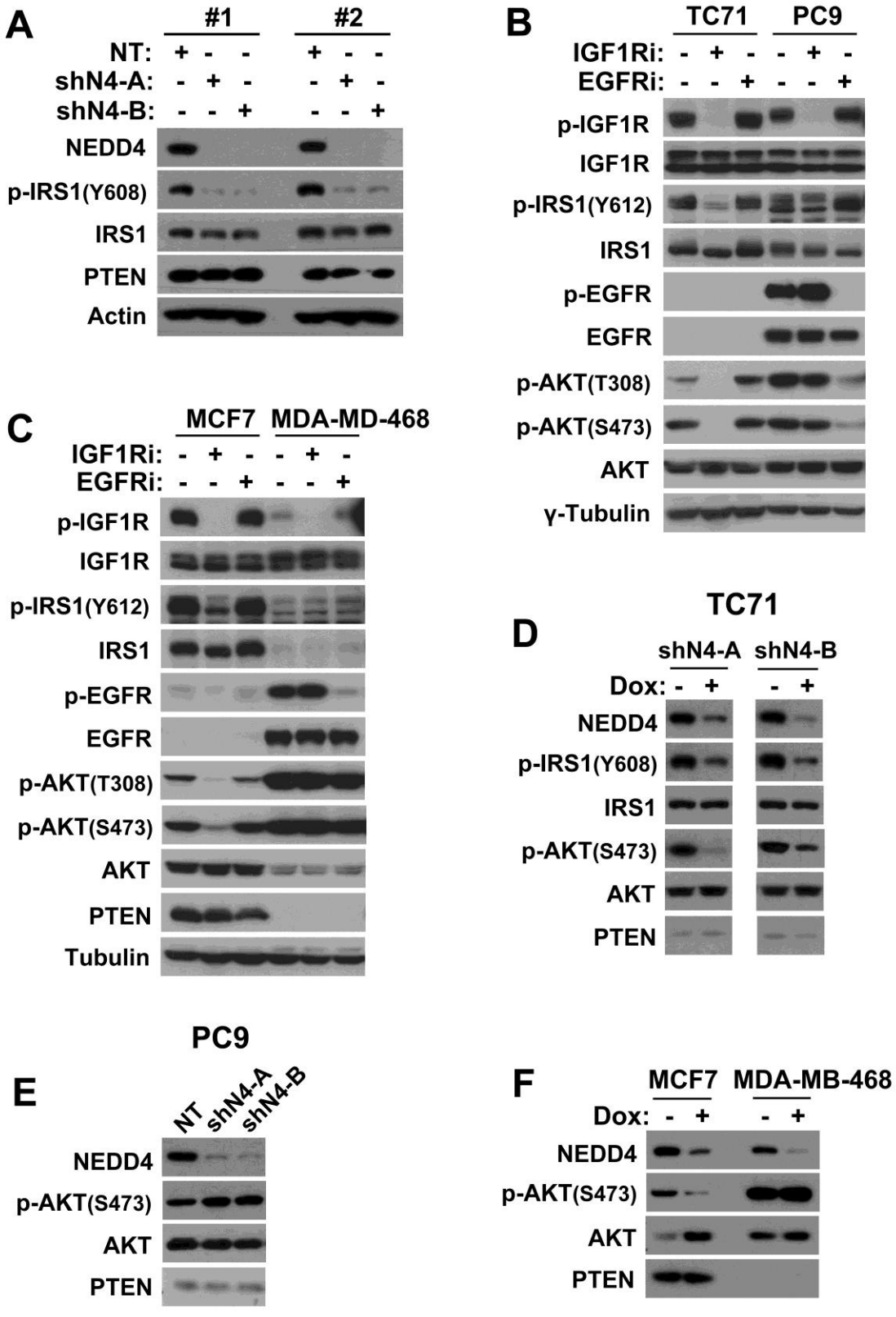
A
#1
#2
NT: + - - + - -
shN4-A: - + - - + -
shN4-B: - - + - - +
NEDD4
p-IRS1(Y608)
IRS1
PTEN
Actin
B
TC71
PC9
IGF1Ri: - + - - + -
EGFRi: - - + - - +
p-IGF1R
IGF1R
p-IRS1(Y612)
IRS1
p-EGFR
EGFR
p-AKT(T308)
p-AKT(S473)
AKT
γ-Tubulin
C
MCF7
MDA-MD-468
IGF1Ri: - + - - + -
EGFRi: - - + - - +
p-IGF1R
IGF1R
p-IRS1(Y612)
IRS1
p-EGFR
EGFR
p-AKT(T308)
p-AKT(S473)
AKT
PTEN
Tubulin
D
TC71
shN4-A
shN4-B
Dox: - + - +
NEDD4
p-IRS1(Y608)
IRS1
p-AKT(S473)
AKT
PTEN
E
PC9
NT
shN4-A
shN4-B
NEDD4
p-AKT(S473)
AKT
PTEN
F
MCF7
MDA-MB-468
Dox: - + - +
NEDD4
p-AKT(S473)
AKT
PTEN

Figure 2.8

NEDD4 is required for growth of IGF1R-dependent tumor cells. (A) Dox-inducible NEDD4 RNAi inhibits proliferation of TC71 cells. TC71 cells expressing indicated shRNA constructs were seeded for cell growth assay and colony formation assay, in the presence of 1μg/ml Dox. (B) Dox-inducible NEDD4 RNAi does not inhibit proliferation of PC9 cells. PC9 cells expressing indicated shRNA constructs were seeded for cell growth assay and colony formation assay in the presence of 1μg/ml Dox.

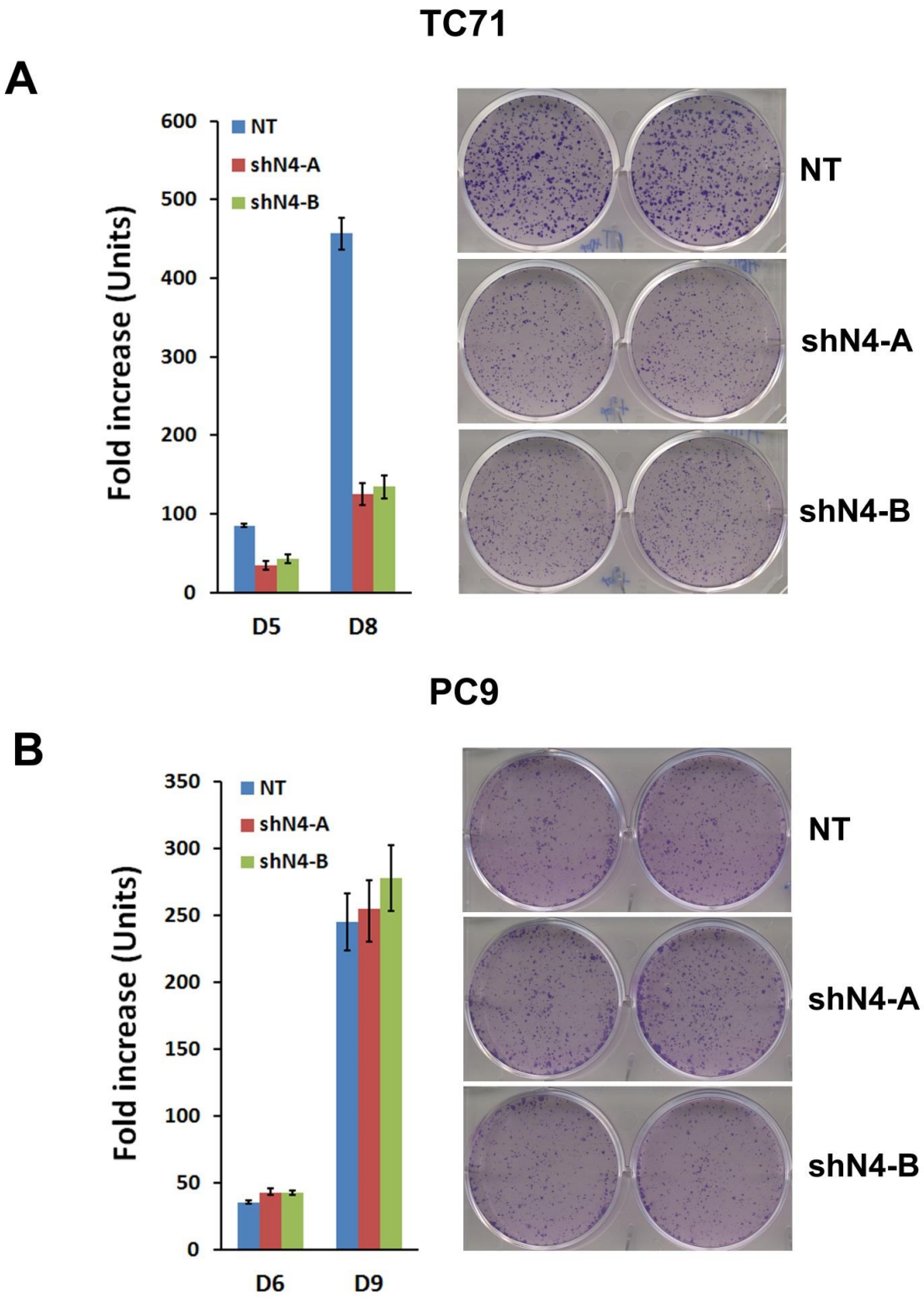
TC71
A
600
500
400
300
200
100
0
NT
shN4-A
shN4-B
Fold increase (Units)
D5
D8
NT
shN4-A
shN4-B
PC9
B
350
300
250
200
150
100
50
0
NT
shN4-A
shN4-B
Fold increase (Units)
D6
D9
NT
shN4-A
shN4-B

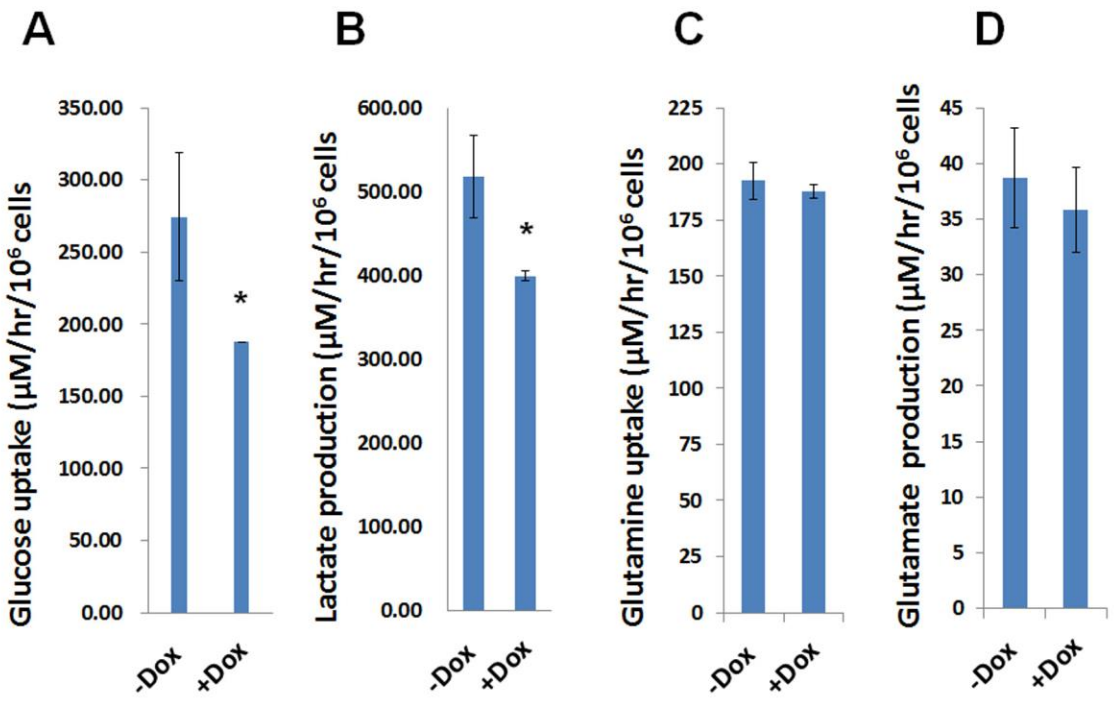

Figure 2.9

NEDD4 regulates insulin-induced glucose metabolism. MEFs harboring Dox-inducible NEDD4 shRNA were cultured in the absence or presence of Dox as indicated. Cells were serum starved for 6 hrs and then incubated in serum-free medium containing 200 ng/ml insulin for 18 hrs. Media were taken from each culturing condition to measure glucose uptake (A), lactate production (B), glutamine uptake (C), and glutamate production (D). Error bars indicate standard deviation from multiple independent experiments ("*": $p<0.05$).

DISCUSSION

In this study, we demonstrated that NEDD4 was specifically required for IGF and insulin signaling, but not EGF or serum signaling. By using inducible-RNAi, we showed that the function of NEDD4 in maintaining IGF1-induced AKT activation was through suppressing PTEN activity. Particularly we pinpointed that NEDD4 blocked the interaction between IRS1 and PTEN, and this was dependent on its ubiquitin E3 ligase activity. Furthermore, the impact of NEDD4 on the biological functions of IGF/insulin signaling was defined by the results that NEDD4 regulated IGF1R-dependent cancer cell growth and insulin-mediated glucose metabolism.

This work is conceptually important for our general understanding of RTK signaling. Diverse growth factors function by activating their corresponding RTKs, which stimulate a variety of downstream signaling programs, including those mediated by PLC, STAT phosphorylation, RAS and PI3K-AKT pathways (Casaletto and McClatchey, 2012). The variety of proliferative RTK pathways might provide differential nodes for regulation. However, the mechanisms that enable specificity of signaling through these pathways and how specific receptors mediate very different biologic effects remains poorly understood. The observation that NEDD4 was specifically required for IGF signaling but not EGF signaling provides mechanistic insights into how various RTK pathways could be distinctly regulated even though they all function through common downstream effector molecules. Interestingly, IGF1R and Insulin Receptor require adaptor IRS proteins to mediate the binding to downstream effectors, unlike other RTKs which bind directly to downstream effectors

(Taniguchi et al., 2006). The specific requirement of NEDD4 in IGF and Insulin signaling could be attributed to the effects of NEDD4 on IRS1 tyrosine phosphorylation.

By inhibiting the activity of PTEN, NEDD4 could contribute to the effects of insulin and IGFs on multiple important physiological processes, including growth, metabolism, and glucose homeostasis (Engelman et al., 2006). Further, because NEDD4 has other protein substrates such as RNA polymerase II (Anindya et al., 2007), Cbl-b (Yang et al., 2008), and Activated Cdc42-associated tyrosine kinase (Lin et al., 2010), this ubiquitin ligase might possess additional biological functions independent of PTEN or IGF/insulin signaling (Persaud et al., 2009). Very recently, NEDD4 was reported to interact, ubiquitinate and degrade Ras, playing a role in Ras-driven tumorigenesis (Zeng et al., 2014). This might help explain why NEDD4 was not required for proliferation of EGFR-dependent cancer cell lines.

It has been reported that NEDD4 deficiency leads to the internalization and degradation of IGF1R or insulin receptors, hours after agonist stimulation (Cao et al., 2008). While such a NEDD4-regulated receptor desensitization mechanism might play a role in the later stages of IGF/insulin signaling, it does not provide an explanation for the involvement of PTEN, neither does it account for the rapid inhibition of IRS1 and AKT activation by NEDD4 elimination, which could be observed as early as 5 min after agonist stimulation. Further, NEDD4 elimination only blocked activation of IRS1 and AKT but not that of IGF1R or insulin receptor, indicating that even in the

absence of NEDD4, receptors were available on the cell surface for activation by their agonists at early time points.

However, the precise mechanism by which NEDD4 regulated PTEN in response to IGF/insulin stimulation was not clear at this stage. We did not observe any changes in total PTEN protein level when NEDD4 expression was knocked down in MEFs or when cells were treated with IGF1 or insulin. One possibility is that only a small subpopulation of total PTEN is required to suppress IGF signaling, and that NEDD4 selectively antagonizes this sub-fraction. In line with this possibility, it was recently reported that NEDD4 preferentially ubiquitinates membrane-localized PTEN, and that PTEN ubiquitination is sufficient to suppress its phosphatase activity even in the absence of proteasomal degradation (Maccario et al., 2010). It is also possible that insulin-stimulated production of reactive oxygen species (ROS) could contribute to this process, as PTEN modified by ROS has been shown to be a better substrate for NEDD4 (Kwon et al., 2004). Furthermore, a recent paper reported that NEDD4 mediates K63-specific polyubiquitination on PTEN during T cell activation and lysine 13 was the major ubiquitination site for PTEN (Guo et al., 2012). We also showed that NEDD4 forms K63-specific, and not K48-specific, polyubiquitination chains on PTEN in vitro. Therefore, we hypothesize that IGF stimulus promotes PTEN K-63 polyubiquitination, subsequently inhibiting PTEN activity.

CHAPTER THREE

PTEN IS A PROTEIN TYROSINE PHOSPHATASE FOR IRS1*

INTRODUCTION

PTEN is a physiological lipid (PIP3) phosphatase but may also possess protein phosphatase activity. The protein tyrosine phosphatase activity of PTEN has been suggested based on its domain structure (Lee et al., 1999; Li and Sun, 1997) and on the observation that PTEN could dephosphorylate synthetic phosphor-tyrosine peptides (Myers et al., 1997). Additionally, it has been suggested that such protein phosphatase activity may be relevant to various functions of PTEN, such as cell migration and invasion (Maier et al., 1999; Tamura et al., 1999; Tibarewal et al., 2012; Zhang et al., 2012). However, no phosphoprotein substrates of PTEN have been conclusively identified in vivo. Therefore, whether PTEN is a physiologically relevant protein phosphatase remains an open question.

In MCF7 breast cancer cells, overexpression of WT PTEN resulted in general inhibition of AKT activation stimulated by various growth factors, but selective inhibition of MEK/ERK phosphorylation induced by insulin and IGF1(Weng et al., 2001). These data suggested that PTEN could block insulin-stimulated IRS1 phosphorylation and IRS1/Grb2/Sos complex formation. Interestingly, loss of PTEN correlated specifically with a suppression of IGF1/insulin signaling in a number of cell

*: citation 4

lines, but had no effect on platelet-derived growth factor (PDGF) or EGF signaling (Lackey et al., 2007). This phenotype could be partially explained by reduced protein levels of IRS1, IGF1R and insulin receptor.

Our previous studies in chapter one showed that PTEN could interact with IRS1 and regulated IRS1 tyrosine phosphorylation. Using biochemical and cellular studies, we tested if IRS1 was a direct protein substrate of PTEN.

RESULTS

PTEN is a protein tyrosine phosphatase for IRS1 in vitro

To address this question, we engineered WT MEFs expressing PTEN shRNA, and then reconstituted these cells by expressing RNAi-resistant GFP-S-tagged wild-type (WT) PTEN, C124S (CS) mutant PTEN, or G129E (GE) mutant PTEN. CS mutant PTEN is defective in total enzymatic activity, while GE mutant PTEN cannot dephosphorylate lipid substrates, such as PIP3, but maintains protein phosphatase activity, and can still dephosphorylate synthetic peptides containing phospho-tyrosine. As shown in Figure 3.1A, PTEN RNAi caused a substantial increase of basal p-AKT, and introducing back WT PTEN, but not CS or GE mutants, inhibited the elevation of pAKT. This conclusion was also validated in cells with EGF treatment. WT PTEN but not the CS or GE mutants could inhibit EGF-induced AKT phosphorylation (Figure

3.1B). This conclusion was further validated in cells lacking PTEN: WT PTEN but not the CS or GE mutants could inhibit cellular PIP3 production in PTEN-negative PC3 cells (Figure 3.1C).

We generated purified recombinant WT PTEN protein, CS PTEN mutant protein, and GE PTEN mutant protein (Figure 3.2A). Their lipid phosphatase activities were confirmed by an in vitro lipid assay that confirmed WT PTEN, but not the CS or GE mutants, could dephosphorylate PIP3, even though the concentrations of CS or GE mutant proteins were 100 times that of WT PTEN (Figure 3.2B). We then generated phospho-IRS1 substrate by overexpressing HA-tagged IRS1 and HA-tagged IGF1R in 293 cells and subsequently treating the cells with IGF1. The IRS1 substrates were isolated by immuno-precipitation. When the isolated IRS1 was incubated with recombinant PTEN, we observed dephosphorylation of IRS1 in a PTEN dose-dependent manner, as monitored with a specific antibody against pY608 of IRS1 (Figure 3.2C). This activity could be blocked by a general protein phosphatase inhibitor cocktail (Y inhibitor). Dephosphorylation of IRS1 was a property of the GE mutant but not the CS mutant (Figure 3.2D). The IRS1 protein tyrosine phosphatase activity of PTEN could also be detected using the pY989-specific IRS1 antibody and a general phospho-tyrosine antibody. Importantly, in these experiments, we found that the protein phosphatase activity of PTEN was specific for phospho-IRS1 and that phosphorylation status of IGF1R (both Y1135/1136 and Y980 sites) was not affected by PTEN (Figure 3.2C, D).

To further disentangle the lipid and protein phosphatase activities of PTEN, we also generated recombinant protein (Figure 3.3) with a recently reported PTEN mutation, Y138L(YL), possessing lipid but not protein phosphatase activity (Davidson et al., 2010). Indeed, the YL mutant could not dephosphorylate IRS1 in vitro (Figure 3.3). However, unlike the GE or CS mutants, the YL mutant did possess lipid phosphatase activity, but this activity was considerably lower than that of WT PTEN (Figure 3.3).

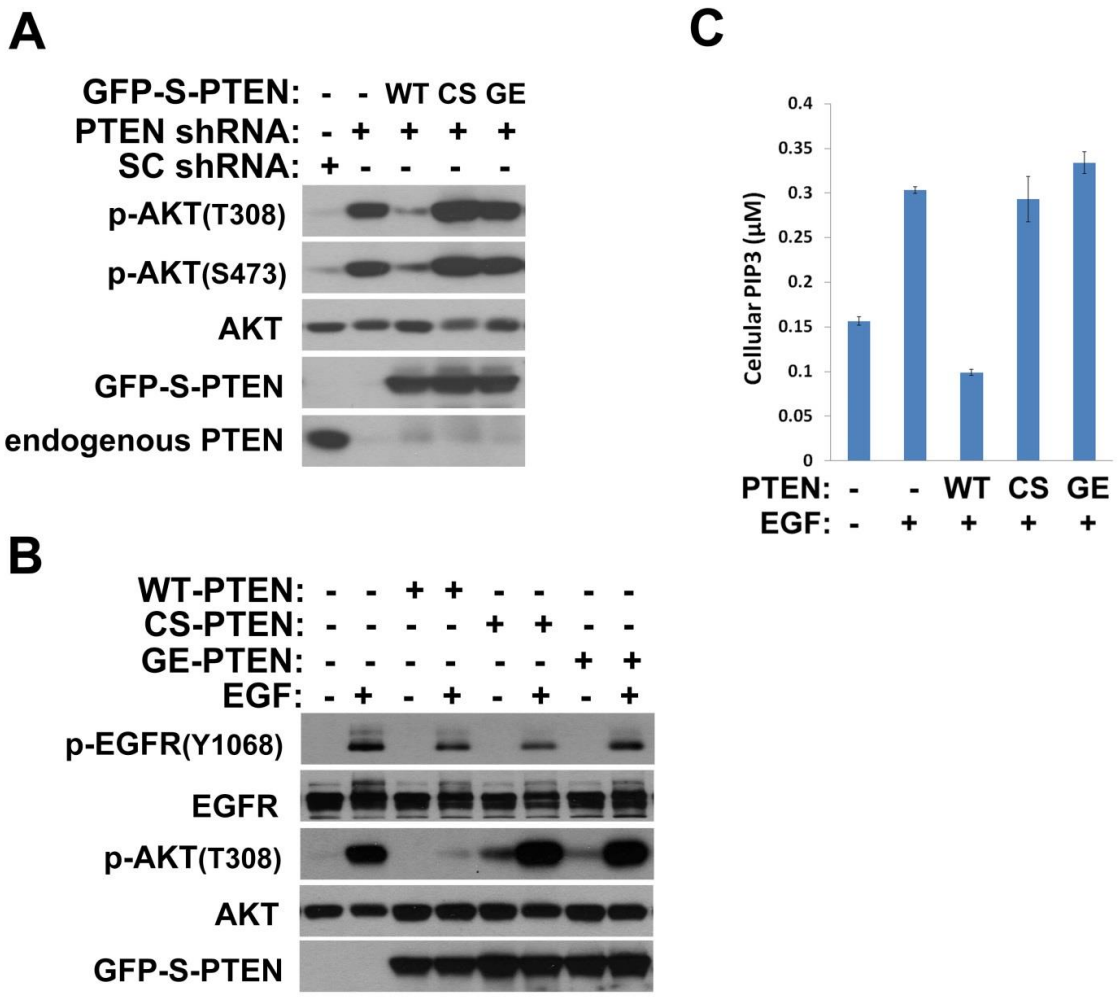

Figure 3.1

WT PTEN but not the CS or GE mutant has lipid phosphatase activity. (A) Validation of PTEN shRNA MEFs reconstituted with GFP-S-tagged PTEN (WT/CS/GE). (B) WT PTEN but not the CS or GE mutant can inhibit EGF-induced AKT activation. GFP-S-tagged PTEN (WT/CS/GE) was overexpressed in MEFs with stable PTEN shRNA. Cells were serum starved for 3 hrs and then treated with 100 ng/ml EGF for 5 min. (C) WT PTEN but not the CS or GE mutant PTEN can inhibit EGF-induced cellular PIP3 generation. GFP-S-tagged PTEN (WT/CS/GE) was overexpressed in PTEN negative PC3 cells. Cells were serum starved for 6 hrs and then treated with 100 ng/ml EGF for 5 min. Cellular PIP3 concentration was measured as described in methods.

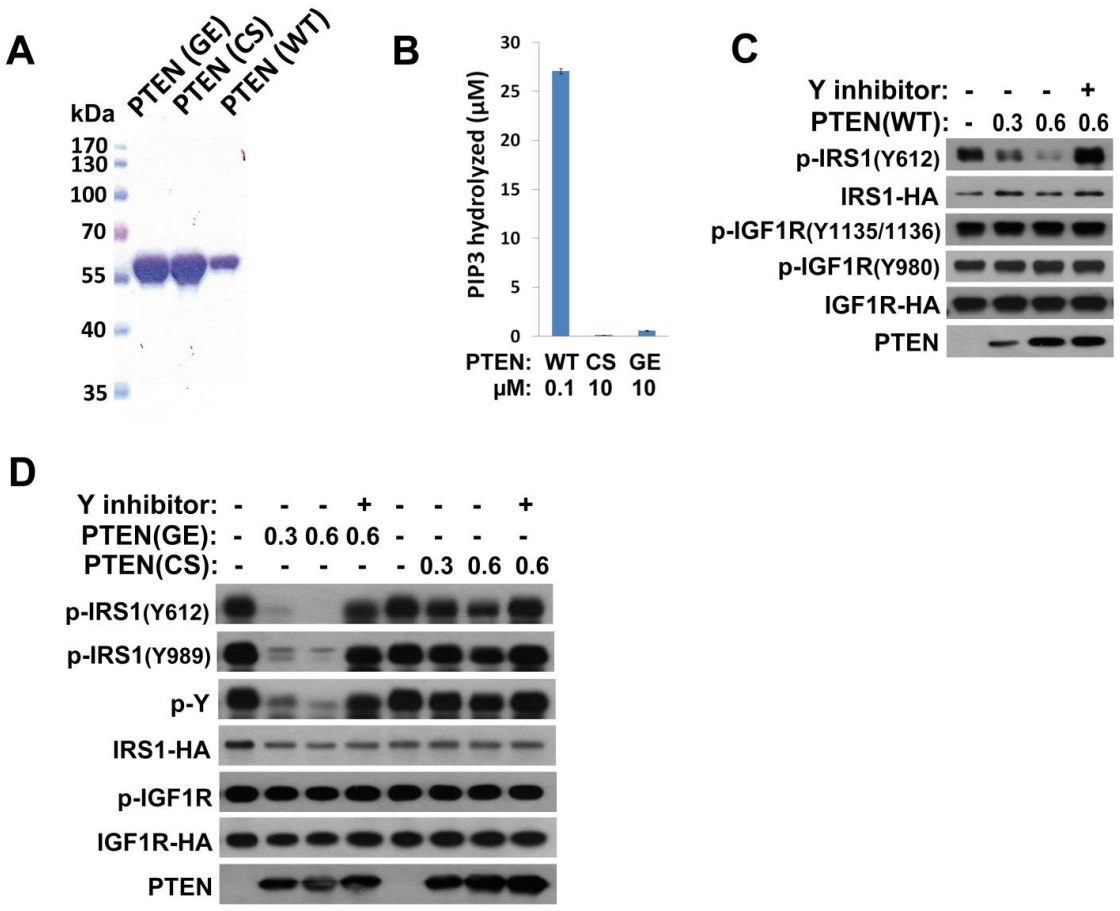

Figure 3.2

PTEN is a protein phosphatase for IRS1 in vitro. (A) Coomassie blue gel showing purified recombinant PTEN proteins. WT: wild-type; CS: C124S mutant; GE: G129E mutant. (B) WT PTEN but not the CS or GE mutant dephosphorylates PIP3. The assay was performed as described in Methods. 40 μM PIP3 and 0.1 μM PTEN (WT), 10 μM PTEN (CS) and 10 μM PTEN (GE) proteins were used in the assay. (C) WT-PTEN dephosphorylates IRS1 but not IGF1R. HA-IRS1 and HA-IGF1R were co-expressed in 293 cells, and cells were treated with IGF1 to trigger their phosphorylation. IRS1 and IGF1R were immunoprecipitated from cell lysates by HA-antibody, and were subsequently incubated with recombinant PTEN (WT) protein (0.3 or 0.6 μM, as indicated) with or without phosphatase inhibitor cocktail (Y inhibitor) for 1 hr at 30^{o}C. (D) GE but not CS mutant PTEN can dephosphorylate IRS1 but not IGF1R. Immunoprecipitated IRS1 and IGF1R were incubated with recombinant PTEN (GE or CS mutant) protein (0.3 or 0.6 μM) with or without phosphatase inhibitor cocktail (Y inhibitor) for 1 hr at 30^{o}C.

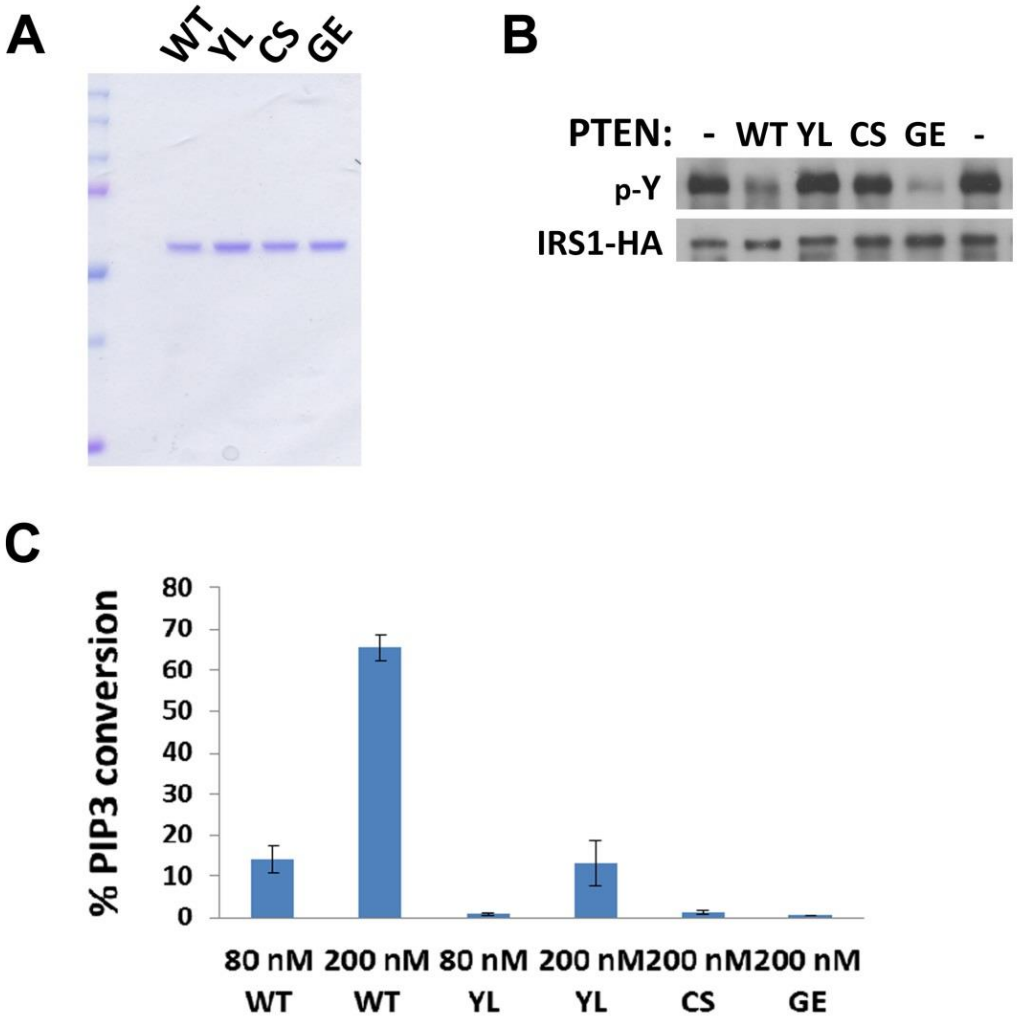

Figure 3.3

Characterization of recombinant PTEN protein in lipid and protein phosphatase assays. (A) Coomassie blue gel showing purified recombinant PTEN proteins. WT: wild-type; YL: Y138L mutant; CS: C124S mutant; GE: G129E mutant. (B) WT-PTEN or GE but not YL or CS mutant can dephosphorylate IRS1. Immunoprecipitated IRS1 was incubated with recombinant PTEN (WT, YL GE or CS mutant) protein (0.6 μM) for 1 hr at 30^{o}C. (C) Comparing PTEN (WT or mutants) activity in a lipid phosphatase assay. The assay was performed similar to that in Figure 3.2B, with 40 μM PIP3 and PTEN (WT/YL/CS/GE) proteins of indicated concentrations.

PTEN is a protein tyrosine phosphatase for IRS1 in cells

Given the data that purified PTEN was an IRS1 phosphatase, we sought to determine whether it also functioned as a NEDD4-suppressed IRS1 phosphatase in cells. In cellular reconstitution experiments, we blocked IGF1 induction of IRS1 phosphorylation with Dox-inducible NEDD4 RNAi, and restored IRS1 phosphorylation by knocking down PTEN expression (Figure 3.4A). After induction of NEDD4 RNAi with Dox, IGF1-induced phosphorylation of IRS1 and AKT was greatly reduced in the PTEN-RNAi cells in which wild-type PTEN was re-expressed (Figure 3.4B), but not reduced in the PTEN-RNAi cells in which CS mutant PTEN was re-expressed (Figure 3.4C). Similar to wild-type PTEN, after induction of NEDD4 RNAi with Dox, IGF1-induced phosphorylation of IRS1 and AKT was greatly reduced in the PTEN-RNAi cells in which GE mutant PTEN was re-expressed (Figure 3.4D). Effects of wild-type PTEN or PTEN mutants on NEDD4-mediated IRS1 phosphorylation were also quantified in Figure 3.4E, demonstrating the reproducibility of the experiments.

These data demonstrate that PTEN acts as an IRS1 phosphatase in cells and that this activity is dependent on the protein phosphatase activity but not PIP3 phosphatase activity of the enzyme. In these cells, the effect of PTEN on IGF-induced IRS1 phosphorylation could be detected by using antibodies specific to both pY608 site and pY989 site of IRS1 (Figure 3.5), which was consistent with our in vitro observations.

The result that the PIP3 phosphatase-defective GE mutant could also reduce IRS1 phosphorylation, like WT PTEN, indicated that the effect of PTEN on IRS1 phosphorylation was not likely through indirect feedback regulation caused by the change of downstream PIP3 level or AKT activity. To further rule out the possible feedback mechanisms caused by PIP3/AKT changes, we performed similar experiments in the presence of a pharmacological inhibitor of PI3K (GDC0941). This inhibitor prevented IGF1-induced PIP3 generation, as demonstrated by the lack of downstream AKT activation, although the upstream phosphorylation of IGF1R or IRS1 remained intact (Figure 3.6A). In the presence of the inhibitor, Dox-induced NEDD4 RNAi ablated IGF1-induced IRS1 phosphorylation in PTEN-knockdown cells only when PTEN was re-expressed in the cells (Figure 3.6B). While in the absence of PTEN expression, and in the presence of the PI3K inhibitor, Dox-induced NEDD4 RNAi could not ablate IGF1-induced IRS1 phosphorylation (Figure 3.6C).

To demonstrate the specificity of the regulation of NEDD4-PTEN on IGF signaling, we did similar experiments with serum or EGF treatment (Figure 3.7). Generally, serum-induced AKT activation was not affected, while NEDD4 knockdown led to elevated EGFR phosphorylation, but little change in p-AKT level upon EGF treatment.

Figure 3.4

PTEN is a protein phosphatase for IRS1 in cells. (A) When PTEN expression is knocked down, IGF1 can induce IRS1 phosphorylation in the absence of NEDD4. MEFs harboring inducible NEDD4 shRNA (with or without Dox treatment as indicated) were subjected to transient PTEN knockdown and followed by serum-starvation and then 50 ng/ml IGF1 stimulation. (B) Re-expressing wild-type PTEN blocked IGF1-induced IRS1 phosphorylation in NEDD4-RNAi/PTEN-RNAi MEFs. MEFs as in panel A were reconstituted with shRNA-resistant GFP-S-PTEN (WT) by transient retroviral infection and subjected to the same treatment as in panel A. (C) Re-expressing the CS mutant of PTEN cannot block IGF1-induced IRS1 phosphorylation in NEDD4-RNAi/PTEN-RNAi MEFs. (D) Re-expressing the GE mutant of PTEN can block IGF1-induced IRS1 phosphorylation in NEDD4-RNAi/PTEN-RNAi MEFs. (E) Quantification of the effect of PTEN (WT or indicated mutants, as in Panel a-d) on NEDD4-mediated IRS 1phosphorylation. Each pIRS1 signal on western blots was quantitated by densitometer and normalized by total IRS1 signal. The ratio of pIRS1 (+ DOX, thus in the absence of NEDD4 expression) versus pIRS1 (- DOX) was plotted for specific conditions as indicated. Error bars show s.e.m. from four independent experiments.

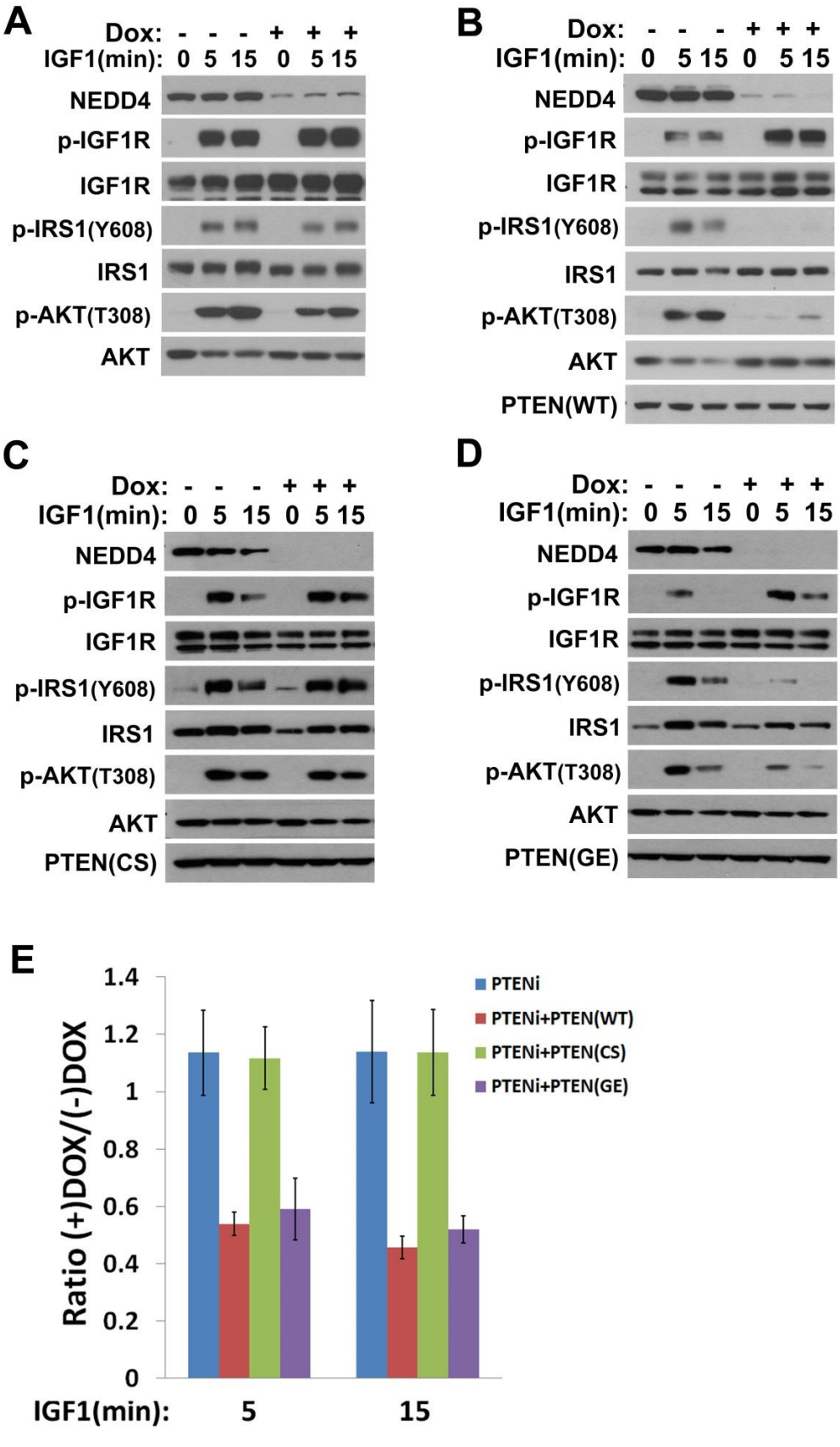
A
Dox: - - - + + +
IGF1(min): 0 5 15 0 5 15
NEDD4
p-IGF1R
IGF1R
p-IRS1(Y608)
IRS1
p-AKT(T308)
AKT
B
Dox: - - - + + +
IGF1(min): 0 5 15 0 5 15
NEDD4
p-IGF1R
IGF1R
p-IRS1(Y608)
IRS1
p-AKT(T308)
AKT
PTEN(WT)
C
Dox: - - - + + +
IGF1(min): 0 5 15 0 5 15
NEDD4
p-IGF1R
IGF1R
p-IRS1(Y608)
IRS1
p-AKT(T308)
AKT
PTEN(CS)
D
Dox: - - - + + +
IGF1(min): 0 5 15 0 5 15
NEDD4
p-IGF1R
IGF1R
p-IRS1(Y608)
IRS1
p-AKT(T308)
AKT
PTEN(GE)
E
Ratio (+)DOX/(-)DOX
1.4
1.2
1
0.8
0.6
0.4
0.2
0
IGF1(min): 5 15
PTENi
PTENi+PTEN(WT)
PTENi+PTEN(CS)
PTENi+PTEN(GE)

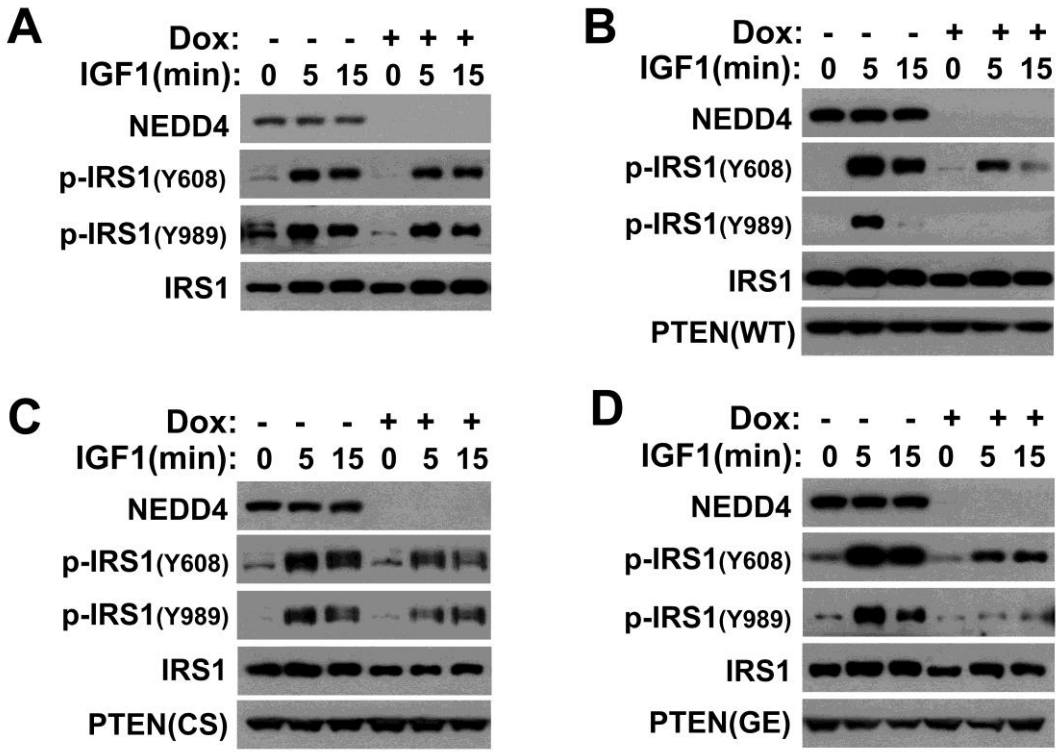

Figure 3.5

WT and GE mutant, but not CS mutant, PTEN can dephosphorylate the phospho-tyrosine 989 site of IRS1 in cells. The experiments were performed the same as that in Figure 3.4 except that both p-IRS1 (Y608) and p-IRS1 (Y989) were assessed here.

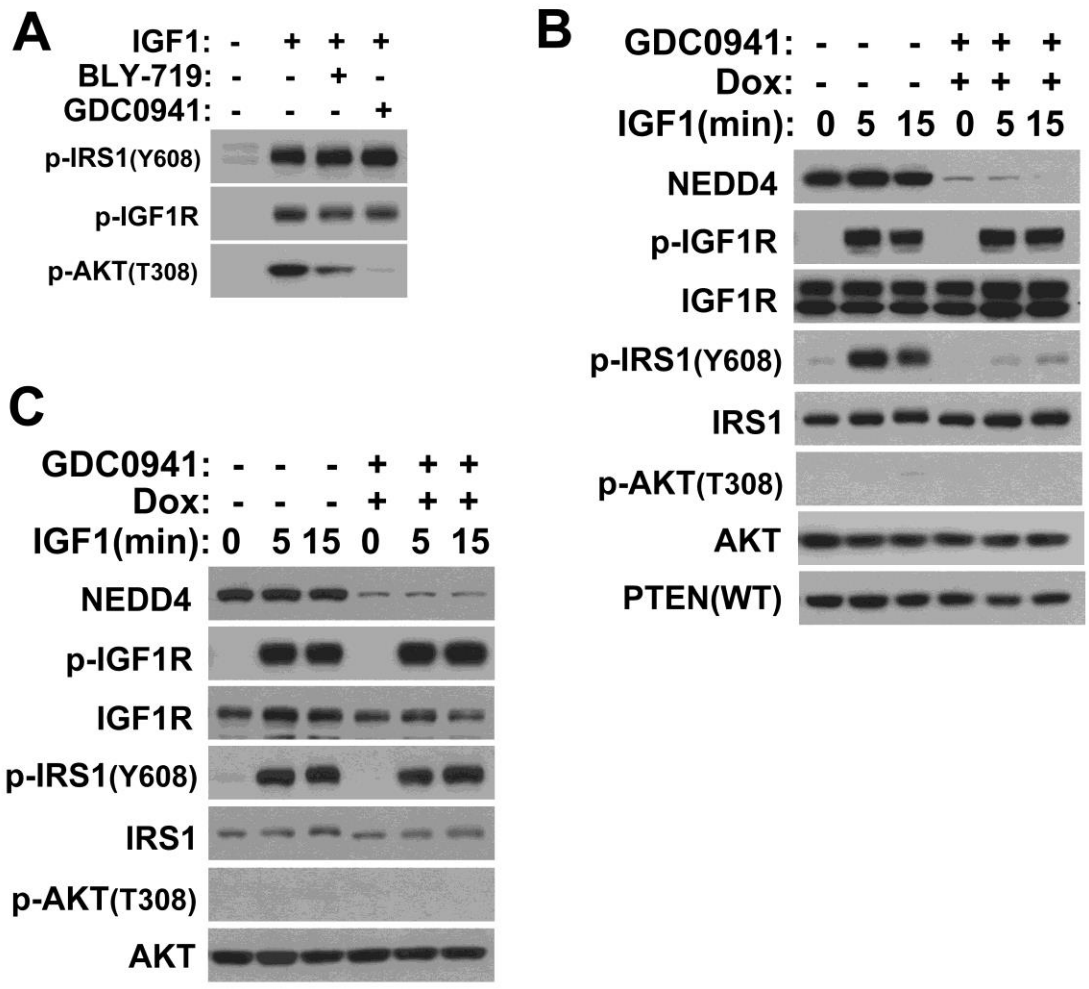

Figure 3.6

PI3K inhibitor does not affect the PTEN function as IRS1 protein phosphatase. (A) PI3K inhibitors block IGF1-induced phosphorylation of AKT but not that of IGF1R or IRS1. WT MEFs were pretreated for 1 hr with either 2 μM BYL-719 or 1 μM GDC0941, followed by 50 ng/ml IGF1 for 10 min. (B) PI3K inhibitor (GDC0941) does not affect the function of wild-type PTEN on IGF1-induced IRS1 phosphorylation in NEDD4-RNAi/PTEN-RNAi MEFs. (C) PI3K inhibitor (GDC0941) has no effect on IGF1-induced IRS1 phosphorylation in NEDD4-RNAi/PTEN-RNAi MEFs.

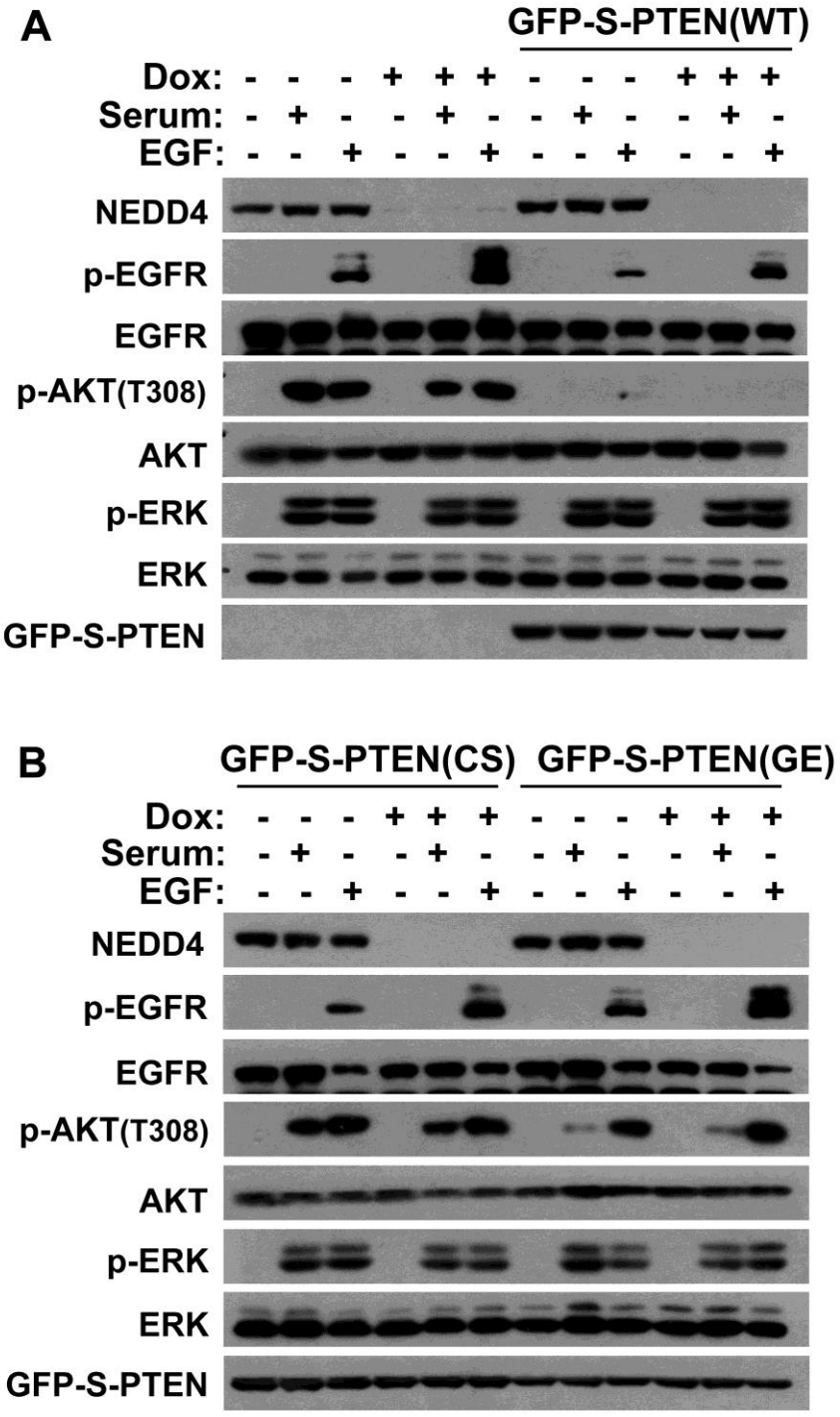

Figure 3.7

NEDD4 RNAi has no inhibitory effect on EGF signaling. (A) Re-expressing wild-type PTEN does not block EGF signaling in NEDD4-RNAi/PTEN-RNAi MEFs. (B) Re-expressing the CS or GE mutant of PTEN cannot block EGF signaling in NEDD4-RNAi/PTEN-RNAi MEFs.

It should be noted that, in these cellular experiments, we used transient PTEN knockdown because, as we and other have previously demonstrated, permanent PTEN loss causes a marked decrease in IGF1R expression and thus deficiency of IGF signaling, and AKT inhibition increases IGF1R expression by relieving feedback inhibition of FOXO (Chandarlapaty et al., 2011; Qin et al., 2011). As shown in Figure 3.8, both genetic deletion of PTEN gene and long-term, stable PTEN shRNA caused a decline in IGF1R levels. Indeed, treating $PTEN^{-/-}$ MEFs or PTEN-shRNA MEFs with an AKT inhibitor enhanced IGF1R expression (Figure 3.8A, B). Re-expressing wild-type but not CS or GE mutant PTEN could also restore IGF1R expression in $PTEN^{-/-}$ MEFs but had no effect on EGFR levels (Figure 3.8C). Nevertheless, AKT inhibition by AKTi increased IGF1R to similar level in all the cell lines. Consistent with such feedback regulation, stable knockdown of PTEN only minimally enhanced IRS1 phosphorylation in $NEDD4^{-/-}$ MEFs, although it substantially restored IGF1-induced AKT activation, presumably by suppressing the PIP3 phosphatase activity of PTEN (Figure 3.8D).

To better understand the mechanism of how PTEN regulates IRS1, we mapped domains for the interaction between PTEN and IRS1. PTEN contains multiple domains, including an N-terminal phosphatase domain, a central C2 domain and a C-terminal tail. The C-terminal tail is a long flexible fragment that is mainly involved in PTEN regulation (Lee et al., 1999). So we generated a series of PTEN truncation fragments and tested their interaction with IRS1, indicating C2 domain is necessary and sufficient for interaction (Figure 3.9A). IRS1 has both PH domain and PTB

domains near the N terminus. The central and C terminus of the IRS proteins contain up to 20 potential tyrosine-phosphorylation sites that, after phosphorylation by the IR, bind to intracellular molecules that contain SH2 domains (Copps and White, 2012). Preliminary truncation studies revealed that the N-terminal of IRS1 was required for binding to PTEN (Figure 3.9B).

Taken together, these results reveal the novel function of PTEN as a protein phosphatase for IRS1, as well as mechanisms underlying specific regulation of IGF signaling by PTEN and NEDD4 (see Figure 3.10 for a model). It has been a long-standing debate concerning whether PTEN is a biologically relevant protein phosphatase. Thus, our demonstration of the biochemical nature of PTEN as both a protein and lipid phosphatase is significant. Additionally, until now, the biochemical effects of PTEN in PI3K signaling have been completely ascribed to its lipid phosphatase activity. Through this work, we have now obtained evidence showing that PTEN is a protein phosphatase and can down-regulate PI3K signaling in a least two ways: generally by decreasing PIP3 levels, and in a manner specific to IGF/insulin signaling, by dephosphorylating IRS1.

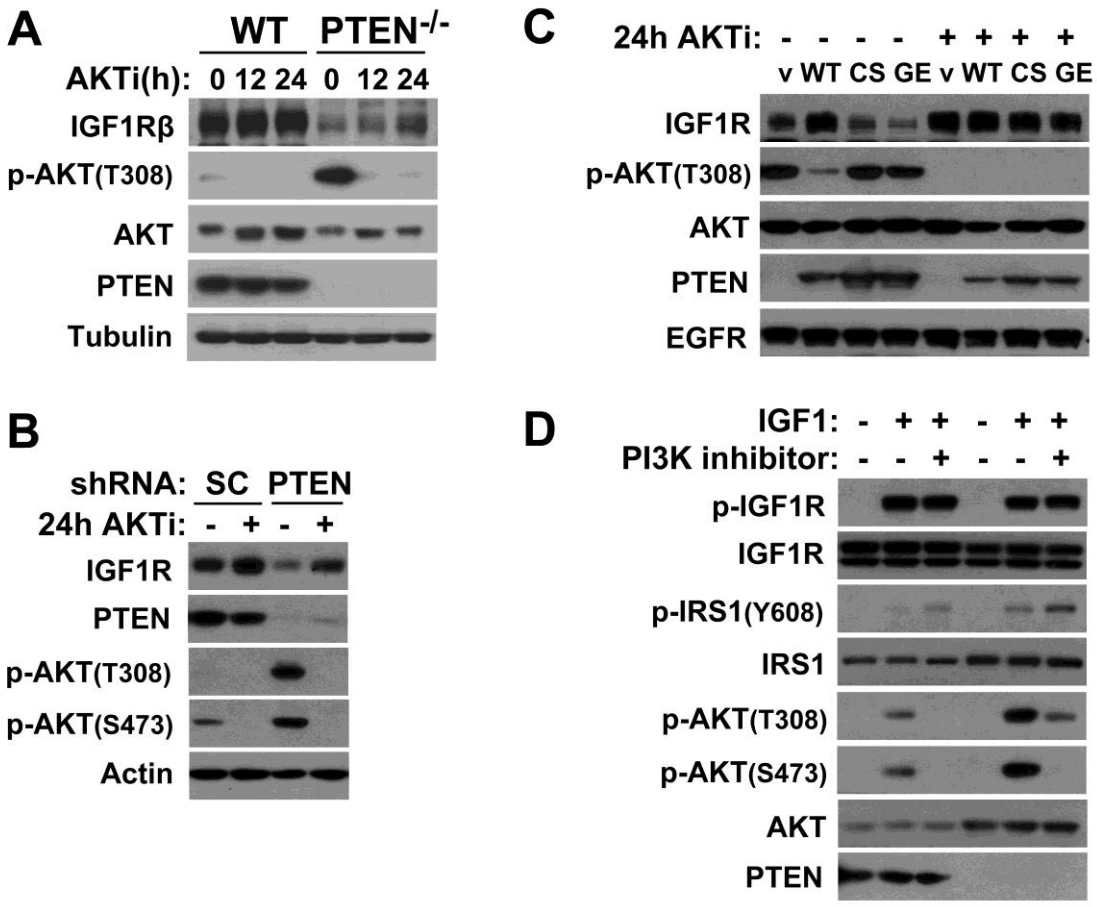

Figure 3.8

PTEN and AKT regulate IGF1R expression via feedback mechanism. (A) PTEN$^{-/-}$ MEFs express lower levels of IGF1R which can be increased by AKT inhibition. WT or PTEN$^{-/-}$ MEFs were treated with 1 μM AKTi for 12 or 24 hrs. (B) MEFs harboring long-term PTEN shRNA have decreased IGF1R expression, which can be reversed by AKT inhibition. (C) Expression of wild-type but not CS or GE mutant PTEN increased IGF1R expression in PTEN$^{-/-}$ MEFs. PTEN$^{-/-}$ MEFs were reconstituted with GFP or GFP-S-PTEN (WT/CS/GE), and treated with or without 1 μM AKTi for 24 hrs. (D) Stable PTEN shRNA restored IGF1-induced AKT activation in NEDD4$^{-/-}$ MEFs but had minimal effect on IRS1 phosphorylation. NEDD4$^{-/-}$ MEFs with control knockdown or stable PTEN knockdown were serum-starved, and then stimulated with 50 ng/ml IGF1 for 5 min, with or without 1 μM PI3K inhibitor.

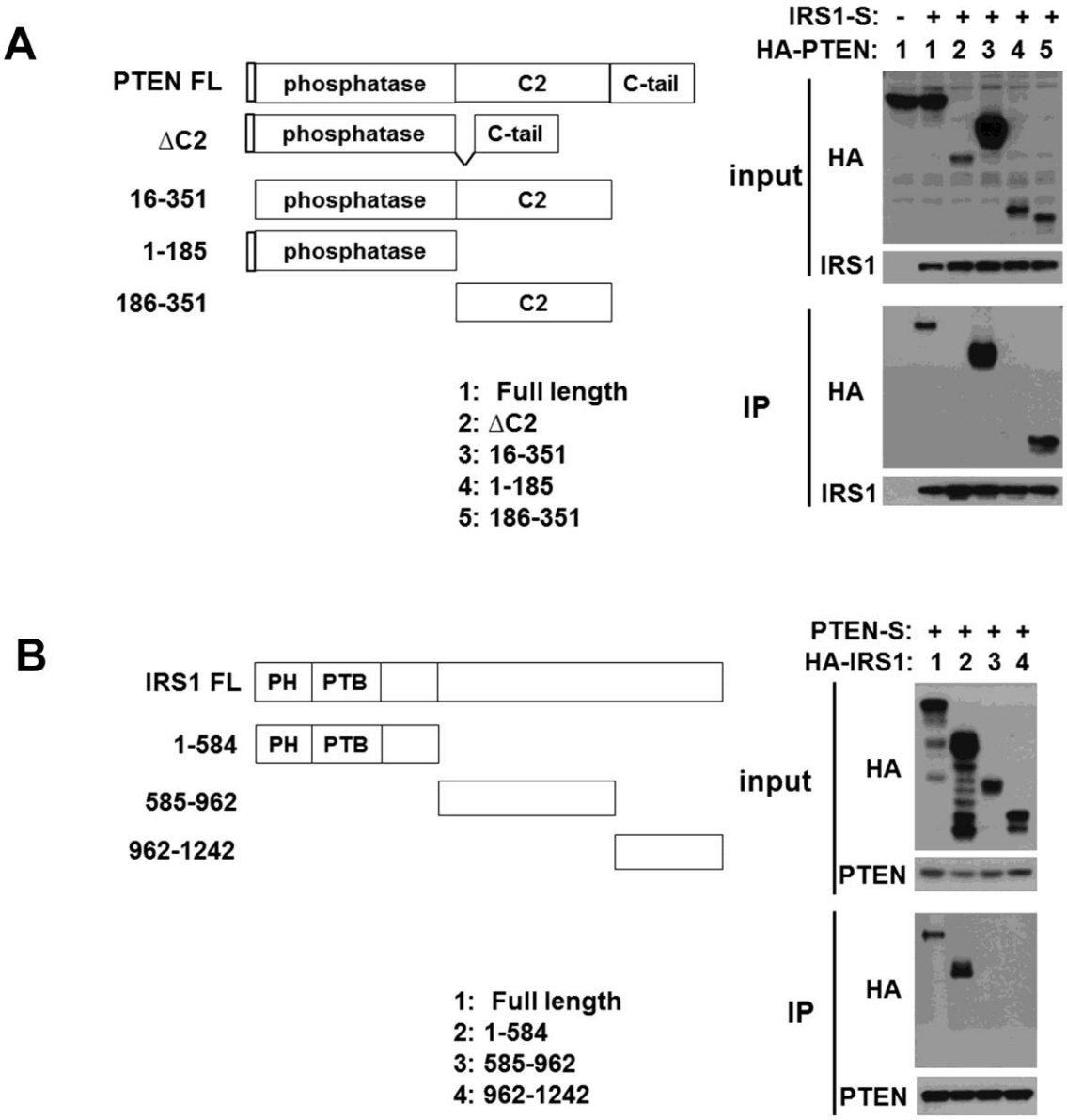

Figure 3.9

Domain mapping for interaction between PTEN and IRS1. (A) Schematic of PTEN fragments. 293T cells were transfected with S-tagged IRS1 and indicated PTEN fragments. Cell lysates were immunoprecipitated by S-protein agarose and followed by immunoblotting for PTEN and IRS1. (B) Schematic of IRS1 fragments. 293T cells were transfected with S-tagged PTEN and indicated IRS1 fragments. Cell lysates were immunoprecipitated by S-protein agarose followed by immunoblotting for PTEN and IRS1.

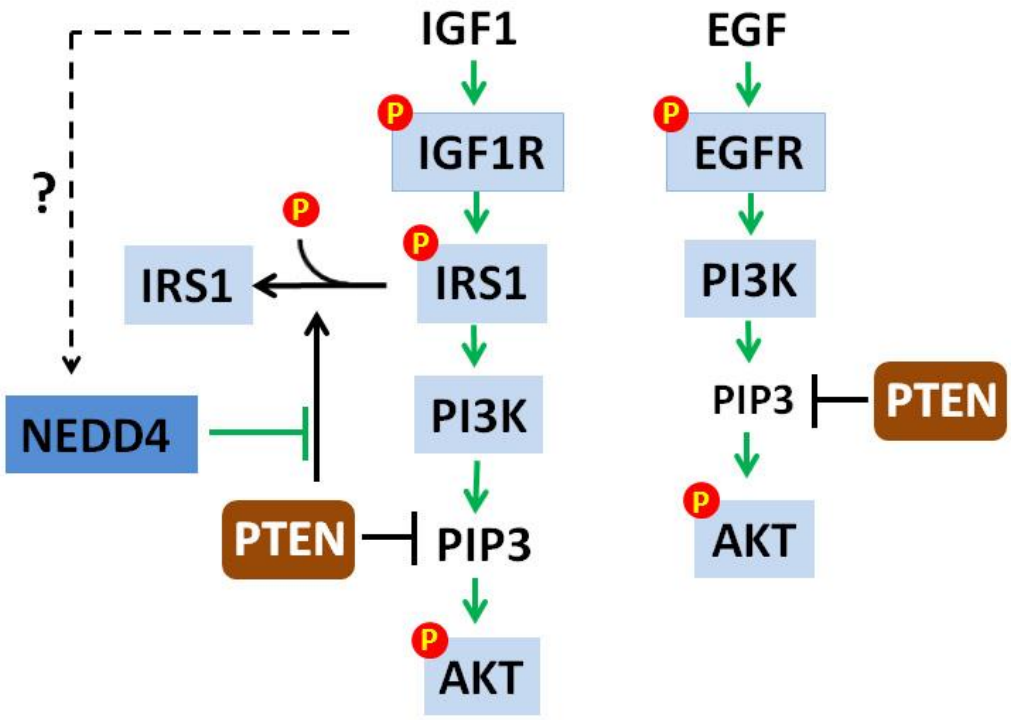

Figure 3.10

Model showing that IGF but not EGF signaling pathway is regulated by the NEDD4-PTEN circuitry. Upon IGF and insulin signaling, the IRS1 protein phosphatase activity of PTEN is antagonized by NEDD4. This mechanism accounts for the specific requirement of NEDD4 in IGF signaling but not EGF signaling. The lipid phosphatase activity of PTEN down-regulates both IGF and EGF signals.

DISCUSSION

This study establishes that PTEN is a protein tyrosine phosphatase for IRS1, which is under specific regulation by NEDD4. Therefore, PTEN has dual functions for IGF or insulin signaling, as a lipid phosphatase for PIP3 and as a protein tyrosine phosphatase for IRS1. PTEN's function as an IRS1 tyrosine phosphatase is usually masked by the negative feedback regulation of the PI3K-AKT pathway (Chandarlapaty et al., 2011; Qin et al., 2011). Generally, manipulation of PTEN protein levels lead to immediate change in AKT phosphorylation, thus the expression and phosphorylation of multiple RTKs. In addition, IRS1 is negatively regulated by serine phosphorylation due to mTORC1-S6K1 signaling (Copps and White, 2012; Harrington et al., 2004; Ozes et al., 2001), which is also activated by AKT. That's why stable PTEN knockdown or knockout often led to a decrease in IRS1 tyrosine phosphorylation, while over-expression of WT PTEN increased tyrosine phosphorylated IRS1 (unpublished data). Luckily, the novel function of PTEN was revealed when NEDD4 is absent upon IGF or insulin stimulation. It seems that the ubiquitin E3 ligase constitutively suppresses protein phosphatase activity of PTEN towards IRS1.

So far, six of family members of IRS proteins have been identified and termed IRS1-6. IRS1 and IRS2 are widely distributed, whereas IRS3, 4, 5, 6 had limited expression (Taniguchi et al., 2006). IRS1 and IRS2 contain highly similar N-terminal PH and PTB domains, followed by long unstructured C-terminal tail regions. For the conserved N-terminal region which is responsible for interaction between

IRS1 and PTEN, IRS1 and IRS2 only share 49% identical sequences. Furthermore, IRS2 contains fewer YXXM motifs than IRS1 that could be tyrosine phosphorylated and mediate binding to PI3K. Our preliminary data showed that IRS2 is probably not a protein substrate for PTEN (unpublished data).

In addition to PTEN, other protein phosphatases could also negatively regulate IGF/insulin signaling. For example, TCPTP and PTP1B can inactivate insulin signaling by dephosphorylating the insulin receptor, and PTP1B may also dephosphorylate IRS1 (Galic et al., 2005; Goldstein et al., 2000; Tiganis, 2013). How does the IRS1 phosphatase activity of PTEN coordinate with these additional regulatory mechanisms, and do these protein phosphatases function differentially, e.g., in a tissue and/or context-specific manner? Understanding these questions will provide further insights into the mechanisms and biology of IGF/insulin signaling.

Noticeably, NEDD4 RNAi resulted in increased EGF signaling, especially elevated EGFR phosphorylation. This could be explained by the indirect effect of NEDD4 on EGFR protein level, through ubiquitinating ACK (activated Cdc42-associated tyrosine kinase) which is involved in EGF-induced degradation of EGFR (Lin et al., 2010). This might also contribute to the special requirement of NEDD4 for IGF/insulin signaling.

This work also raises many important questions for future study. It is likely that the intensity and duration of IGF signaling in different tissues could be achieved by tuning the expression and activity of the PTEN and NEDD4 enzymes. It can also

be speculated that NEDD4 may be specifically stimulated by IGF/insulin signaling but not other RTKs to neutralize the inhibitory activity of PTEN. Furthermore, we speculate that the regulation of IGF/insulin signaling by PTEN and NEDD4 could play key roles in the pathophysiology of cancers (such as Ewing's sarcoma) and metabolic diseases (such as diabetes and obesity). Beyond IGF signaling, our findings warrant a systematic search and functional investigation of other cellular phosphoproteins that might be subject to regulation by the protein phosphatase activity of PTEN.

CHAPTER FOUR

CHARACTERIZATION OF A NEW FORM OF PTEN

INTRODUCTION

The classic "Kozak sequence" CCACC**ATG**G, has been shown to the most favorable sequence context for translation initiation (Kozak, 1991). In certain transcripts, translation initiation could occur from non-AUG codons. Kozak found that GUG and CUG were both capable of initiating translation in vitro far less efficiently (Kozak, 1989). The transcription factor, c-myc, has an alternate upstream CUG initiation codon, which adds 14 amino acids to the N-terminus of the protein (Hann et al., 1988). Actual subcellular localization of a protein can be dictated by alternate initiation codons. For example, human FGF3, if translation is initiated from AUG it enters the secretory pathway while protein translated from an upstream CUG localizes to the nucleus (Kiefer et al., 1994).

In addition to 403-amino acid PTEN, a 576-amino acid translational variant of PTEN was identified, which was generated from an alternative translation start site (Hopkins et al., 2013). The same group also showed that this longer version of PTEN could be secreted from cells and entered other cells. A very recent paper reported that translation of the same upper band was initiated from a CUG codon upstream and

Eukaryotic translation initiation factor 2A (eIF2A) controls its translation (Liang et al., 2014). Furthermore, they found that the protein induced cytochrome c oxidase activity and ATP production in mitochondria.

Intriguingly, two groups identified the same PTEN protein species as PTEN by SUMOylation (SUMO, small ubiquitin-like modifier). One group showed that PTEN was covalently modified by SUMO1 at both K266 and K254 sites in the C2 domain (Huang et al., 2012). The other group mapped the SUMOylation site at position 254, which controls PTEN nuclear localization (Bassi et al., 2013).

RESULTS

Identify of UPP

During immunoblotting for endogenous PTEN in cell lysates, we noticed an upper protein band of PTEN (termed UPP) of molecular mass ~75-kD (Figure 4.1A). This upper band could be detected by with two PTEN-specific antibodies in various mammalian cells, including human breast (MCF7), WT MEFs, human 293 and human osteosarcoma (U2OS) cells. While UPP cannot be detected in known PTEN-negative cells including breast cancer (MDA-MB-468) and prostate cancer (PC3) cells. We also tested more mammalian cells (Figure 4.1B) and UPP coexisted with PTEN in all PTEN positive cells such as epidermoid carcinoma (A431), monkey Cos-1, mouse NIH3T3, and colorectal carcinoma (HCT116). As expected, UPP was absent from cells lacking PTEN (prostate cancer (LNCaP, PC3) and $PTEN^{-/-}$ MEFs).

To study the connection between PTEN and UPP, we engineered MEFs to express two different Dox-inducible shRNA against PTEN (Figure 4.2A). When PTEN RNAi was induced for 24 hours, PTEN protein level barely changed while UPP was substantially depleted. Nevertheless, 48 hours PTEN RNAi resulted in notable reduction of both PTEN and UPP, supporting that UPP and PTEN were correlated on mRNA level. To test if exogenous PTEN could induce UPP generation (Figure 4.2B), PTEN cDNA with different tags were transfected into 293T cells, then immunoblotted with PTEN antibody. However, none could give rise to the UPP band, contradicting the notion that UPP was a posttranslational modification of PTEN.

To identify the UPP band, we attempted to separate endogenous UPP from PTEN in HeLa cell extracts, using ammonium sulfate precipitation, a series of chromatography and final immune-precipitation with PTEN antibody (Figure 4.3A). The eluate from last step of purification was silver stained and sent for mass spectrometry (Figure 4.3B). When the sequencing result was compared with the NCBI database from before June 2013, it was only identified as PTEN.

In 2013, a group published the identity of PTEN upper band in science (Hopkins et al., 2013). They named it PTEN-Long, as 576-amino acid translational variant of PTEN. When we compared the mass spectrometry result for UPP with that of PTEN-Long, there was a complete match (Figure 4.4A). UPP shares the same identity as PTEN-long, translated from upstream CTG as diagrammed in Figure 4.4B. Then we generated UPP mutants for distinctive expression patterns (Figure 4.4C). UPP-CTG expressed as a major PTEN band and a minor UPP band. When the original

CTG was mutated into ATG, the ratio of UPP vs PTEN is about 1:1. While the original ATG was mutated into ATA, only UPP band could be detected. We used UPP(ATG/ATA) for our following studies of UPP.

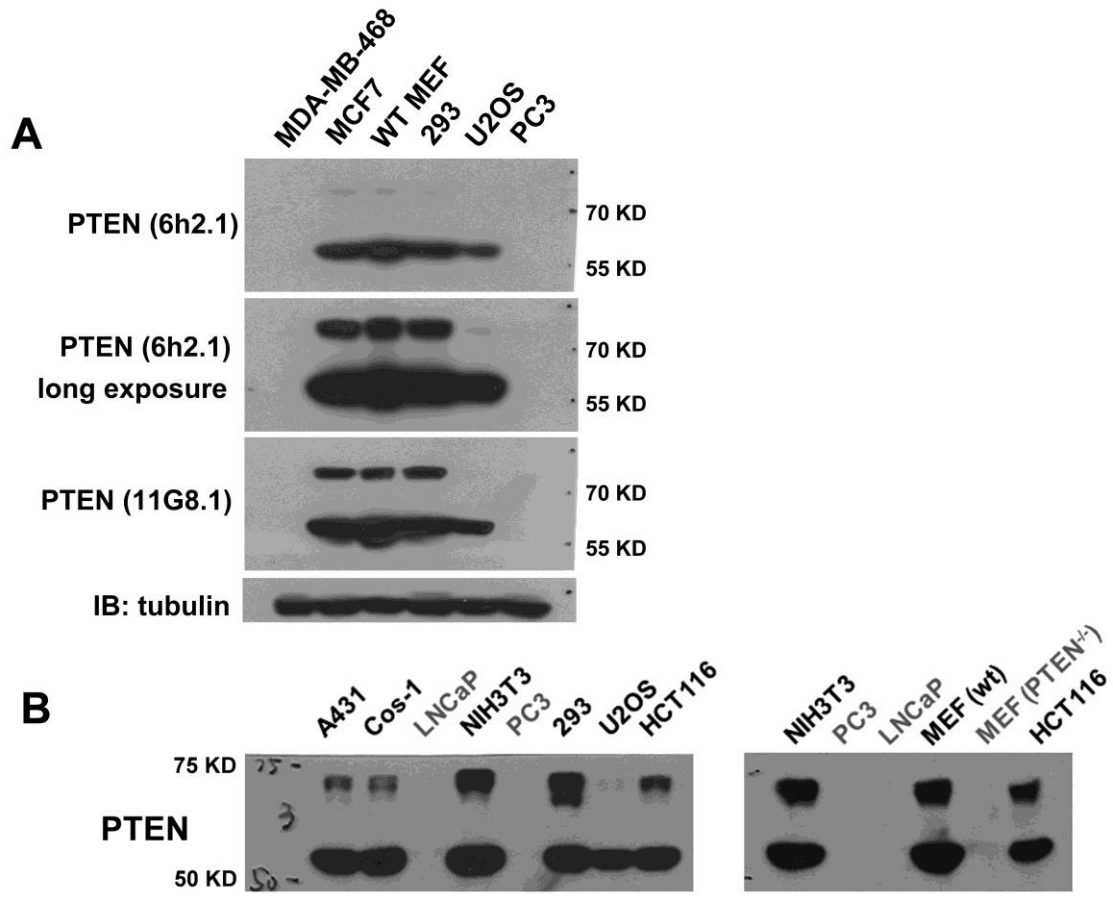

Figure 4.1

Immunoblot of whole-cell lysates of cell lines of known PTEN status. (A) Western blots of whole-cell lysates of MDA-MB-468, MCF7, WT MEFs, 293, U2OS and PC3. MDA-MB-468 and PC3 are PTEN negative. (B) Western blots of whole-cell lysates of A431, Cos-1, LNCaP, NIH3T3, PC3, 293, U2OS, HCT116, WT MEFs and $PTEN^{-/-}$ MEFs. LNCaP, PC3 and $PTEN^{-/-}$ MEFs are PTEN negative.

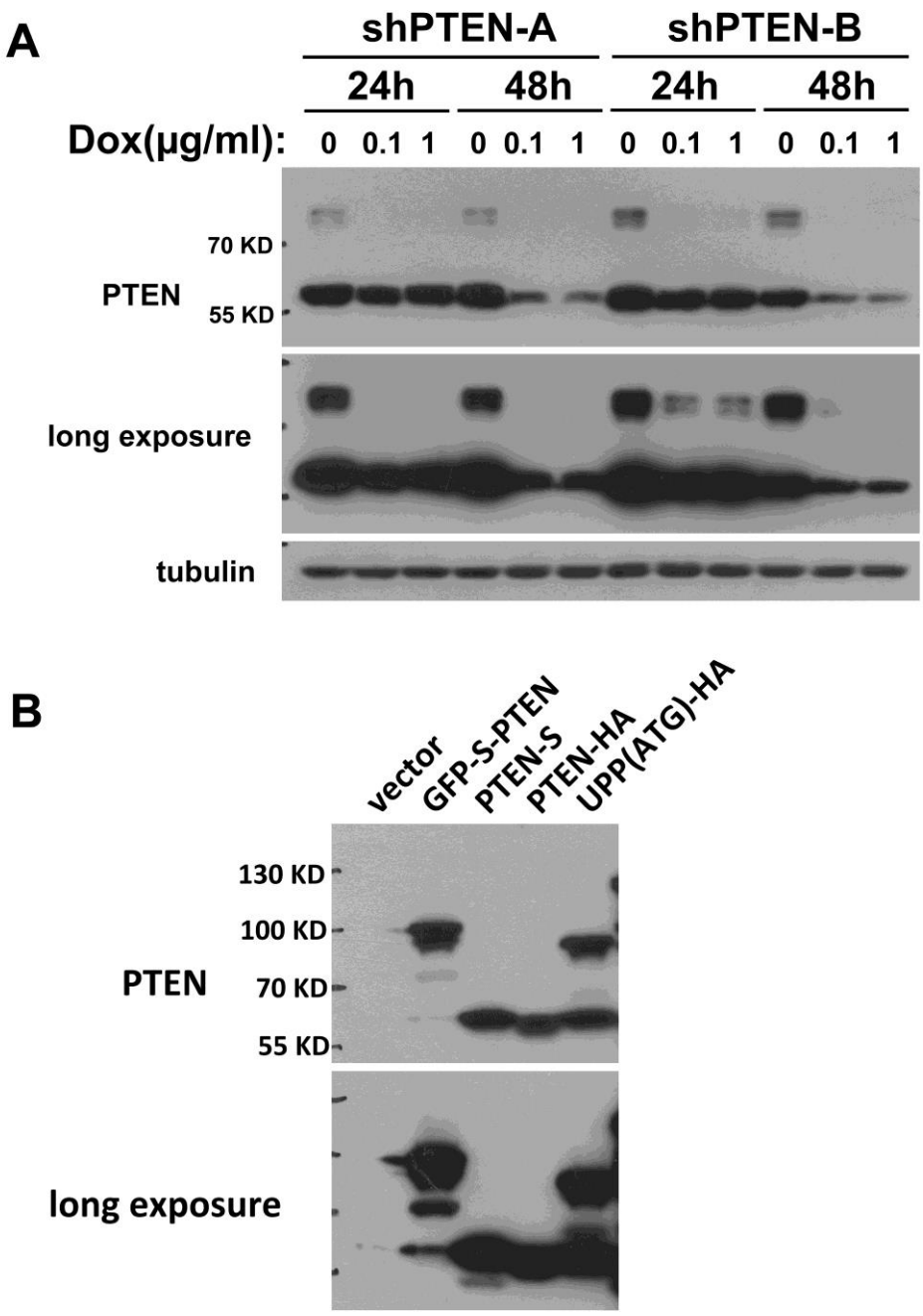

Figure 4.2

Correlation between UPP and endogenous PTEN. (A) UPP decreases when PTEN is knocked down by RNAi. WT MEFs haring Dox-inducible PTEN shRNA constructs (shPTEN-A, shPTEN-B) were treated with Doxycycline with indicated concentration and time. (B) Expression of exogenous PTEN fails to generate UPP. 293T cells were transfected with indicated plasmids and UPP (ATG)-HA as positive control.

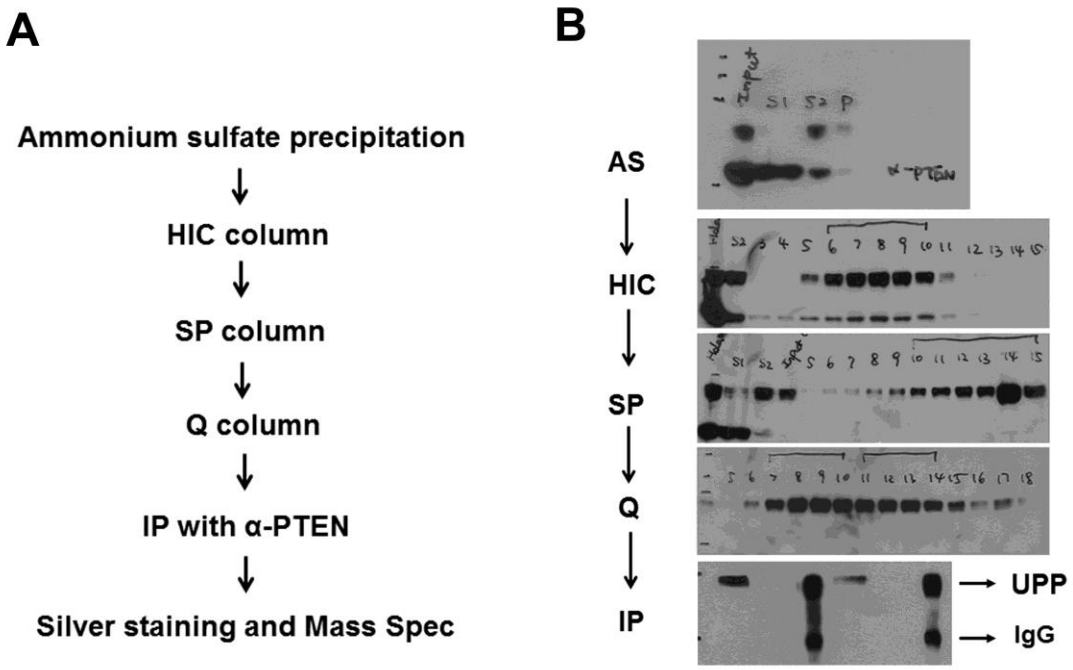

Figure 4.3

Purification of endogenous UPP. (A) Endogenous UPP purification strategies. Starting material is supernatant of HeLa nuclei extracted with 1% Triton. After ammonium sulfate precipitation, UPP is completely separated from PTEN by chromatography. Endogenous UPP is enriched by immunoprecipitation by PTEN antibody. (B) Immunoblot of UPP from purification steps. (Data were generated by Wei Pan in Dr.Jiang's lab)

Figure 4.4

Identity of UPP. (A) Mass spec data and comparison with known PTEN-long sequence. Matched sequence is highlighted in red. (B) PTEN and UPP domain structures. Normal PTEN translation starts at ATG, while UPP is translated from upstream CTG codon. (C) Schematics of UPP mutants and expression in 293T cells.

A

UPP

```
  1 LERGGEAAAA AAAAAAAPGR GSESPVTISR AGNAGELVSP LLLPPTRRRR
 51 RRHIQGPGPV LNLPSAAAAP PVARAPEAAG GGSRSEDYSS SPHSAAAAAR
101 PLAAEEKQAQ SLQPSSSRRS SHYPAAVQSQ AAAERGASAT AKSRAISILQ
151 KKPRHQQLLP SLSSFFFSHR LPDLMTAIIKE IVSRNKRRYQ EDGFDLDLTY
201 IYPNIIAMGF PAERLEGVYR NNIDDVVRFL DSKHKNHYKI YNLCAERHYD
251 TAKFNCRVAQ YPFEDHNPPQ LELIKPFCED LDQWLSEDDN HVAAIHCKAG
301 KGRTGVMICA YLLHRGKFLK AQEALDFYGE VRTRDKKGVT IPSQRRYVYY
351 YSYLLKNHLD YRPVALLFHK MMFETIPMFS GGTCNPQFVV CQLKVKIYSS
401 NSGPTRREDK FMYFEFPQPL PVCGDIKVEF FHKQNKMLKK DKMFHFWVNT
451 FFIPGPEETS EKVENGSLCD QEIDSICSIE RADNDKEYLV LTLTKNDLDK
501 ANKDKANRYF SPNFKVKLYF TKTVEEPSNP EASSSTSVTP DVSDNEPDHY
551 RYSDTTDSDP ENEPFDEDQH TQITKV
```

PTEN

Protein sequence coverage: 50%

B

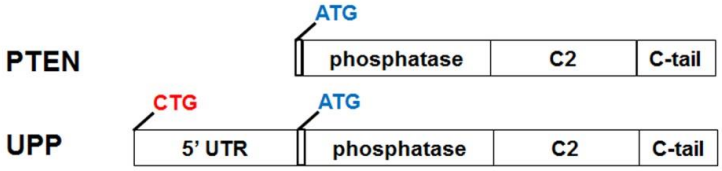

C

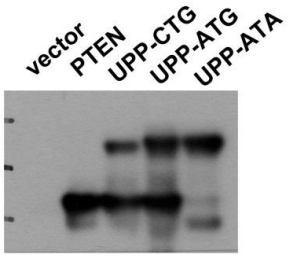

Subcellular localization of UPP

Since UPP contains over 150 additional amino acids at its N-terminus, we wanted to study if they altered the biochemical properties of the protein. To study the stability and subcellular localization of UPP, we treated WT MEFs with cycloheximide, an inhibitor of protein synthesis, and fractionated cell lysate using hypotonic buffer and ultracentrifugation (Figure 4.5A). The majority of endogenous PTEN was in the cytosol soluble fraction, while most of UPP was in the pellet. When protein synthesis was blocked, UPP levels decreased dramatically, while PTEN remained quite stable, suggesting UPP had a shorter half-life than PTEN. Similarly, when MG132, a proteasome inhibitor, was used to block degradation of ubiquitin-conjugated proteins, only UPP accumulated in the pellet fraction, supporting that UPP is the fast turnover subpopulation of PTEN (Figure 4.5B).

Our fractionation data showed that UPP has a distinct subcellular localization from PTEN. To verify this, we engineered MCF7 cells expressing Dox-inducible expression of C-terminal GFP-tagged PTEN or UPP. As shown in Figure 4.5C, PTEN-GFP was present in both cytosol and nucleus, but UPP-GFP was excluded from nucleus and exhibited a unique pattern from PTEN.

For a better understanding of the subcellular localization of UPP, we recorded the Dox-inducible expression of UPP-GFP or PTEN-GFP using time-lapse microscopy. Still images from different time points showed that UPP-GFP was synthesized in cytoplasm, stayed outside the nucleus and transient translocations to the

plasma membrane and cell-cell junctions (Figure 4.6B). In contrast, PTEN-GFP was synthesized in cytoplasm, but trans-located to the nucleus and demonstrated less frequent localization to plasma membrane (Figure 4.6A).

To pinpoint the localization of UPP on the membrane networks of cells, we checked different organelle markers for potential co-localization. As reported recently (Liang et al., 2014), UPP was detected predominantly in the cytoplasm and mitochondria. We tested if UPP co-localized with mitochondria using MitoTracker in live cells (Figure 4.7A) and immunofluorescence by cytochrome C antibody (Figure 4.7B). However, we did not observe the subcellular localization of UPP or PTEN on mitochondria.

Next we tested a series of antibodies for organelle markers (Figure 4.8). As a maker for endoplasmic reticulum (ER), carboxyl-terminal tetrapeptide KDEL signal is essential for retention of resident proteins in the lumen of ER (Pelham, 1990). Nevertheless, immunofluorescence with KDEL antibody showed little co-localization with UPP-GFP (Figure 4.8A). Then we tested several early endosome markers, including Rab5 (Figure 4.8B) and EEA1 (Figure 4.8C). Rab5 is a key regulator of early endocytosis and localizes at the plasma membrane and early endosomes (Zerial and McBride, 2001), while EEA1 is a Rab5 effector required for early endosomal membrane fusion and trafficking (Christoforidis et al., 1999). Interestingly, there was partial co-localization of UPP-GFP with both Rab5 and EEA1. Furthermore, Syntaxin 6, a member of SNARE protein which is localized to the trans-Golgi network and within endosomes (Wendler and Tooze, 2001), showed partial co-localization with

UPP-GFP as well (Figure 4.8D). Taken together, UPP-GFP appears to be involved in the endocytic pathway involving membrane trafficking.

From live imaging of Dox-inducible expression of UPP-GFP, we noticed the transient localization of UPP-GFP on ruffled plasma membranes and areas of cell-cell adhesion (Figure 4.6B). Therefore, we tested if UPP-GFP was localized on adherens junctions, employing E-caderin (Figure 4.9A) and β-catenin antibody as markers (Figure 4.9B). As a member of transmembrane glycoproteins which mediated calcium-dependent cell-cell adhesion (Wheelock and Johnson, 2003), E-caherin staining showed substantial co-localization with UPP-GFP. Additionally, we also detected clear co-localization of UPP-GFP and β-catenin, which binds to the cytoplasmic tail of E-cadherin at adherens junctions (Xu and Kimelman, 2007). These data supported the localization of UPP on adherens junctions.

Figure 4.5

UPP is the fast turnover subpopulation with distinctive subcellular localization. (A) Cycloheximide treatment and fractionation. WT MEFs were treated with 10μg/ml cycloheximide for indicated time, and then subjected to fractionation using hypotonic buffer and ultracentrifuge. (B) MG132 treatment and fractionation. WT MEFs were treated with 25μM MG132 for indicated time and subjected to fractionation. (C) UPP shows a different subcellular localization from PTEN. MCF7 cells were transduced with lentivirus expressing PTEN-GFP or UPP-GFP.

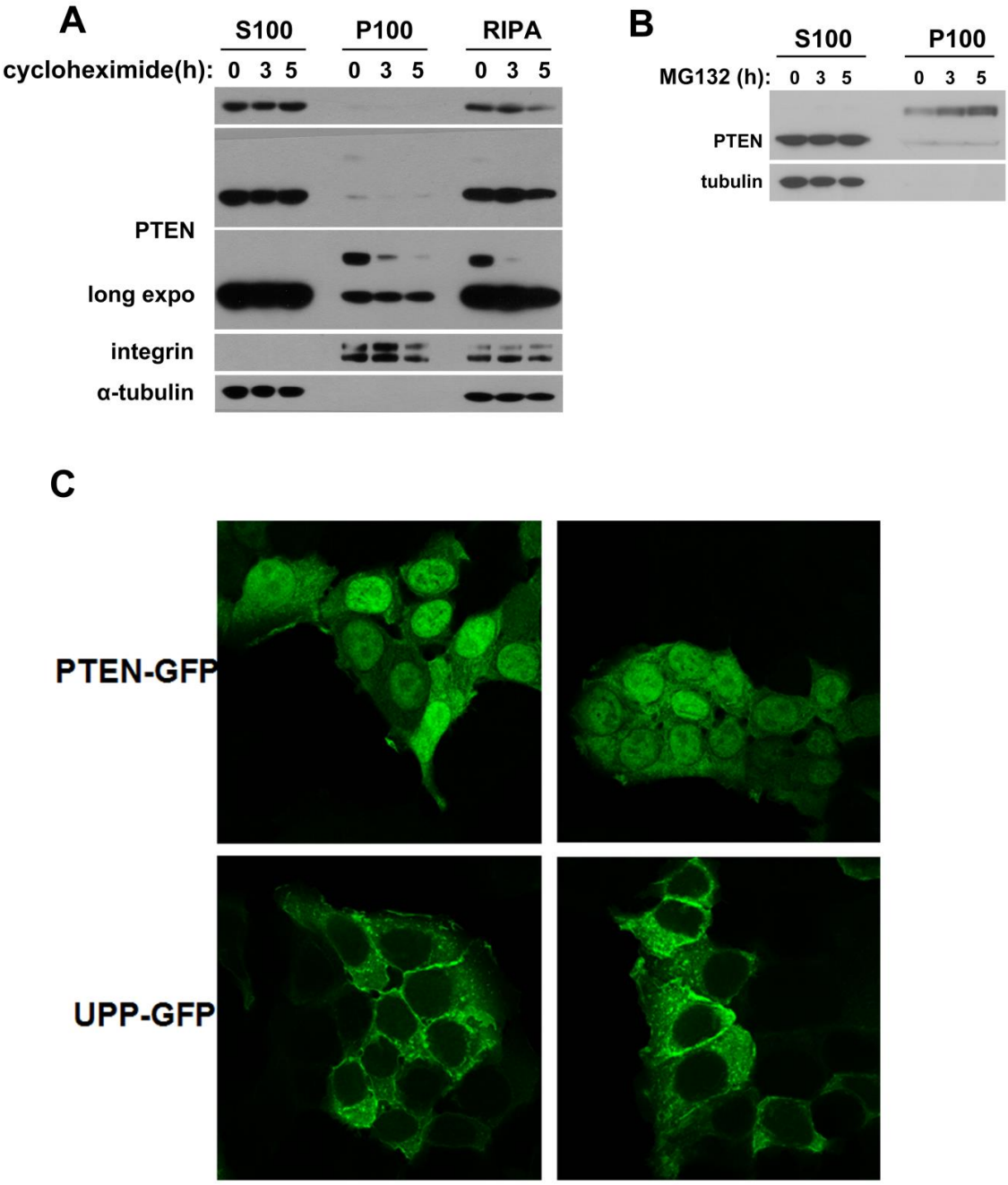
A
S100
P100
RIPA
cycloheximide(h):
0 3 5 0 3 5 0 3 5
PTEN
long expo
integrin
α-tubulin
B
S100
P100
MG132 (h):
0 3 5 0 3 5
PTEN
tubulin
C
PTEN-GFP
UPP-GFP

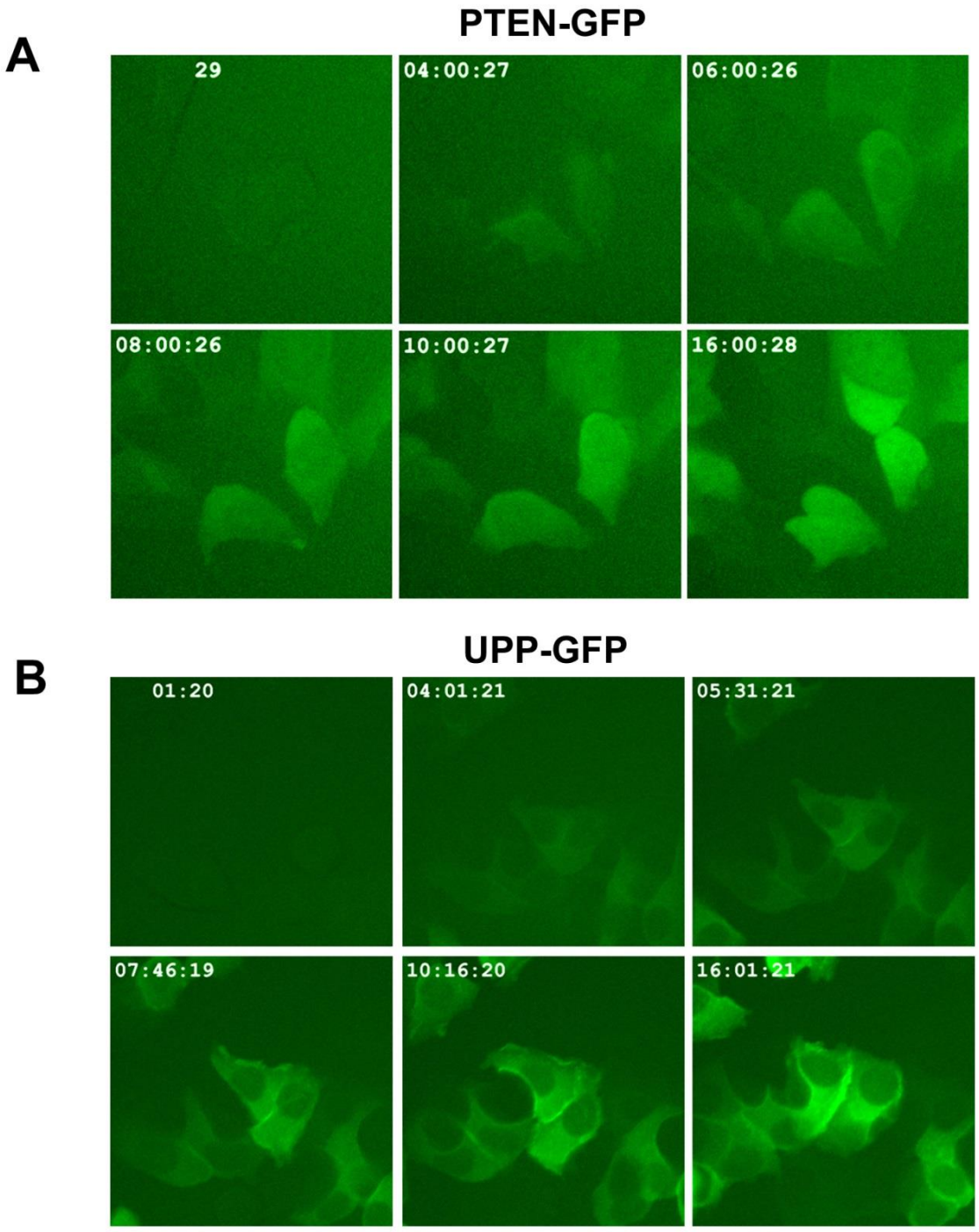

Figure 4.6

Live cell imaging: Dox-inducible expression of PTEN-GFP or UPP-GFP in MCF7. MCF7 cells were transduced with lentivirus expressing PTEN-GFP (A) or UPP-GFP (B). After changing to fresh medium with 1μg/ml Dox, cells were subjected to live cell imaging.

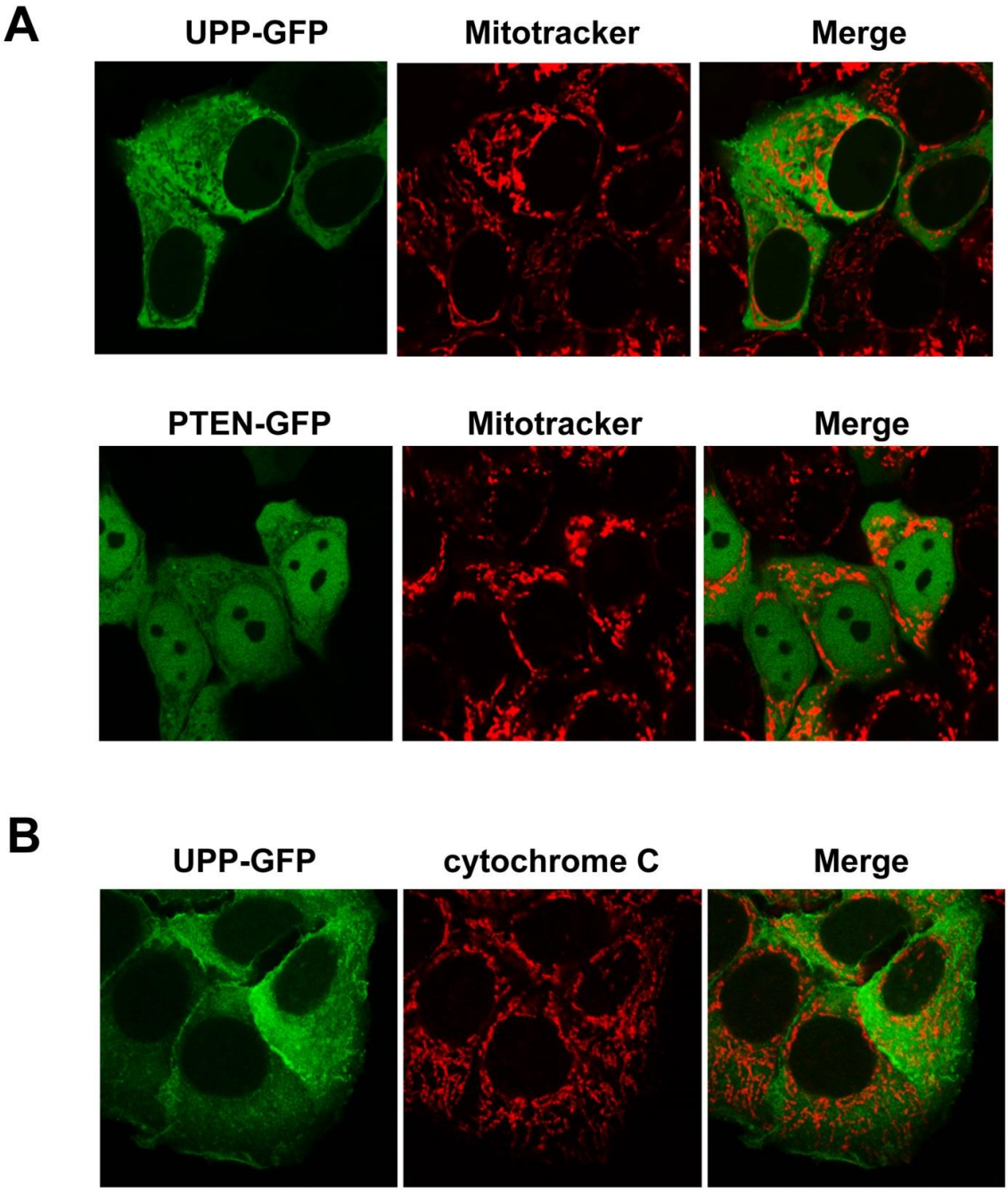

Figure 4.7

UPP does not localize on mitochondria. (A) MCF7 cells expressing UPP-GFP or PTEN-GFP were treated with 10μM MitoTracker for 20min then subjected to confocal fluorescence microscopy. (B) MCF7 cells expressing UPP-GFP were subjected to immunofluorescence by cytochrome C antibody.

Figure 4.8

UPP is localized on endosomes. MCF7 cells expressing UPP-GFP were subjected to immunofluorescence by antibodies (A) KDEL, (B) Rab5, (C) EEA1 and (D) Syntaxin 6.

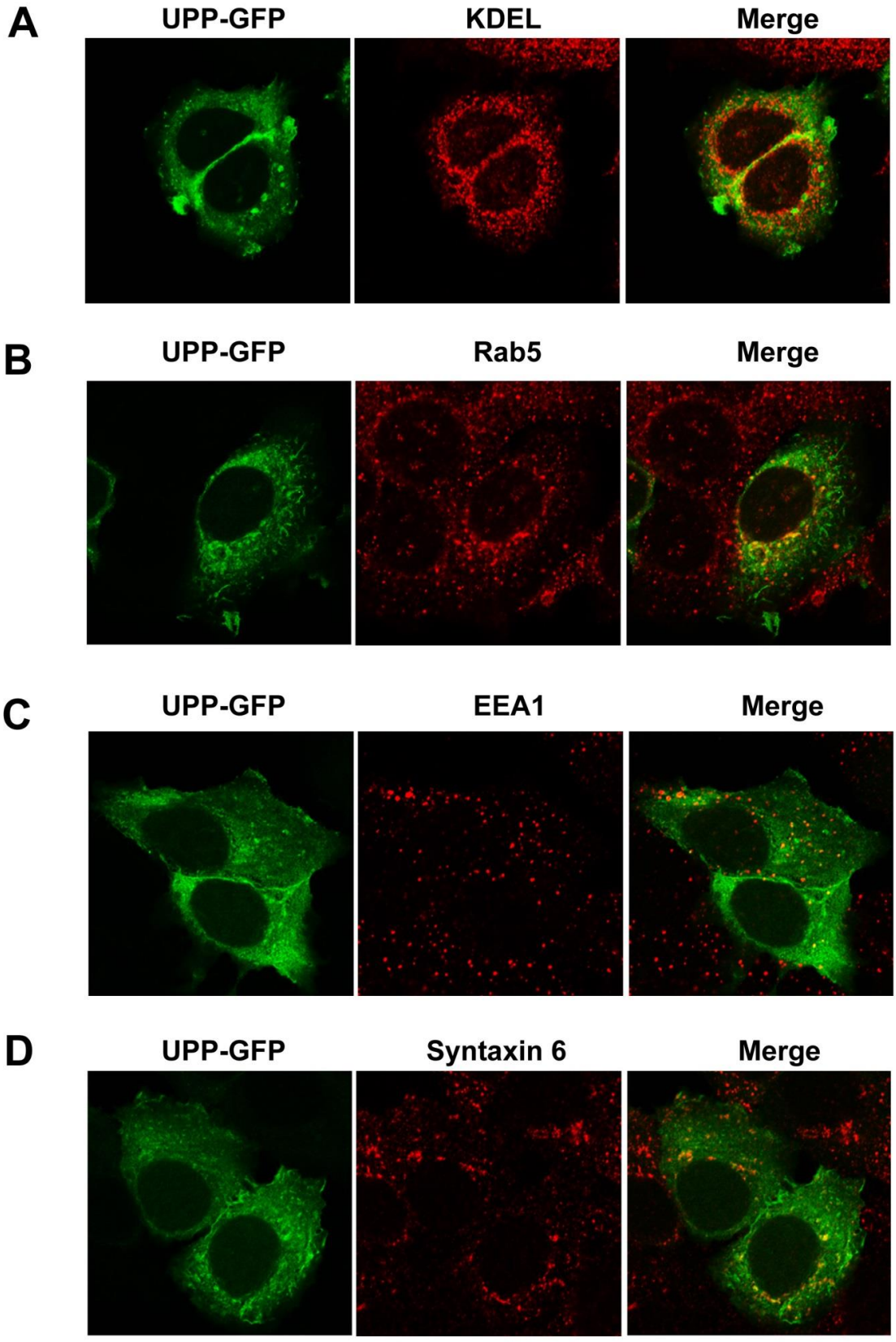
A
UPP-GFP
KDEL
Merge
B
UPP-GFP
Rab5
Merge
C
UPP-GFP
EEA1
Merge
D
UPP-GFP
Syntaxin 6
Merge

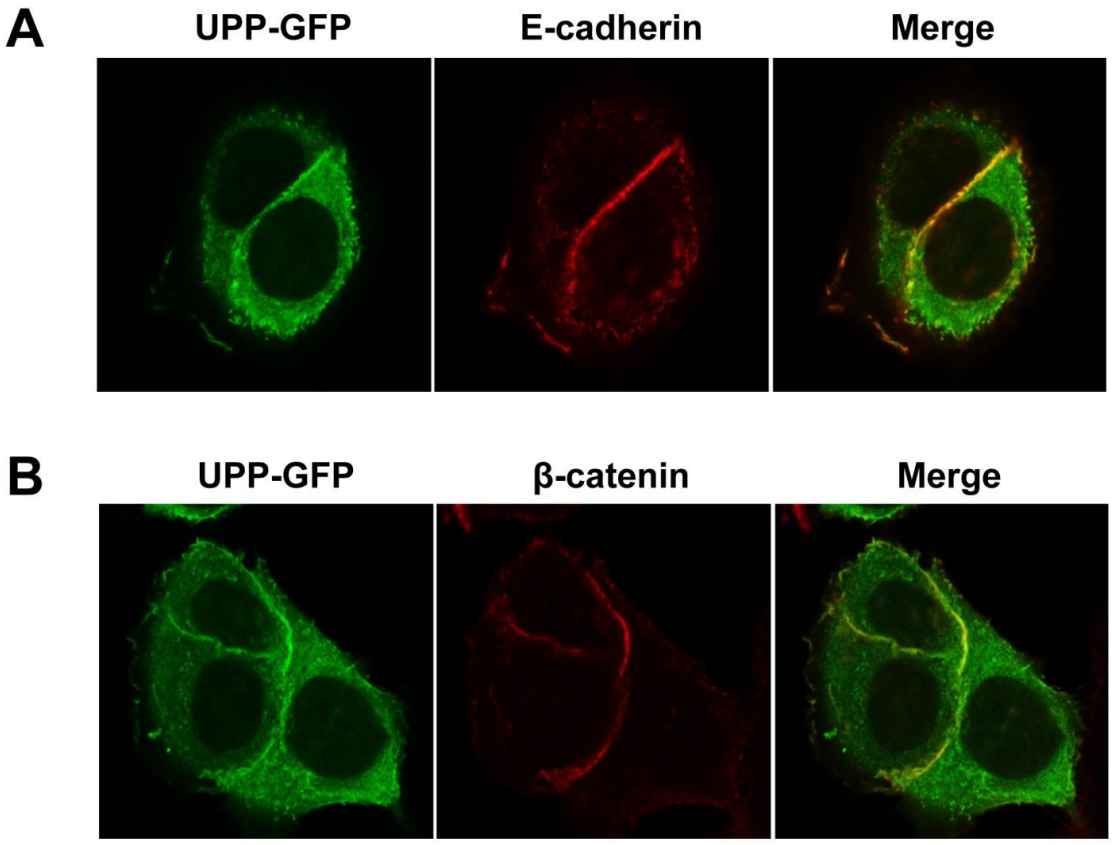

Figure 4.9

UPP co-localizes with E-cadherin/β-catenin. MCF7 cells expressing UPP-GFP were subjected to immunofluorescence by antibodies (A) E-cadherin and (B) β-catenin.

Interestingly, when WT MEFs were treated with 1% oxygen hypoxia for a few hours, we noticed a slight decrease in the UPP band, but not PTEN, which correlated with an increase in p-AKT(S473) (Figure 4.10A). When cells were subjected to fractionation, the down-regulation of UPP is obvious in the membrane fraction (Figure 4.10B).

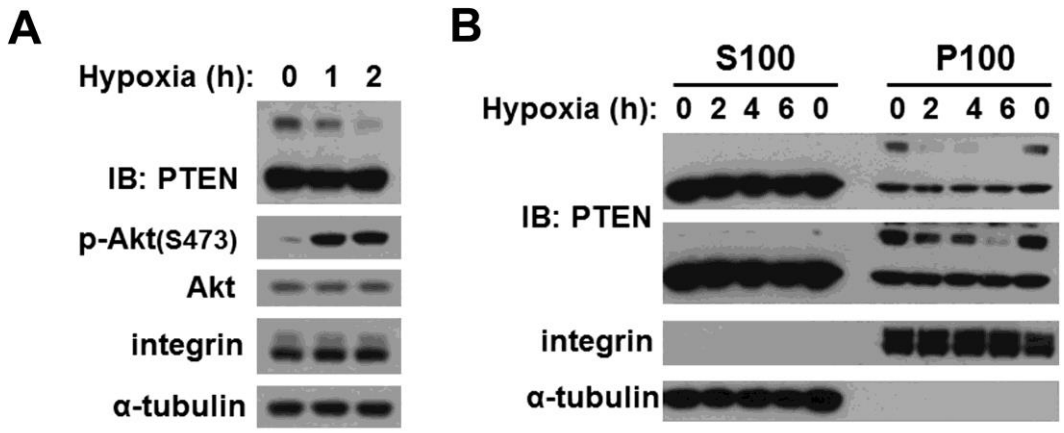

Figure 4.10

UPP regulation during hypoxia. (A) Hypoxia treatment on WT MEFs. WT MEFs were treated with 1% oxygen hypoxia for indicated time and whole cell lysate were analyzed. (B) Hypoxia treatment and fractionation. WT MEFs were treated with 1% oxygen hypoxia for indicated time and subject to fractionation.

UPP is an active lipid phosphatase

Since UPP is a translational variant of PTEN, we tested if additional amino acids regulated its enzymatic activity. Analysis of the extra peptide using SignalIP3.0 predicted a signal peptide which might be cleaved at amino acid 22 (Figure 4.11A). To compare the enzymatic activities of PTEN and UPP, recombinant C-terminal his-tagged PTEN, UPP or UPP without signal peptide (UPP (-) S) protein were generated in SF9 cells. Then their enzymatic activities were measured against the lipid substrate PtdIns(3,4,5)P_3. UPP demonstrated comparable lipid phosphatase activity dephosphorylating diC_8PIP_3 , either in phospholipid vesicles (PLV) (Figure 4.11B) or water (Figure 4.11C).

Then lipid phosphatase activities of PTEN and UPP were compared in PTEN-negative cells. PTEN$^{-/-}$ MEFs were transduced with retrovirus expressing either PTEN or UPP. Even though the level of exogenous UPP was much lower than exogenous PTEN, they had comparable inhibition on basal AKT phosphorylation (Figure 4.12A). We also transiently over-expressed PTEN or UPP in various PTEN-negative cancer cell lines, including PC3, MDA-MB-468 and T89G. UPP, expressed at much lower levels, demonstrated similar inhibition of basal p-AKT, in comparison with PTEN (Figure 4.12B). Then we measured lipid phosphatase activities of PTEN and UPP on insulin-stimulated AKT phosphorylation in cells through imaging. MCF7 cells transiently expressing either PTEN-GFP or UPP-GFP were serum starved, then stimulated with insulin. Immunofluorescence of endogenous p-AKT (S473) showed

that UPP-GFP blocked insulin-induced AKT phosphorylation similarly as PTEN-GFP (Figure 4.12C and D).

For better control of the expression levels of the proteins, we engineered PC3 cells with Dox-inducible over-expression of PTEN or UPP and picked stable clones. 24 hour of Dox treatment induced comparable levels of expression of PTEN or UPP, with similar suppression of p-AKT (T308/S473) (Figure 4.13A). Next we tested the growth potential of the stable clones in colony formation assay. Dox-inducible UPP over-expression led to slightly better inhibition on colony numbers, however, UPP was expressed at slightly higher levels (Figure 4.13B).

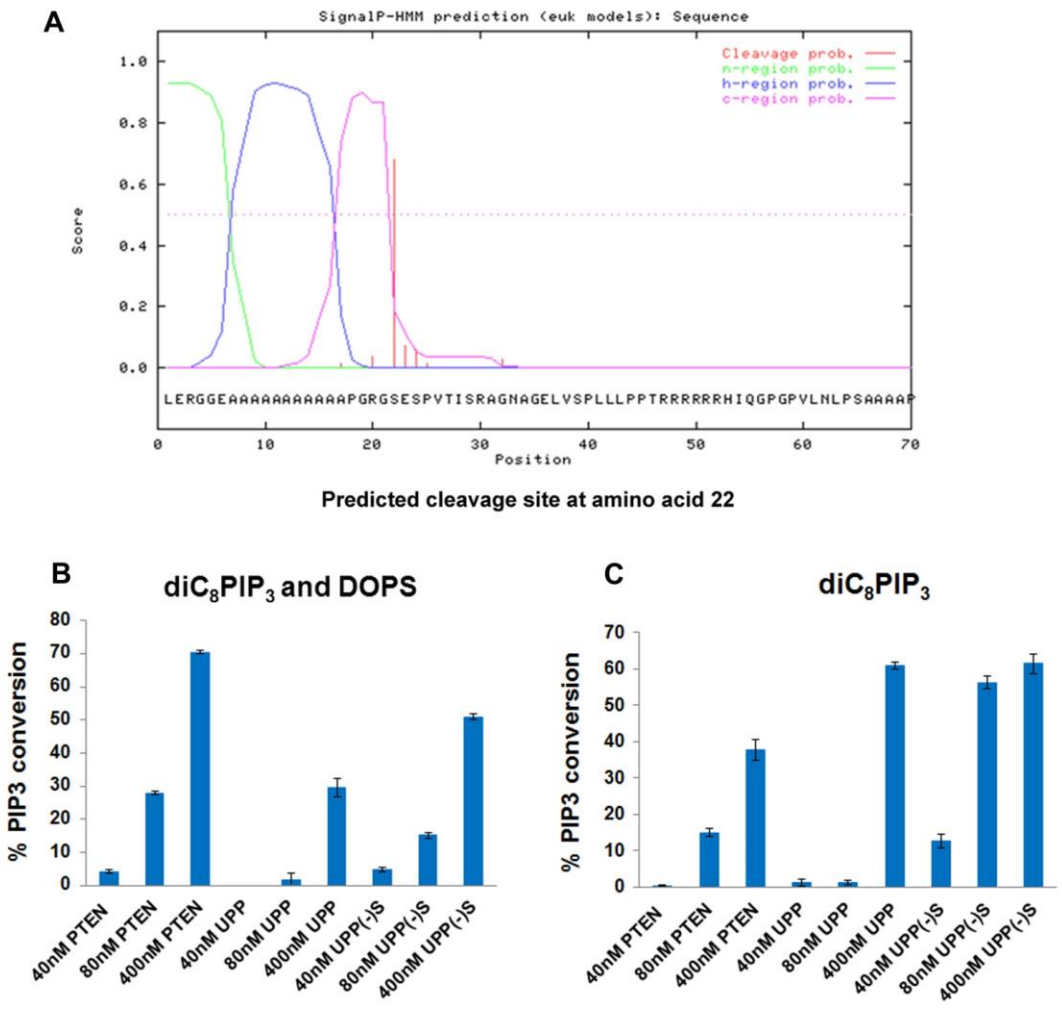

Figure 4.11

Comparison of lipid phosphatase activity of PTEN and UPP in vitro. (A) Sequence analysis of UPP-specific sequence. (B) Lipid phosphatase assays were performed with indicated recombinant protein with 40 μM diC_8PIP_3 and 0.5mM DOPS. (C) Lipid phosphatase assays were performed with indicated recombinant protein with 40 μM diC_8PIP_3.

Figure 4.12

Lipid phosphatase activity of UPP in cells. (A) Transient o/e of PTEN or UPP in $PTEN^{-/-}$ MEFs. PTEN-/- MEFs were transduced with retrovirus expressing PTEN or UPP. 48 hours later, cells were harvested and subjected to western blot. (B) Transient o/e of PTEN or UPP in PTEN negative cancer cells. PC3, MDA-MB-468 and T89G were transduced with retrovirus expressing PTEN or UPP. 48 hours later, cells were harvested and subjected to western blot. (C) Immunofluorescence of Dox-inducible o/e of PTEN in MCF7 cells upon insulin treatment. MCF7 cells expressing PTEN-GFP were serum starved, then treated with 1μg/ml insulin for 10 min. p-AKT (S374) antibody was used for immunofluorescence. (D) Immunofluorescence of Dox-inducible o/e of UPP in MCF7 cells upon insulin treatment. MCF7 cells expressing UPP-GFP were serum starved, then treated with 1μg/ml insulin for 10 min. p-AKT (S374) antibody was used for immunofluorescence.

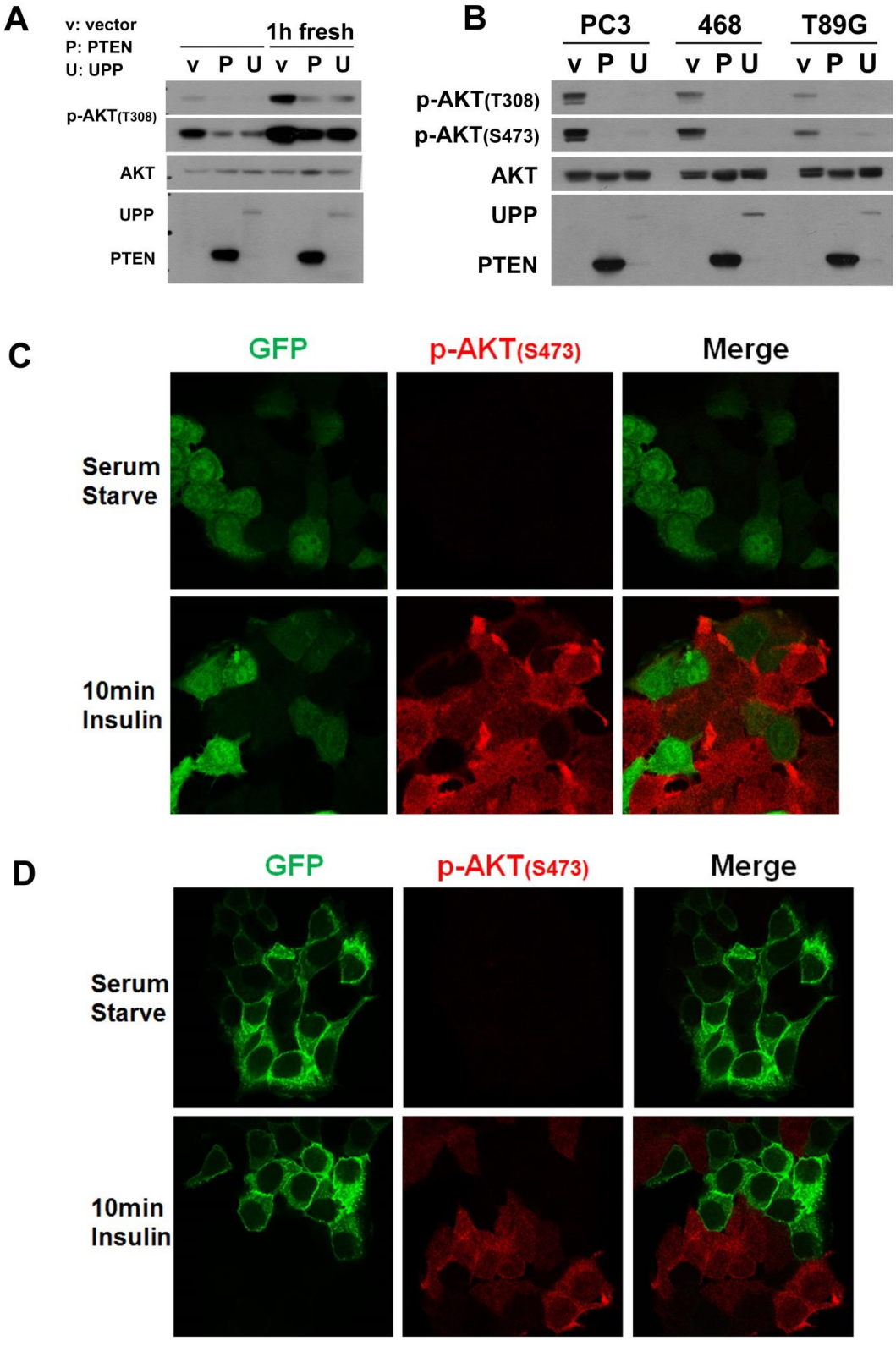
A
v: vector
P: PTEN
U: UPP
1h fresh
v P U v P U
p-AKT(T308)
AKT
UPP
PTEN
B
PC3
468
T89G
v P U v P U v P U
p-AKT(T308)
p-AKT(S473)
AKT
UPP
PTEN
C
GFP
p-AKT(S473)
Merge
Serum Starve
10min Insulin
D
GFP
p-AKT(S473)
Merge
Serum Starve
10min Insulin

Figure 4.13

Growth Suppression activity of UPP in PC3 cells. (A) Dox-inducible o/e of PTEN or UPP in PC3 cells. Stable clones of PC3 harboring Dox-inducible PTEN or UPP expression were treated with or without 1μg/ml Dox for 24 hours. (B) Dox-inducible o/e of PTEN or UPP in colony formation assay. $1X10^3$ cells of stable clones of PC3 harboring Dox-inducible PTEN or UPP expression were seeded in 6-well plates, and then treated with or without 1μg/ml Dox for 10 days.

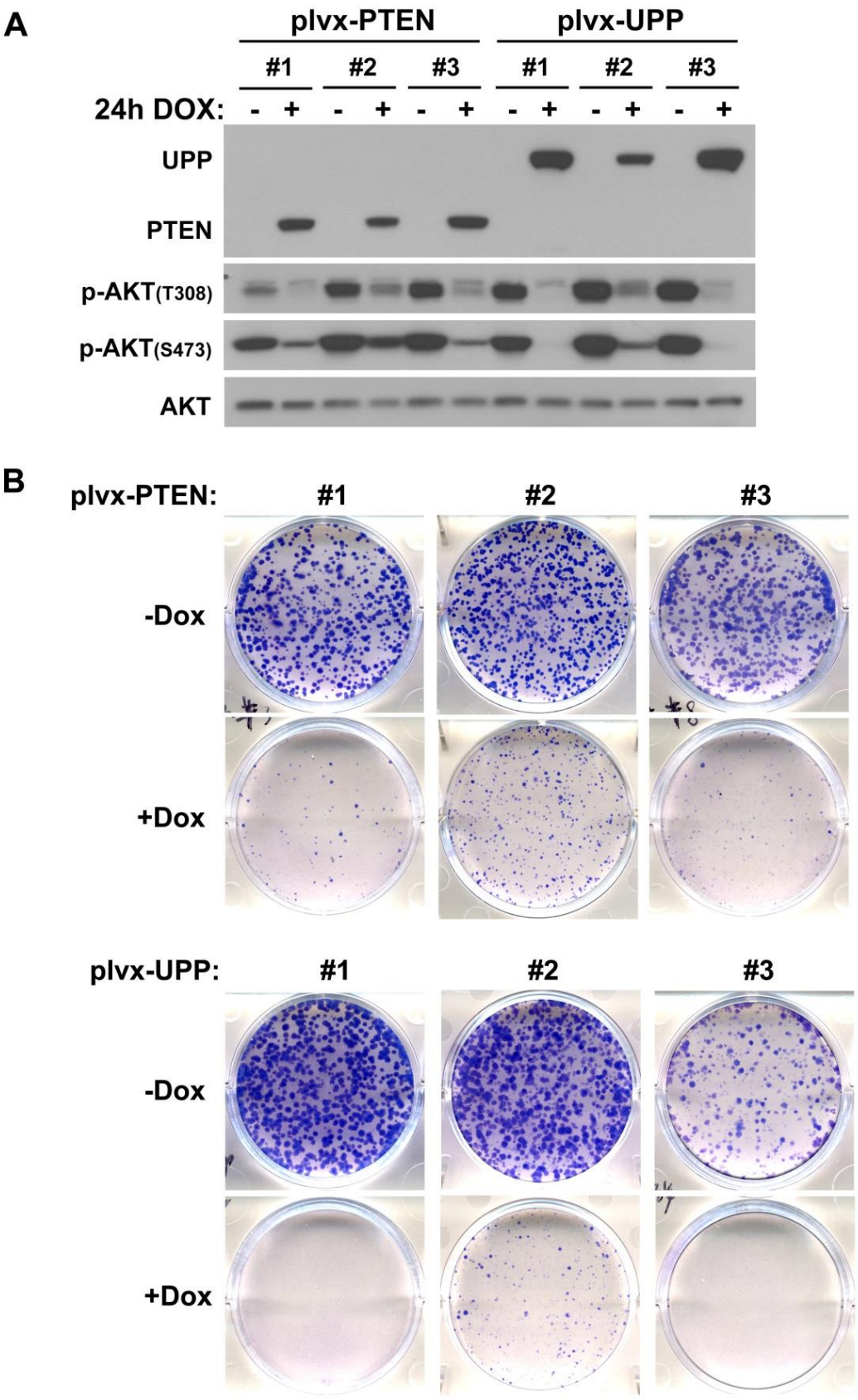
A
plvx-PTEN
plvx-UPP
#1
#2
#3
#1
#2
#3
24h DOX:
- + - + - + - + - + - +
UPP
PTEN
p-AKT(T308)
p-AKT(S473)
AKT
B
plvx-PTEN:
#1
#2
#3
-Dox
+Dox
plvx-UPP:
#1
#2
#3
-Dox
+Dox

UPP is a better binding partner for IRS1

As discussed in chapter two, PTEN is a binding partner and protein tyrosine phosphatase for IRS1. Naturally, we measured the capacity of UPP to bind to IRS1. When S-tagged PTEN or UPP were IPed from cells expressing HA-tagged IRS1, much more IRS1 were in the complex with UPP than with PTEN, independent of the predicted signal peptide on N-terminus of UPP (Figure 4.14A).

To confirm the Co-IP data, we IPed S-tagged IRS1 from cells expressing equal amounts of exogenous PTEN or UPP, using UPP (ATG/ATG) mutant. Consistently, IRS1 bound with UPP preferentially, and the interaction could also be blocked by overexpressing wild-type NEDD4, but not enzymatically dead NEDD4 (Figure 4.14B). To rule out the possibility that the longer UPP protein randomly stuck to beads or proteins, S-tagged IGF1R were pulled down from cells expressing equal amounts of PTEN or UPP. In contrast with IRS1, IGF1R bound equally to both PTEN and UPP (Figure 4.14C).

One dilemma about the importance of endogenous UPP is that its protein level is much lower than that of endogenous PTEN in cells. To address the biological function of UPP, we generated UPP-knockout or PTEN-knockout MCF7 cells, using CRISPR/Cas9 technology. Among the four PTEN knockout stable clones, complete PTEN loss (stable clones #1 and #2) led to dramatic increase in p-AKT (T308), but little change in IRS1 tyrosine phosphorylation, probably due to negative feedback regulation (Figure 4.15). While partial PTEN loss (stable clone #3) and complete UPP

depletion (stable clones UPP #1,2,3,4) resulted in slight up-regulation of pAKT (T308) and substantial increase of IRS1 tyrosine phosphorylation, suggesting UPP might be a physiological tyrosine phosphatase for IRS1 in MCF7.

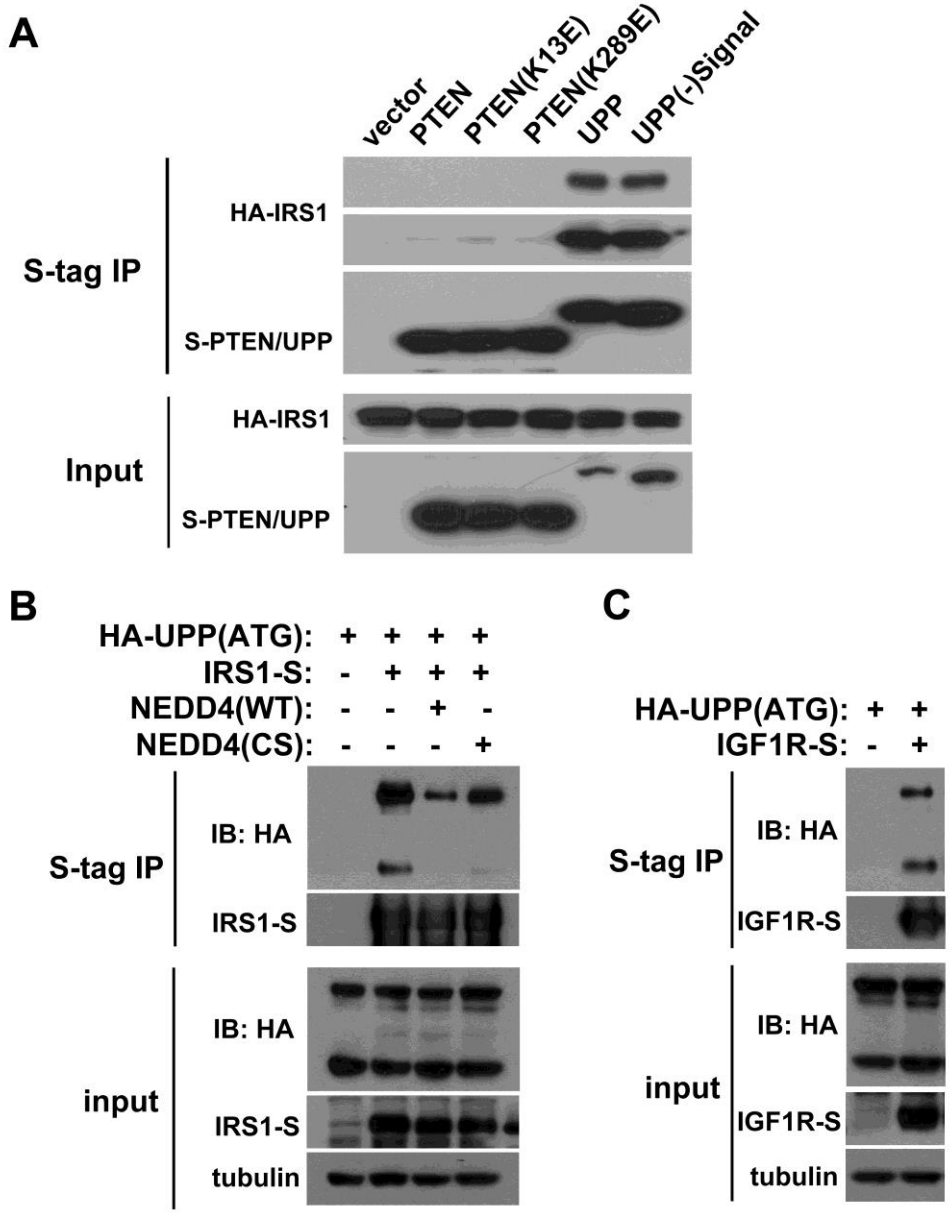

Figure 4.14

UPP is better binding partner to IRS1, but not IGF1R. (A) Compared with PTEN, UPP is a better binding partner for IRS1. 293T cells were transfected with IRS1-HA and indicated GFP-S-tagged constructs. PTEN or UPP were pulldown by S-protein agarose. Interaction with IRS1 were detected by HA antibody. (B) IRS1 binds preferentially to UPP. 293T cells were transfected with S-tagged IRS1 and C-terminal HA-tagged UPP (ATG) mutant expressing equal amount of PTEN and UPP. IRS1 were pulldown by S-protein agarose. (C) IGF1R binds equally to PTEN or UPP. 293T cells were transfected with S-tagged IGF1R and C-terminal HA-tagged UPP (ATG) mutant expressing equal amount of PTEN and UPP. IGF1R was pulldown by S-protein agarose.

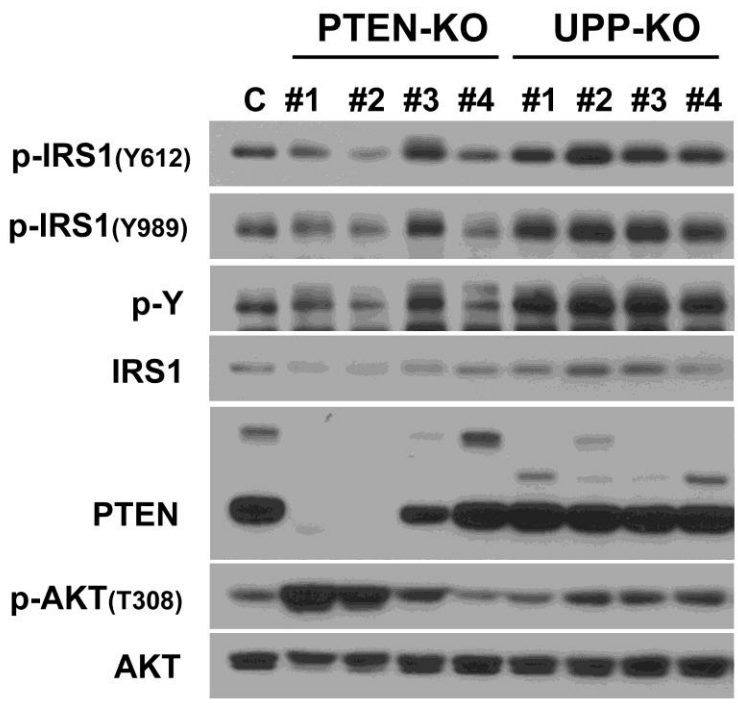

Figure 4.15

UPP-KO leads to more basal IRS1 tyrosine phosphorylation, but not AKT phosphorylation. Single clones of either PTEN or UPP knockout were generated by CRISPR/Cas9.

DISCUSSION

In this study, we purified the endogenous upper protein band of PTEN and the mass spectrometry result confirmed that it was indeed alternative translation of PTEN from the alternative CTG start codon. Surprisingly, exogenous over-expression of different-tagged versions using PTEN cDNA failed to generate the upper protein band, suggesting UPP is not a post-translational modification of PTEN. Subcellular fractionation and imaging data revealed a distinctive localization and shorter half-life of UPP compared to PTEN. Using biochemical assays, cellular experiments and colony formation assays, we demonstrated that UPP is a comparable lipid phosphatase as PTEN.

To determine the distinct localization of UPP we examined the colocalization of UPP with different organelle markers. Data from immunofluorescence and live cell imaging by confocal microscopy indicated a potential function of UPP in endocytosis and membrane trafficking. As UPP/PTEN-long has been shown to be a membrane-permeable lipid phosphatase that can be secreted from cells and enter neighboring cells (Hopkins et al., 2013), UPP might simply be a cargo protein in the endocytic pathway.

Moreover, we observed UPP co-localized with E-cadherin/β-catenin at adherens junctions. General investigations of PTEN localization has found its accumulation at cell-cell contacts and co-localization with E-cadherin/β-catenin upon

formation of growth-arrested structures in human mammary epithelial cells (Fournier et al., 2009). Change of expression of E-cadherin is a cell surface biomarker of epithelial-mesenchymal transition (EMT), which is an important early event in the invasion and metastasis of cancer (Zeisberg and Neilson, 2009). Additionally, PTEN loss promoted EMT in human colon cancer cell lines HCT116 and SW480 (Bowen et al., 2009). Furthermore, PTEN loss has been shown to cooperate with activation of the RAS/MAPK pathway to induce EMT and metastasis initiated from prostate stem/progenitor cells (Mulholland et al., 2012). However, those studies could not distinguish PTEN from UPP, and thus it is possible that UPP contributes to these functions.

We also demonstrated that UPP is a better binding partner for IRS1, but not IGF1R, suggesting a differential function of UPP. The physiological significance of UPP should be further evaluated in UPP specific knockout cell lines or mice. According to the preliminary data from UPP specific knockout cells, there is no drastic effect on pAKT levels, suggesting endogenous UPP is not the principle lipid phosphatase for PIP_3 in cells. In the future, we would like to measure the protein phosphatase activity of UPP in vitro and in cells. Additionally, to identify novel functions of UPP, we could look for UPP-specific binding proteins using tandem affinity purification. Once we confirm the physiological function of UPP, we would try to identify ubiquitin E3 ligase responsible for the unique regulation of UPP.

CHAPTER FIVE

MATERIALS AND METHODS

MATERIALS

Antibodies

p-Akt (T308) (cat#C31E5E), p-Akt (S473) (cat#D9E), Akt (cat#40D4), p-Erk1/2 (T202/Y204) (cat#D13.14.4E), Erk1/2 (cat#3A7), p-IGF1Rβ (Y1135/1136)/IRβ (Y1150/1151) (cat#19H7), p-IGF1Rβ(Y980) (Cat#4568), p-EGFR(Y1068) (cat#2234), E-cadherin (24E10) (cat#3195), Rab5 (C8B1) Rabbit mAb (cat#3547), Syntaxin 6 (C34B2) (Cat# 2869) are from Cell Signaling Technology.

Anti-IRS-1 (pY612) (Cat# 44-816G) and anti-IRS-1(pY896) (Cat# 44818G) are from Invitrogen. IGF1Rβ(C-20) (Cat# sc-713), anti-PTEN (clone A2B1) (Cat# sc-7974), p-IRS-1 (Y989) (Cat# sc-17200), NEDD4-1 (H-135) (Cat# sc-25508), and EGFR (1005) (Cat# sc-03) are from Santa Cruz Biotechnology.

Anti-IRS1 antibody (clone 4.2.2) (Cat# 05-1085), anti-IRS1 (Cat# 06-248) and anti-NEDD4 (Cat# 07-049) are from Millipore.

Anti-Mouse NEDD4 (Cat# 611480), Mouse Anti-β-Catenin (Cat# 610153), mouse Anti-EEA1 (Cat# 610457), Mouse Anti-cytochrome c (Cat# 556432) is from BD Transduction laboratories.

Anti-human PTEN (clone 6H2.1) (Cat# ABM-2052) and anti-human PTEN (clone 11G8.1) (Cat# ABM-2055) are from Cascade Bioscience.

Anti-phosphotyrosine clone PY-20 (Cat# P4110), anti-β-actin (Cat# A5316) and anti-γ-tubulin (clone GTU-88) (Cat# T6557) are from Sigma.

HA.11 clone 16B12 (Cat# MMS-101P) is from Covance.

Anti-α-tubulin (Cat# DM1A) is from Calbiochem.

Anti-KDEL, mAb (10C3) is from Enzo.

Other reagents

Mouse Insulin-like growth factor I (IGF-I) (Cat# I8779), human insulin-like growth factor-II (IGF-II) (cat# I2526), and human insulin (Cat# I2643) are from Sigma. Recombinant human epidermal growth factor (EGF) (Cat# AF-100-15) is from PEPROTECH. Doxycycline (Cat# 324385), and MG-132 (Cat# 474790) are from Calbiochem. Ubiquitin (Cat# U-100H), KO-Ubiquitin(Cat# UM-NOK), Ubiquitin Mutant with K48 only (Cat#: UM-K480), and Ubiquitin Mutant with K63 only (Cat#: UM-K630) were from bostonbiochem. Phosphatase inhibitor cocktail-2 (Y inhibitor) (Cat# P5726) for tyrosine protein phosphatases, phosphatase inhibitor cocktail-1 (Cat# P2850) for serine/threonine protein phosphatases, monoclonal anti-HA agarose conjugate clone HA-7 (Cat# A2095) and HA peptide (Cat# I2149) are from Sigma. IGF1Ri (OSI-906) and PI3Ki (GDC-0941) are from Selleck Chemicals; PI3Ki (BYL-719) is from Novartis. EGFRi Erlotinib (E-4007) is from LC laboratories. AKTi-1/2/3 (MK-2206) is from Merck. MitoTracker Red CMXRos (Cat#M-7512) is from

Invitrogen. Protein A or G sepharose is from GE Healthcare. Protein A/G plus-agarose (Cat# sc-2003) is from Santa Cruz. S-protein agarose (Cat# 69704) is from Millipore.

Plasmids and RNA interference

pcDNA3.1-IRS1-HA, pcDNA3.1-IGF1Rβ-HA, pQCXIP-GFP, pQCXIP-GFP-S-PTEN (WT/CS/GE), pQCXIP-NEDD4(WT), pQCXIP-NEDD4(CS) and pQCXIP-PTEN-S: For expression in cell lines, PTEN (WT/CS/GE) were subcloned into pQCXIP containing an N-terminal GFP and S tag. IRS1 and IGF1Rβ cDNAs were purchased from Addgene. For expression in 293T cells, PTEN, IRS1 and IGF1Rβ were subcloned into pcDNA3.1 containing a C-terminal HA tag. All the PTEN or IRS1 truncation mutants were amplified by PCR or two-step PCR and subcloned into pQCXIP with N-terminal HA tag.

To make UPP construct, PTEN cDNA with 5'UTR was PCR amplified from human PTEN cDNA pOTB7/PTEN (open biosystems) and cloned into pQCXIP containing a C-terminal S tag. Different UPP mutants were created using site-directed mutagenesis. For UPP and PTEN imaging, UPP and PTEN were sub-cloned into pQCXIP with a C-terminal GFP tag. To generate Dox-inducible expression constructs, UPP and PTEN were sub-cloned into pLVX-Tight-Puro (Clontech) and used with pLVX-Tet-On Advanced to generate cell line.

pLko.1-PTENi constructs: The PTEN DNA sequence used in the RNAi construct is CGACTTAGACTTGACCTATAT. Two-step PCRs were carried out to generate shRNA-resistant PTEN constructs with new sequence as

TGATCTCGATTTGACGTACAT. Control pLko.1-sc sequence is: CAACAAGATGAAGAGCACCAA. The Dox-inducible PTEN RNAi constructs were cloned into pLKO-Tet-On (Novartis). The sequences against mouse PTEN are: CGACTTAGACTTGACCTATAT and GCTAGAACTTATCAAACCCTT.

The Dox-inducible RNAi constructs against mouse NEDD4, human NEDD4 and mouse PTEN were generated using pTRIPZ vector according to manufacturer's procedure (Open biosystems). The mouse NEDD4 sequences are: GGAGTATATCTACCTTGTAAT and TGGGCGAGTCTTCTTCATAAA. The human NEDD4 sequences are: GGAGGGAACATACAAAGTATA and ATGGAAGAATCTTCTACATAA. The mouse PTEN sequences are: GCTAGAACTTATCAAACCCTT and CAGCTAAAGGTGAAGATAT. Control pTRIPZ-NT sequence is: CAACAAGATGAAGAGCACCAA.

To knockout genes using CRISRP/Cas9, the sequences used for human PTEN are: CCTTTTGAAGACCATAACCCACC and TATCCAAACATTATTGCTATGGG. The sequences for human UPP are: GCTCCGGAGGCCGCCGGCGGAGG and GCGGCGGCGGCGGCACATCCAGG.

Cell lines

NEDD4$^{-/-}$ MEFs and paired NEDD4$^{+/+}$ MEFs were provided by Dr. Baoli Yang (University of Iowa). TC71, PC9, MCF7 and MDA-MB-468 were from Dr. Neal Rosen.

METHODS

Western blotting

Cells were washed twice with ice-cold phosphate-buffered saline and lysed in ice-cold cell lysis buffer (10mM Tris, pH7.5, 100mM NaCl, 1% Triton-X100, 0.1% SDS, 0.5% sodium deoxycholate, 10% glycerol, 1mM EGTA, 1mM EDTA, 0.1% 2-mercaptoethanol and protease and phosphatase inhibitors). Equal amount of proteins were subjected to SDS-PAGE at 150 V and transferred to polyvinylidene difluoride membranes at 400 mM for 90min. The membrane is blocked with 5% milk for 30 min at room temperature, then washed with 3X10min with 0.1% Tween-20 in TBS (Tris Buffered Saline), the membrane is incubated with primary antibody diluted in 1% BSA in TBST for 1 hr at room temperature or overnight at 4^{o}C. After washing 3X10min with 0.1% Tween-20 in TBS, the membrane is then incubated with secondary antibody diluted in 1% BSA in TBST for 30-60 min at room temperature, washed and subjected to enhanced chemiluminescence (ECL).

Cell culture and transfection

Cell culture- MEFs, 293T, U2OS and PC3 were cultured in high glucose Dullbecco's modified Eagle's medium supplemented with 10% fetal bovine serum, 2mM L-glutamine and penicillin-streptomycin at 37^{o}C with 5% CO_2. TC71 and PC9 cell lines were cultured in PRMI supplemented 10% FBS, L-glutamine and penicillin-

streptomycin at 37^{o}C with 5% CO_2. MCF7 and MDA-MB-468 were maintained in DEM HG: F12 medium supplemented with 10% FBS, L-glutamine and penicillin-streptomycin at 37^{o}C with 5% CO_2. Transfections were carried out with Lipofectamine 2000 following the instruction manual, or with 1mg/ml PEI (DNA: PEI=1:3). For MCF7, transfection was performed by electroporation, using Amaxa cell line Nucleotector kit V.

Co-immunoprecipitations

Following indicated treatments in individual experiments, cells grown in 10-cm plates were placed on ice and washed with ice-cold PBS, followed by lysis in IP buffer (50 mM HEPES, pH7.4, 150 mM NaCl, 1 mM EDTA, 0.5 mM DTT, 10% glycerol, 0.5% Triton-X100) plus protease inhibitors, phosphatase inhibitors and 25 μM MG132. Lysates were then centrifuged at 4^{o}C for 10 min. Clarified lysates were then incubated with S-protein agarose (EMD, Cat# 69704-3) pre-washed in IP buffer overnight with rotation at 4^{o}C. Beads were then washed five times with IP buffer, eluted in 1 x SDS-sample buffer and analyzed by immunoblot. For endogenous PTEN IP, cell lysates were incubated with anti-human PTEN (clone 6H2.1) overnight at 4^{o}C. Then protein-G Sepharose (GE Healthcare, Cat# 17-0618-01) was added and incubated for 3 hrs at 4^{o}C, washed with IP buffer for three times and eluted with 1 x SDS-sample buffer.

Subcellular fractionation

Harvest 5 million cells per sample by scraping in ice-cold PBS, then resuspend cell pellet in hypotonic buffer ((10mM HEPES, pH7.5; 1mM DTT; 10mM NaCl; 0.1mM EDTA; 0.1mM EGTA; 200mM Sucrose), with phosphates, protease inhibitors and incubate on ice for 15min. After Freeze-thaw cycles three times, cells were further broken down by passing through 27G1/2 needles. Cell lysates were subjected to differential centrifugation: 1000g for 10min (pellet: whole cells and nucleus), then 12,000 g for 10 min (pellet: heavy membrane including mitochondria and lysosome), then 100,000 g for 2 hours (pellet: light membrane including microsome and other small vesicles), supernatant includes cytosol fraction. For each pellet, wash with PBS twice before resuspend in extraction buffer.

Recombinant PTEN and NEDD4 protein preparation

For recombinant protein expression, PTEN (WT/C124S/G129E) or NEDD4 were subcloned into pFastBac containing N-terminal His tag and UPP was subcloned into pFastBac containing C-terminal His tag. Recombinant PTEN, NEDD4 and UPP proteins were expressed in Sf9 cells using the Bac-to-Bac expression system from Invitrogen. Cell pellets were re-suspended in Buffer A (20 mM Tris-HCl, pH7.5, 50 mM NaCl, 1 mM DTT) and purified by Ni-NTA affinity chromatography according to standard procedures. Following extensive washing, proteins were eluted stepwise in Buffer A containing 10-250 mM imidazole. Pure fractions were pooled and dialyzed in 25 mM Tris, pH 7.5, 100 mM NaCl and 1 mM DTT. PTEN Proteins were further

purified by gel filtration (Superdex-200 column). Single peak fractions were collected, snap frozen and stored at -80^{o}C in aliquots.

In vitro PTEN ubiquitination assay

The reaction was carried out at 30^{o}C for indicated time in a volume of 15µl containing 50mM HEPES(pH7.5), 2mM DTT, 5mM $MgCl_2$, 10µg of wild-type ubiquitin, K48-Ub, K63-Ub or ko-Ub (Boston Biochem) as indicated, 50nM hE1, 1µM UbCH5c, 5mM ATP, 50ng of recombinant HA-tagged PTEN, 1µM purified rNEDD4-1 from baculovirus-infected insect cells. The reaction was then stopped by adding 5µl of 4XSDS/PAGE sample buffer and boiled for 5 min. The samples were then resolved by SDS/8% PAGE and the ubiquitinated PTEN species were detected by western blotting using HA tag.

In vitro Lipid phosphatase assay

Soluble di-C8-D-myo-Phosphatidylinositol 3,4,5 trisphosphate (PIP3) was purchased from Echelon and diluted to 0.1 mM in a phosphate-free buffer (20 mM HEPES, pH 7.4, 1 mM EGTA). Then phospholipid vesicles (PLV) were prepared by sonication of 0.1 mM diC8PIP3 and 0.5 mM DOPS (Sigma # P-1060). In a 25-µl final volume (100 mM Tris-HCl, pH 8.0, 2 mM DTT), indicated amounts of purified PTEN recombinant proteins were incubated with 10 µl of PLV (thus final diC8PIP3 concentration was 40 µM), for 15 min at 37 ℃. 100 µl of Malachite Green solution were added to terminate

the enzyme reaction and incubated for 20 minutes at room temperature. The released phosphate was measured by absorption at 620 nm.

In vitro PTEN protein phosphatase assay

To prepare p-IRS-1 and p-IGF1R, HEK293T cells were co-transfected with IRS-1-HA/IGF1R-HA, serum starved and then stimulated with 100 ng/ml IGF1 for 10 min. After cells were lysed in cell lysis buffer (10 mM Tris, pH7.4, 100 mM NaCl, 1 mM EDTA, 1 mM EGTA, 0.1% SDS, 0.5% sodium deoxycholate, 1% Triton-X 100, 10% glycerol) containing protease inhibitors and phosphatase inhibitors, tyrosyl-phosphorylated IRS-1 and IGF1R were immunoprecipitated from the lysates using anti-HA agarose beads overnight with rotation at 4^{o}C. Beads were thrice washed in cell lysis buffer, then washed with phosphatase assay buffer (20 mM HEPES, pH7.5, 50 mM NaCl, 5 mM $MgCl_2$, 1mM DTT, 0.1% NP40). IRS-1-HA and IGF1R-HA were then eluted in phosphatase assay buffer containing 100 μg/ml HA peptide for 30 min at 4^{o}C. The eluant was incubated with indicated recombinant PTEN protein in the absence or presence of phosphatase inhibitor cocktail-2 (Y inhibitor) at 30^{o}C for 1 hr. The reaction was terminated by adding SDS sample buffer, boiling for 5 min, and subjecting to immunoblotting.

Cellular PI(3,4,5)P3 measurement

Cellular PtdInsP3 content was measured using PI3 kinase homogenous cell-based assay kit TR-FRET (Millipore, Cat#17-494). Lipids were extracted from $2X10^6$ PC3 cells and cellular PIP_3 level was detected following the instruction manual.

Cell growth assay and colony formation assay

For cell growth assay, $2x10^4$ TC71 or $5x10^4$ PC9 cells were seeded in 6-well plates. Twenty-four hours later, 1 μg/ml Dox was added to the cells. Then cells were trypsinized and counted after indicated days of culture. For colony formation assay, $2x10^3$ TC71, $1x10^3$ PC9 or $1x10^3$ PC3 cells were seeded in 6-well plates; 24-hr later cells were treated with 1 μg/ml Dox in fresh growth media for 2 weeks. To visualize cell colonies, cells were fixed with 3.7% formaldehyde and stained with Giemsa stain (Sigma).

Glucose metabolism

MEFs with inducible NEDD4 shRNA (shN4-A) were treated with or without 1 μg/ml Dox for 2 days, then $1.5x10^5$ cells were seeded in 6-well plates, serum-starved for 6 hrs, and then stimulated with 200 ng/ml insulin for 18 hours. Conditioned media were taken before and after insulin treatment. Concentration of glucose, lactate, glutamine and glutamate in the media were measured using an YSI 7100 nutrient analyzer (YSI Life Sciences). Rates of consumption or secretion were calculated, normalizing to cell

numbers (average of the starting and final cell numbers). Statistical significance was determined using a one-tailed student's t test.

Microscopy and live cell imaging

For fluorescence analysis, cells were grown stably on glass coverslips in a six-well plate. After 24 hrs, treated cells were then fixed with 3.7% paraformaldehyde in 20mM HEPES pH7.5 for 20min at room temperature, followed by permeabilization in 0.2% Triton in PBS for 5min. Slides were then incubated with primary antibodies in blocking buffer (PBS supplemented with 1% BSA) at room temperature for 1hr or at 4 degree for overnight followed by incubation with Alexa Fluo secondary antibodies (Invitrogen) for 30 min at room temperature. After extensive washing, coverslips were mounted on microscope slides and visualized with a Nikon Eclipse Ti-U confocal microscope using a x20 or x60 objective. Images were acquired using Nikon EZ-C1 image acquisition software and edited using Photoshop. For live cell imaging cells were grown in 35 mm glass bottom dishes (MatTek) and imaged using an Ultraview Vox (Perkin Elmer) spinning disc confocal with a Nikon Ti-E microscope, Hamamatsu C9100-13 EMCCD camera, heated incubation chamber with CO2 and Volocity image acquisition software (Improvision).

REFERENCES

Al-Khouri, A.M., Ma, Y., Togo, S.H., Williams, S., and Mustelin, T. (2005). Cooperative phosphorylation of the tumor suppressor phosphatase and tensin homologue (PTEN) by casein kinases and glycogen synthase kinase 3beta. J Biol Chem *280*, 35195-35202.

Amodio, N., Scrima, M., Palaia, L., Salman, A.N., Quintiero, A., Franco, R., Botti, G., Pirozzi, P., Rocco, G., De Rosa, N.*, et al.* (2010). Oncogenic role of the E3 ubiquitin ligase NEDD4-1, a PTEN negative regulator, in non-small-cell lung carcinomas. Am J Pathol *177*, 2622-2634.

Anan, T., Nagata, Y., Koga, H., Honda, Y., Yabuki, N., Miyamoto, C., Kuwano, A., Matsuda, I., Endo, F., Saya, H.*, et al.* (1998). Human ubiquitin-protein ligase Nedd4: expression, subcellular localization and selective interaction with ubiquitin-conjugating enzymes. Genes Cells *3*, 751-763.

Anindya, R., Aygün, O., and Svejstrup, J.Q. (2007). Damage-induced ubiquitylation of human RNA polymerase II by the ubiquitin ligase Nedd4, but not Cockayne syndrome proteins or BRCA1. Mol Cell *28*, 386-397.

Bassi, C., Ho, J., Srikumar, T., Dowling, R.J., Gorrini, C., Miller, S.J., Mak, T.W., Neel, B.G., Raught, B., and Stambolic, V. (2013). Nuclear PTEN controls DNA repair and sensitivity to genotoxic stress. Science *341*, 395-399.

Boura-Halfon, S., and Zick, Y. (2009). Phosphorylation of IRS proteins, insulin action, and insulin resistance. Am J Physiol Endocrinol Metab *296*, E581-591.

Bowen, K.A., Doan, H.Q., Zhou, B.P., Wang, Q., Zhou, Y., Rychahou, P.G., and Evers, B.M. (2009). PTEN loss induces epithelial--mesenchymal transition in human colon cancer cells. Anticancer Res *29*, 4439-4449.

Cantley, L.C. (2002). The phosphoinositide 3-kinase pathway. Science *296*, 1655-1657.

Cao, X.R., Lill, N.L., Boase, N., Shi, P.P., Croucher, D.R., Shan, H., Qu, J., Sweezer, E.M., Place, T., Kirby, P.A.*, et al.* (2008). Nedd4 controls animal growth by regulating IGF-1 signaling. Sci Signal *1*, ra5.

Casaletto, J.B., and McClatchey, A.I. (2012). Spatial regulation of receptor tyrosine kinases in development and cancer. Nat Rev Cancer *12*, 387-400.

Chandarlapaty, S., Sawai, A., Scaltriti, M., Rodrik-Outmezguine, V., Grbovic-Huezo, O., Serra, V., Majumder, P.K., Baselga, J., and Rosen, N. (2011). AKT inhibition relieves feedback suppression of receptor tyrosine kinase expression and activity. Cancer Cell *19*, 58-71.

Chen, M., Pratt, C.P., Zeeman, M.E., Schultz, N., Taylor, B.S., O'Neill, A., Castillo-Martin, M., Nowak, D.G., Naguib, A., Grace, D.M.*, et al.* (2011). Identification of PHLPP1 as a tumor

suppressor reveals the role of feedback activation in PTEN-mutant prostate cancer progression. Cancer Cell *20*, 173-186.

Christoforidis, S., McBride, H.M., Burgoyne, R.D., and Zerial, M. (1999). The Rab5 effector EEA1 is a core component of endosome docking. Nature *397*, 621-625.
Copps, K.D., and White, M.F. (2012). Regulation of insulin sensitivity by serine/threonine phosphorylation of insulin receptor substrate proteins IRS1 and IRS2. Diabetologia *55*, 2565-2582.

Dai, B., Pieper, R.O., Li, D., Wei, P., Liu, M., Woo, S.Y., Aldape, K.D., Sawaya, R., Xie, K., and Huang, S. (2010). FoxM1B regulates NEDD4-1 expression, leading to cellular transformation and full malignant phenotype in immortalized human astrocytes. Cancer Res *70*, 2951-2961.

Davidson, L., Maccario, H., Perera, N.M., Yang, X., Spinelli, L., Tibarewal, P., Glancy, B., Gray, A., Weijer, C.J., Downes, C.P.*, et al.* (2010). Suppression of cellular proliferation and invasion by the concerted lipid and protein phosphatase activities of PTEN. Oncogene *29*, 687-697.

Drinjakovic, J., Jung, H., Campbell, D.S., Strochlic, L., Dwivedy, A., and Holt, C.E. (2010). E3 ligase Nedd4 promotes axon branching by downregulating PTEN. Neuron *65*, 341-357.

Engelman, J.A., Luo, J., and Cantley, L.C. (2006). The evolution of phosphatidylinositol 3-kinases as regulators of growth and metabolism. Nat Rev Genet *7*, 606-619.

Esposito, D.L., Li, Y., Cama, A., and Quon, M.J. (2001). Tyr(612) and Tyr(632) in human insulin receptor substrate-1 are important for full activation of insulin-stimulated phosphatidylinositol 3-kinase activity and translocation of GLUT4 in adipose cells. Endocrinology *142*, 2833-2840.

Fouladkou, F., Landry, T., Kawabe, H., Neeb, A., Lu, C., Brose, N., Stambolic, V., and Rotin, D. (2008). The ubiquitin ligase Nedd4-1 is dispensable for the regulation of PTEN stability and localization. Proc Natl Acad Sci U S A *105*, 8585-8590.

Fournier, M.V., Fata, J.E., Martin, K.J., Yaswen, P., and Bissell, M.J. (2009). Interaction of E-cadherin and PTEN regulates morphogenesis and growth arrest in human mammary epithelial cells. Cancer Res *69*, 4545-4552.

Galic, S., Hauser, C., Kahn, B.B., Haj, F.G., Neel, B.G., Tonks, N.K., and Tiganis, T. (2005). Coordinated regulation of insulin signaling by the protein tyrosine phosphatases PTP1B and TCPTP. Mol Cell Biol *25*, 819-829.

Goldstein, B.J., Bittner-Kowalczyk, A., White, M.F., and Harbeck, M. (2000). Tyrosine dephosphorylation and deactivation of insulin receptor substrate-1 by protein-tyrosine phosphatase 1B. Possible facilitation by the formation of a ternary complex with the Grb2 adaptor protein. J Biol Chem *275*, 4283-4289.

Gu, J., Tamura, M., Pankov, R., Danen, E.H., Takino, T., Matsumoto, K., and Yamada, K.M. (1999). Shc and FAK differentially regulate cell motility and directionality modulated by PTEN. J Cell Biol *146*, 389-403.

Guo, H., Qiao, G., Ying, H., Li, Z., Zhao, Y., Liang, Y., Yang, L., Lipkowitz, S., Penninger, J.M., Langdon, W.Y.*, et al.* (2012). E3 ubiquitin ligase Cbl-b regulates Pten via Nedd4 in T cells independently of its ubiquitin ligase activity. Cell Rep *1*, 472-482.

Hann, S.R., King, M.W., Bentley, D.L., Anderson, C.W., and Eisenman, R.N. (1988). A non-AUG translational initiation in c-myc exon 1 generates an N-terminally distinct protein whose synthesis is disrupted in Burkitt's lymphomas. Cell *52*, 185-195.
Harrington, L.S., Findlay, G.M., Gray, A., Tolkacheva, T., Wigfield, S., Rebholz, H., Barnett, J., Leslie, N.R., Cheng, S., Shepherd, P.R.*, et al.* (2004). The TSC1-2 tumor suppressor controls insulin-PI3K signaling via regulation of IRS proteins. J Cell Biol *166*, 213-223.

Heit, B., Robbins, S.M., Downey, C.M., Guan, Z., Colarusso, P., Miller, B.J., Jirik, F.R., and Kubes, P. (2008). PTEN functions to 'prioritize' chemotactic cues and prevent 'distraction' in migrating neutrophils. Nat Immunol *9*, 743-752.

Hopkins, B.D., Fine, B., Steinbach, N., Dendy, M., Rapp, Z., Shaw, J., Pappas, K., Yu, J.S., Hodakoski, C., Mense, S.*, et al.* (2013). A secreted PTEN phosphatase that enters cells to alter signaling and survival. Science *341*, 399-402.

Howitt, J., Lackovic, J., Low, L.H., Naguib, A., Macintyre, A., Goh, C.P., Callaway, J.K., Hammond, V., Thomas, T., Dixon, M.*, et al.* (2012). Ndfip1 regulates nuclear Pten import in vivo to promote neuronal survival following cerebral ischemia. J Cell Biol *196*, 29-36.

Huang, J., Yan, J., Zhang, J., Zhu, S., Wang, Y., Shi, T., Zhu, C., Chen, C., Liu, X., Cheng, J.*, et al.* (2012). SUMO1 modification of PTEN regulates tumorigenesis by controlling its association with the plasma membrane. Nat Commun *3*, 911.

Ikeda, F., and Dikic, I. (2008). Atypical ubiquitin chains: new molecular signals. 'Protein Modifications: Beyond the Usual Suspects' review series. EMBO Rep *9*, 536-542.

Ikenoue, T., Inoki, K., Zhao, B., and Guan, K.L. (2008). PTEN acetylation modulates its interaction with PDZ domain. Cancer Res *68*, 6908-6912.

Karreth, F.A., Tay, Y., Perna, D., Ala, U., Tan, S.M., Rust, A.G., DeNicola, G., Webster, K.A., Weiss, D., Perez-Mancera, P.A.*, et al.* (2011). In vivo identification of tumor- suppressive PTEN ceRNAs in an oncogenic BRAF-induced mouse model of melanoma. Cell *147*, 382-395.

Kiefer, P., Acland, P., Pappin, D., Peters, G., and Dickson, C. (1994). Competition between nuclear localization and secretory signals determines the subcellular fate of a single CUG-initiated form of FGF3. EMBO J *13*, 4126-4136.

Kim, H.T., Kim, K.P., Lledias, F., Kisselev, A.F., Scaglione, K.M., Skowyra, D., Gygi, S.P., and Goldberg, A.L. (2007). Certain pairs of ubiquitin-conjugating enzymes (E2s) and ubiquitin-

protein ligases (E3s) synthesize nondegradable forked ubiquitin chains containing all possible isopeptide linkages. J Biol Chem *282*, 17375-17386.

Kim, J.S., Xu, X., Li, H., Solomon, D., Lane, W.S., Jin, T., and Waldman, T. (2011). Mechanistic analysis of a DNA damage-induced, PTEN-dependent size checkpoint in human cells. Mol Cell Biol *31*, 2756-2771.

Kim, Y.C., Kitaura, H., Taira, T., Iguchi-Ariga, S.M., and Ariga, H. (2009). Oxidation of DJ-1-dependent cell transformation through direct binding of DJ-1 to PTEN. Int J Oncol *35*, 1331-1341.

Kitamura, T., Kahn, C.R., and Accili, D. (2003). Insulin receptor knockout mice. Annu Rev Physiol *65*, 313-332.
Kozak, M. (1989). Context effects and inefficient initiation at non-AUG codons in eucaryotic cell-free translation systems. Mol Cell Biol *9*, 5073-5080.

Kozak, M. (1991). An analysis of vertebrate mRNA sequences: intimations of translational control. J Cell Biol *115*, 887-903.

Kumar, S., Harvey, K.F., Kinoshita, M., Copeland, N.G., Noda, M., and Jenkins, N.A. (1997). cDNA cloning, expression analysis, and mapping of the mouse Nedd4 gene. Genomics *40*, 435-443.

Kumar, S., Tomooka, Y., and Noda, M. (1992). Identification of a set of genes with developmentally down-regulated expression in the mouse brain. Biochem Biophys Res Commun *185*, 1155-1161.

Kwak, Y.D., Ma, T., Diao, S., Zhang, X., Chen, Y., Hsu, J., Lipton, S.A., Masliah, E., Xu, H., and Liao, F.F. (2010a). NO signaling and S-nitrosylation regulate PTEN inhibition in neurodegeneration. Mol Neurodegener *5*, 49.

Kwak, Y.D., Wang, B., Pan, W., Xu, H., Jiang, X., and Liao, F.F. (2010b). Functional interaction of phosphatase and tensin homologue (PTEN) with the E3 ligase NEDD4-1 during neuronal response to zinc. J Biol Chem *285*, 9847-9857.

Kwon, J., Lee, S.R., Yang, K.S., Ahn, Y., Kim, Y.J., Stadtman, E.R., and Rhee, S.G. (2004). Reversible oxidation and inactivation of the tumor suppressor PTEN in cells stimulated with peptide growth factors. Proc Natl Acad Sci U S A *101*, 16419-16424.

Lackey, J., Barnett, J., Davidson, L., Batty, I.H., Leslie, N.R., and Downes, C.P. (2007). Loss of PTEN selectively desensitizes upstream IGF1 and insulin signaling. Oncogene *26*, 7132-7142.

Lee, J.O., Yang, H., Georgescu, M.M., Di Cristofano, A., Maehama, T., Shi, Y., Dixon, J.E., Pandolfi, P., and Pavletich, N.P. (1999). Crystal structure of the PTEN tumor suppressor: implications for its phosphoinositide phosphatase activity and membrane association. Cell *99*, 323-334.

Lee, S.R., Yang, K.S., Kwon, J., Lee, C., Jeong, W., and Rhee, S.G. (2002). Reversible inactivation of the tumor suppressor PTEN by H2O2. J Biol Chem *277*, 20336-20342.

Leslie, N.R., Bennett, D., Lindsay, Y.E., Stewart, H., Gray, A., and Downes, C.P. (2003). Redox regulation of PI 3-kinase signalling via inactivation of PTEN. EMBO J *22*, 5501-5510.

Li, D.M., and Sun, H. (1997). TEP1, encoded by a candidate tumor suppressor locus, is a novel protein tyrosine phosphatase regulated by transforming growth factor beta. Cancer Res *57*, 2124-2129.

Li, J., Yen, C., Liaw, D., Podsypanina, K., Bose, S., Wang, S.I., Puc, J., Miliaresis, C., Rodgers, L., McCombie, R.*, et al.* (1997). PTEN, a putative protein tyrosine phosphatase gene mutated in human brain, breast, and prostate cancer. Science *275*, 1943-1947.

Li, Z., Dong, X., Wang, Z., Liu, W., Deng, N., Ding, Y., Tang, L., Hla, T., Zeng, R., Li, L.*, et al.* (2005). Regulation of PTEN by Rho small GTPases. Nat Cell Biol *7*, 399-404.
Liang, H., He, S., Yang, J., Jia, X., Wang, P., Chen, X., Zhang, Z., Zou, X., McNutt, M.A., Shen, W.H.*, et al.* (2014). PTENα, a PTEN Isoform Translated through Alternative Initiation, Regulates Mitochondrial Function and Energy Metabolism. Cell Metab *19*, 836-848.

Lin, Q., Wang, J., Childress, C., Sudol, M., Carey, D.J., and Yang, W. (2010). HECT E3 ubiquitin ligase Nedd4-1 ubiquitinates ACK and regulates epidermal growth factor (EGF)-induced degradation of EGF receptor and ACK. Mol Cell Biol *30*, 1541-1554.

Liu, J.P., Baker, J., Perkins, A.S., Robertson, E.J., and Efstratiadis, A. (1993). Mice carrying null mutations of the genes encoding insulin-like growth factor I (Igf-1) and type 1 IGF receptor (Igf1r). Cell *75*, 59-72.

Maccario, H., Perera, N.M., Davidson, L., Downes, C.P., and Leslie, N.R. (2007). PTEN is destabilized by phosphorylation on Thr366. Biochem J *405*, 439-444.

Maccario, H., Perera, N.M., Gray, A., Downes, C.P., and Leslie, N.R. (2010). Ubiquitination of PTEN (phosphatase and tensin homolog) inhibits phosphatase activity and is enhanced by membrane targeting and hyperosmotic stress. J Biol Chem *285*, 12620-12628.

Maehama, T., and Dixon, J.E. (1998). The tumor suppressor, PTEN/MMAC1, dephosphorylates the lipid second messenger, phosphatidylinositol 3,4,5-trisphosphate. J Biol Chem *273*, 13375-13378.

Mahimainathan, L., and Choudhury, G.G. (2004). Inactivation of platelet-derived growth factor receptor by the tumor suppressor PTEN provides a novel mechanism of action of the phosphatase. J Biol Chem *279*, 15258-15268.

Maier, D., Jones, G., Li, X., Schönthal, A.H., Gratzl, O., Van Meir, E.G., and Merlo, A. (1999). The PTEN lipid phosphatase domain is not required to inhibit invasion of glioma cells. Cancer Res *59*, 5479-5482.

Mani, A., and Gelmann, E.P. (2005). The ubiquitin-proteasome pathway and its role in cancer. J Clin Oncol *23*, 4776-4789.

Manning, B.D., and Cantley, L.C. (2007). AKT/PKB signaling: navigating downstream. Cell *129*, 1261-1274.

Meng, F., Henson, R., Wehbe-Janek, H., Ghoshal, K., Jacob, S.T., and Patel, T. (2007). MicroRNA-21 regulates expression of the PTEN tumor suppressor gene in human hepatocellular cancer. Gastroenterology *133*, 647-658.

Mulholland, D.J., Kobayashi, N., Ruscetti, M., Zhi, A., Tran, L.M., Huang, J., Gleave, M., and Wu, H. (2012). Pten loss and RAS/MAPK activation cooperate to promote EMT and metastasis initiated from prostate cancer stem/progenitor cells. Cancer Res *72*, 1878-1889.

Mund, T., and Pelham, H.R. (2010). Regulation of PTEN/Akt and MAP kinase signaling pathways by the ubiquitin ligase activators Ndfip1 and Ndfip2. Proc Natl Acad Sci U S A *107*, 11429-11434.

Myers, M.P., Stolarov, J.P., Eng, C., Li, J., Wang, S.I., Wigler, M.H., Parsons, R., and Tonks, N.K. (1997). P-TEN, the tumor suppressor from human chromosome 10q23, is a dual-specificity phosphatase. Proc Natl Acad Sci U S A *94*, 9052-9057.

Numajiri, N., Takasawa, K., Nishiya, T., Tanaka, H., Ohno, K., Hayakawa, W., Asada, M., Matsuda, H., Azumi, K., Kamata, H.*, et al.* (2011). On-off system for PI3-kinase-Akt signaling through S-nitrosylation of phosphatase with sequence homology to tensin (PTEN). Proc Natl Acad Sci U S A *108*, 10349-10354.

Odriozola, L., Singh, G., Hoang, T., and Chan, A.M. (2007). Regulation of PTEN activity by its carboxyl-terminal autoinhibitory domain. J Biol Chem *282*, 23306-23315.

Okahara, F., Itoh, K., Nakagawara, A., Murakami, M., Kanaho, Y., and Maehama, T. (2006). Critical role of PICT-1, a tumor suppressor candidate, in phosphatidylinositol 3,4,5-trisphosphate signals and tumorigenic transformation. Mol Biol Cell *17*, 4888-4895.

Okumura, K., Mendoza, M., Bachoo, R.M., DePinho, R.A., Cavenee, W.K., and Furnari, F.B. (2006). PCAF modulates PTEN activity. J Biol Chem *281*, 26562-26568.

Ozes, O.N., Akca, H., Mayo, L.D., Gustin, J.A., Maehama, T., Dixon, J.E., and Donner, D.B. (2001). A phosphatidylinositol 3-kinase/Akt/mTOR pathway mediates and PTEN antagonizes tumor necrosis factor inhibition of insulin signaling through insulin receptor substrate-1. Proc Natl Acad Sci U S A *98*, 4640-4645.

Pautsch, A., Zoephel, A., Ahorn, H., Spevak, W., Hauptmann, R., and Nar, H. (2001). Crystal structure of bisphosphorylated IGF-1 receptor kinase: insight into domain movements upon kinase activation. Structure *9*, 955-965.

Pelham, H.R. (1990). The retention signal for soluble proteins of the endoplasmic reticulum. Trends Biochem Sci *15*, 483-486.

Persaud, A., Alberts, P., Amsen, E.M., Xiong, X., Wasmuth, J., Saadon, Z., Fladd, C., Parkinson, J., and Rotin, D. (2009). Comparison of substrate specificity of the ubiquitin ligases Nedd4 and Nedd4-2 using proteome arrays. Mol Syst Biol *5*, 333.

Poliseno, L., Salmena, L., Zhang, J., Carver, B., Haveman, W.J., and Pandolfi, P.P. (2010). A coding-independent function of gene and pseudogene mRNAs regulates tumour biology. Nature *465*, 1033-1038.

Qin, L., Wang, Y., Tao, L., and Wang, Z. (2011). AKT down-regulates insulin-like growth factor-1 receptor as a negative feedback. J Biochem *150*, 151-156.

Raftopoulou, M., Etienne-Manneville, S., Self, A., Nicholls, S., and Hall, A. (2004). Regulation of cell migration by the C2 domain of the tumor suppressor PTEN. Science *303*, 1179-1181.

Rahdar, M., Inoue, T., Meyer, T., Zhang, J., Vazquez, F., and Devreotes, P.N. (2009). A phosphorylation-dependent intramolecular interaction regulates the membrane association and activity of the tumor suppressor PTEN. Proc Natl Acad Sci U S A *106*, 480-485.

Reddy, P., Liu, L., Adhikari, D., Jagarlamudi, K., Rajareddy, S., Shen, Y., Du, C., Tang, W., Hämäläinen, T., Peng, S.L*., et al.* (2008). Oocyte-specific deletion of Pten causes premature activation of the primordial follicle pool. Science *319*, 611-613.

Rotin, D., and Kumar, S. (2009). Physiological functions of the HECT family of ubiquitin ligases. Nat Rev Mol Cell Biol *10*, 398-409.

Salmena, L., Carracedo, A., and Pandolfi, P.P. (2008). Tenets of PTEN tumor suppression. Cell *133*, 403-414.

Sesti, G., Federici, M., Hribal, M.L., Lauro, D., Sbraccia, P., and Lauro, R. (2001). Defects of the insulin receptor substrate (IRS) system in human metabolic disorders. FASEB J *15*, 2099-2111.

Shi, Y., Paluch, B.E., Wang, X., and Jiang, X. (2012). PTEN at a glance. J Cell Sci *125*, 4687-4692.

Smith, F.M., Holt, L.J., Garfield, A.S., Charalambous, M., Koumanov, F., Perry, M., Bazzani, R., Sheardown, S.A., Hegarty, B.D., Lyons, R.J*., et al.* (2007). Mice with a disruption of the imprinted Grb10 gene exhibit altered body composition, glucose homeostasis, and insulin signaling during postnatal life. Mol Cell Biol *27*, 5871-5886.

Song, M.S., Carracedo, A., Salmena, L., Song, S.J., Egia, A., Malumbres, M., and Pandolfi, P.P. (2011). Nuclear PTEN regulates the APC-CDH1 tumor-suppressive complex in a phosphatase-independent manner. Cell *144*, 187-199.

Song, M.S., Salmena, L., and Pandolfi, P.P. (2012). The functions and regulation of the PTEN tumour suppressor. Nat Rev Mol Cell Biol *13*, 283-296.

Staub, O., Dho, S., Henry, P., Correa, J., Ishikawa, T., McGlade, J., and Rotin, D. (1996). WW domains of Nedd4 bind to the proline-rich PY motifs in the epithelial Na+ channel deleted in Liddle's syndrome. EMBO J *15*, 2371-2380.

Steck, P.A., Pershouse, M.A., Jasser, S.A., Yung, W.K., Lin, H., Ligon, A.H., Langford, L.A., Baumgard, M.L., Hattier, T., Davis, T.*, et al.* (1997). Identification of a candidate tumour suppressor gene, MMAC1, at chromosome 10q23.3 that is mutated in multiple advanced cancers. Nat Genet *15*, 356-362.

Tamura, M., Gu, J., Matsumoto, K., Aota, S., Parsons, R., and Yamada, K.M. (1998). Inhibition of cell migration, spreading, and focal adhesions by tumor suppressor PTEN. Science *280*, 1614-1617.

Tamura, M., Gu, J., Takino, T., and Yamada, K.M. (1999). Tumor suppressor PTEN inhibition of cell invasion, migration, and growth: differential involvement of focal adhesion kinase and p130Cas. Cancer Res *59*, 442-449.

Taniguchi, C.M., Emanuelli, B., and Kahn, C.R. (2006). Critical nodes in signalling pathways: insights into insulin action. Nat Rev Mol Cell Biol *7*, 85-96.

Tibarewal, P., Zilidis, G., Spinelli, L., Schurch, N., Maccario, H., Gray, A., Perera, N.M., Davidson, L., Barton, G.J., and Leslie, N.R. (2012). PTEN protein phosphatase activity correlates with control of gene expression and invasion, a tumor-suppressing phenotype, but not with AKT activity. Sci Signal *5*, ra18.

Tiganis, T. (2013). PTP1B and TCPTP--nonredundant phosphatases in insulin signaling and glucose homeostasis. FEBS J *280*, 445-458.
Torres, J., and Pulido, R. (2001). The tumor suppressor PTEN is phosphorylated by the protein kinase CK2 at its C terminus. Implications for PTEN stability to proteasome-mediated degradation. J Biol Chem *276*, 993-998.

Trotman, L.C., Wang, X., Alimonti, A., Chen, Z., Teruya-Feldstein, J., Yang, H., Pavletich, N.P., Carver, B.S., Cordon-Cardo, C., Erdjument-Bromage, H.*, et al.* (2007). Ubiquitination regulates PTEN nuclear import and tumor suppression. Cell *128*, 141-156.

Vazquez, F., Ramaswamy, S., Nakamura, N., and Sellers, W.R. (2000). Phosphorylation of the PTEN tail regulates protein stability and function. Mol Cell Biol *20*, 5010-5018.

Wang, L., Balas, B., Christ-Roberts, C.Y., Kim, R.Y., Ramos, F.J., Kikani, C.K., Li, C., Deng, C., Reyna, S., Musi, N.*, et al.* (2007a). Peripheral disruption of the Grb10 gene enhances insulin signaling and sensitivity in vivo. Mol Cell Biol *27*, 6497-6505.

Wang, X., Shi, Y., Wang, J., Huang, G., and Jiang, X. (2008). Crucial role of the C-terminus of PTEN in antagonizing NEDD4-1-mediated PTEN ubiquitination and degradation. Biochem J *414*, 221-229.

Wang, X., Trotman, L.C., Koppie, T., Alimonti, A., Chen, Z., Gao, Z., Wang, J., Erdjument-Bromage, H., Tempst, P., Cordon-Cardo, C.*, et al.* (2007b). NEDD4-1 is a proto-oncogenic ubiquitin ligase for PTEN. Cell *128*, 129-139.

Wendler, F., and Tooze, S. (2001). Syntaxin 6: the promiscuous behaviour of a SNARE protein. Traffic *2*, 606-611.

Weng, L.P., Smith, W.M., Brown, J.L., and Eng, C. (2001). PTEN inhibits insulin-stimulated MEK/MAPK activation and cell growth by blocking IRS-1 phosphorylation and IRS-1/Grb-2/Sos complex formation in a breast cancer model. Hum Mol Genet *10*, 605-616.

Wheelock, M.J., and Johnson, K.R. (2003). Cadherins as modulators of cellular phenotype. Annu Rev Cell Dev Biol *19*, 207-235.

White, M.F. (1998). The IRS-signalling system: a network of docking proteins that mediate insulin action. Mol Cell Biochem *182*, 3-11.

Xu, W., and Kimelman, D. (2007). Mechanistic insights from structural studies of beta-catenin and its binding partners. J Cell Sci *120*, 3337-3344.

Yakar, S., and Adamo, M.L. (2012). Insulin-like growth factor 1 physiology: lessons from mouse models. Endocrinol Metab Clin North Am *41*, 231-247, v.

Yang, B., Gay, D.L., MacLeod, M.K., Cao, X., Hala, T., Sweezer, E.M., Kappler, J., Marrack, P., and Oliver, P.M. (2008). Nedd4 augments the adaptive immune response by promoting ubiquitin-mediated degradation of Cbl-b in activated T cells. Nat Immunol *9*, 1356-1363.

Yang, B., and Kumar, S. (2010). Nedd4 and Nedd4-2: closely related ubiquitin-protein ligases with distinct physiological functions. Cell Death Differ *17*, 68-77.

Yim, E.K., Peng, G., Dai, H., Hu, R., Li, K., Lu, Y., Mills, G.B., Meric-Bernstam, F., Hennessy, B.T., Craven, R.J.*, et al.* (2009). Rak functions as a tumor suppressor by regulating PTEN protein stability and function. Cancer Cell *15*, 304-314.

Yim, J.H., Kim, Y.J., Ko, J.H., Cho, Y.E., Kim, S.M., Kim, J.Y., Lee, S., and Park, J.H. (2007). The putative tumor suppressor gene GLTSCR2 induces PTEN-modulated cell death. Cell Death Differ *14*, 1872-1879.

Zeisberg, M., and Neilson, E.G. (2009). Biomarkers for epithelial-mesenchymal transitions. J Clin Invest *119*, 1429-1437.

Zeng, T., Wang, Q., Fu, J., Lin, Q., Bi, J., Ding, W., Qiao, Y., Zhang, S., Zhao, W., Lin, H.*, et al.* (2014). Impeded Nedd4-1-mediated Ras degradation underlies Ras-driven tumorigenesis. Cell Rep *7*, 871-882.

Zerial, M., and McBride, H. (2001). Rab proteins as membrane organizers. Nat Rev Mol Cell Biol *2*, 107-117.

Zhang, X.C., Piccini, A., Myers, M.P., Van Aelst, L., and Tonks, N.K. (2012). Functional analysis of the protein phosphatase activity of PTEN. Biochem J *444*, 457-464.